



QA: QA

ANL-WIS-MD-000008 REV 01

March 2004

## **Clad Degradation – FEPs Screening Arguments**

Prepared for:  
U.S. Department of Energy  
Office of Civilian Radioactive Waste Management  
Office of Repository Development  
1551 Hillshire Drive  
Las Vegas, Nevada 89134-6321

Prepared by:  
Bechtel SAIC Company, LLC  
1180 Town Center Drive  
Las Vegas, Nevada 89144

Under Contract Number  
DE-AC28-01RW12101

## **DISCLAIMER**

This report was prepared as an account of work sponsored by an agency of the United States Government. Neither the United States Government nor any agency thereof, nor any of their employees, nor any of their contractors, subcontractors or their employees, makes any warranty, express or implied, or assumes any legal liability or responsibility for the accuracy, completeness, or any third party's use or the results of such use of any information, apparatus, product, or process disclosed, or represents that its use would not infringe privately owned rights. Reference herein to any specific commercial product, process, or service by trade name, trademark, manufacturer, or otherwise, does not necessarily constitute or imply its endorsement, recommendation, or favoring by the United States Government or any agency thereof or its contractors or subcontractors. The views and opinions of authors expressed herein do not necessarily state or reflect those of the United States Government or any agency thereof.

2. Scientific Analysis Title  
**Clad Degradation – FEPs Screening Arguments**

3. DI (including Revision Number)  
**ANL-WIS-MD-000008 REV 01**

4. Total Appendices Three (3)	5. Number of Pages in Each Appendix A-10; B-4; C-12
----------------------------------	--

	Printed Name	Signature	Date
6. Originator	Eric R. Siegmann	SIGNATURE ON FILE	3/16/04
7. Checker	Emma R. Thomas	SIGNATURE ON FILE	3/16/04
8. QER	Darrell K. Svalstad	SIGNATURE ON FILE	3/16/04
9. Responsible Manager/Lead	Howard Adkins	SIGNATURE ON FILE	03-16-04
10. Responsible Manager	Robert Andrews	SIGNATURE ON FILE	17 MAR 04

11. Remarks  
  
This is associated with task F0050 for TSPA-LA.

**Change History**

12. Revision/ICN No.	13. Total Pages	14. Description of Change
00	69	Initial Issue.
00/01	82	Changed corrosion FEPs to be consistent with the Waste Form PMR. Ensured consistence of FEPs summary in Waste Form PMR. Addressed concerns cited in the self assessment documented in SA-PA-2000-005 (MOL.20000719.0414. Added full FEP discussion for Volume Increase of Corrosion Products - YMP No. 2.1.09.03.00 from ANL-WIS-MD-000009 Gap and Grain release of Cs, I - YMP No. 2.1.02.07.00 from ANL-WIS-MD-000009 Rockfall (Large Block)- YMP No. 2.1.07.01.00 from ANL-WIS-MD-000009
01	126	Modified report to be consistent with new procedures including AP-SIII.9Q. Revised FEP names, numbers, and description to be consistent with the FEPs selected for LA. Revised screening arguments.

INTENTIONALLY LEFT BLANK

## EXECUTIVE SUMMARY

Twenty-four features, events, and processes (FEPs) have been identified as being related to the degradation of cladding (including, in some cases, cladding and fuel pellet degradation) on commercial spent nuclear fuel during the post-closure period, with an emphasis on zirconium-alloyed cladding. This report also addresses the effect of some FEPs on both the cladding and all waste forms where it was considered appropriate to address the effects on both materials together (FEP 2.1.09.09.0A, 2.1.09.11.0A, 2.1.11.05.0A, 2.1.12.02.0A, and 2.1.12.03.0A). Defense spent nuclear fuel, including fuel with aluminum cladding, is addressed in the general waste form FEPs screening report and not in this report. Four FEPs have been identified as having sufficient probability of occurrence and having sufficient effect on the resulting radionuclide exposures to the reasonably maximally exposed individual as to be included in the TSPA-LA. Summaries of their inclusion are presented in this document. Eighteen FEPs have been identified as being excluded from the TSPA-LA because their omission would have low consequence (i.e., they would not significantly change the magnitude and time of the resulting radiological exposures to the reasonably maximally exposed individual or radionuclide releases to the accessible environment). Two FEPs have been excluded based on low probability. Arguments for their exclusion are presented in this report.

INTENTIONALLY LEFT BLANK

**CONTENTS**

	<b>Page</b>
1. PURPOSE.....	1
1.1 SCOPE.....	5
1.2 FEPS IDENTIFICATION AND ANALYSIS.....	6
2. QUALITY ASSURANCE.....	6
3. USE OF SOFTWARE.....	7
4. INPUTS.....	7
4.1 DIRECT INPUTS.....	7
4.1.1 Data.....	7
4.1.2 Parameters and Parameter Uncertainty.....	7
4.1.3 Other Model / Analyses Inputs and Technical Information.....	10
4.2 CRITERIA.....	11
4.3 CODES AND STANDARDS.....	11
5. ASSUMPTIONS.....	11
6. SCIENTIFIC ANALYSIS DISCUSSION.....	11
6.1 DEGRADATION OF CLADDING FROM WATERLOGGED RODS.....	17
6.2 DEGRADATION OF CLADDING PRIOR TO DISPOSAL.....	19
6.3 GENERAL CORROSION OF CLADDING.....	20
6.4 MICROBIALY INFLUENCED CORROSION (MIC) OF CLADDING.....	26
6.5 LOCALIZED (RADIOLYSIS ENHANCED) CORROSION OF CLADDING.....	28
6.6 LOCALIZED (PITTING) CORROSION OF CLADDING.....	31
6.7 LOCALIZED (CREVICE) CORROSION OF CLADDING.....	36
6.8 ENHANCED CORROSION OF CLADDING FROM DISSOLVED SILICA.....	38
6.9 CREEP RUPTURE OF CLADDING.....	39
6.10 INTERNAL PRESSURIZATION OF CLADDING.....	42
6.11 STRESS CORROSION CRACKING (SCC) OF CLADDING.....	44
6.12 HYDRIDE CRACKING OF CLADDING.....	47
6.12.1 Hydride Embrittlement from Zirconium Corrosion (of Cladding).....	50
6.12.2 Hydride Embrittlement from Galvanic Corrosion of Waste Package Contacting Cladding.....	50
6.12.3 Delayed Hydride Cracking (of Cladding).....	52
6.12.4 Hydride Reorientation (of Cladding).....	54
6.12.5 Hydride Axial Migration (of Cladding).....	59
6.12.6 Hydride Embrittlement from Fuel Reaction (Causes Failure of Cladding).....	60
6.13 CLADDING UNZIPPING.....	60
6.14 MECHANICAL IMPACT ON CLADDING.....	61
6.15 NAVAL SNF CLADDING.....	63
6.16 DIFFUSION-CONTROLLED CAVITY GROWTH (DCCG) IN CLADDING.....	63
6.17 LOCALIZED (FLUORIDE ENHANCED) CORROSION OF CLADDING.....	65

## CONTENTS

	<b>Page</b>
6.18 ROCKFALL .....	68
6.19 VOLUME INCREASE OF CORROSION PRODUCTS IMPACTS CLADDING .....	69
6.20 ELECTROCHEMICAL EFFECTS IN EBS .....	69
6.21 CHEMICAL EFFECTS OF WASTE-ROCK CONTACT .....	72
6.22 THERMAL EXPANSION/STRESS OF IN-PACKAGE EBS COMPONENTS .....	73
6.23 GAS GENERATION (HE) FROM WASTE FORM DECAY .....	75
6.24 GAS GENERATION (H <sub>2</sub> ) FROM WASTE PACKAGE CORROSION .....	76
7. CONCLUSIONS .....	79
8. REFERENCES .....	81
8.1 DOCUMENTS CITED .....	81
8.2 CODES, STANDARDS, REGULATIONS, AND PROCEDURES .....	90
8.3 SOURCE DATA, LISTED BY DATA TRACKING NUMBER .....	90

---

**FIGURES**

	<b>Page</b>
6.3-1. The Iso-Corrosion Diagram for Zirconium in Sulfuric Acid (H <sub>2</sub> SO <sub>4</sub> ) .....	22
6.3-2. A Comparison of Oxide Thicknesses for Different Zirconium Alloys.....	25
6.5-1. pH Profiles Showing How the Radiolysis Inputs Affect the pH .....	29
6.6-1. Comparison of In-Package Chemistry with Chemical Conditions Necessary for Pitting.....	33
6.6-2. Chemistry Where Pitting of Zirconium Has Been Observed.....	36
6.9-1. Creep Failure Fraction as a Function of Peak Cladding Temperature.....	41
6.9-2. Comparison of Creep Damage in Dry Storage and Repository Emplacement.....	41
6.12-1. Fracture Toughness vs. Hydrogen Content of Zircaloy-4 .....	49
6.12-2. Comparison of the YMP Reorientation Equation with Additional Experimental Data..	56
6.12-3. Dissolution and Precipitation Solubilities for Hydrogen in Irradiated Zirconium Metal .....	59

**TABLES**

	<b>Page</b>
1-1. FEPs Related to the CSNF Clad Degradation Component.....	3
1-2. Changes to the Cladding FEPs from TSPA-SR to TSPA-LA .....	4
4-1. Information Sources for FEPs Included in TSPA-LA .....	7
4-2. Information Sources for FEPs Excluded from TSPA-LA .....	8
6-1. LA FEP List for Cladding.....	13
6-2. Corroborating Models and Information Used to Develop This Report .....	16
6.3-1. Percent of Cladding Remaining in Waste Packages that Fail at Closure .....	24
6.5-1. Chloride, Ferric Iron, and Hydrogen Peroxide Molality.....	30
6.5-2. Half-Life of Hydrogen Peroxide at Various Temperatures .....	31
6.6-1. Corrosion and Repassivation Potentials for In-Package Chemistry Condition .....	33
6.10-1. Effect of Helium Production on Rod Pressure.....	43
6.11-1. Pressures, Stresses and Stress Intensity Factors for Fuel Rods During Repository Emplacement.....	46
6.12-1. Puls' Zircaloy-2 Strain Tests on Zirconium with Reoriented Hydrides.....	57
6.12-2. Saturation Limits (T <sub>ssd</sub> ) for Hydrogen in Unirradiated Zirconium as a Function of Temperature .....	58
6.17-1. Compositions of J-13 Well Water and Its Concentrates.....	67
7-1. Summary of Cladding Degradation and Waste Form FEPs .....	80

## ACRONYMS AND ABBREVIATIONS

ANL	Argonne National Laboratory
ASTM	American Society for Testing and Materials
BWR	boiling water reactor
CCDF	Complementary Cumulative Distribution Function
CSNF	commercial spent nuclear fuel
DCCG	Diffusion Controlled Cavity Growth
DHC	Delayed Hydride Cracking
DOE	U.S. Department of Energy
DHLW	Defense High Level Waste
DSNF	Defense Spent Nuclear Fuel
EBS	Engineered Barrier System
FEPs	Features, Events, and Processes
HLW	High Level Waste
IAEA	International Atomic Energy Agency
INEEL	Idaho National Engineering and Environmental Laboratory
kgU	kilogram Uranium
KTI	Key Technical Issue
LA	License Application
LWR	Light Water Reactor
MIC	Microbially Influenced Corrosion
MWd	Megawatt days
NRC	U.S. Nuclear Regulatory Commission
OCRWM	Office of Civilian Radioactive Waste Management
PWR	pressurized water reactor
RMEI	reasonably maximally exposed individual
SCC	Stress Corrosion Cracking
SCE	Standard Calomel Electrode scale
SNF	Spent Nuclear Fuel
SR	Site Recommendation
SRB	Sulfate Reducing Bacteria
STP	Standard Temperature and Pressure
TSPA	Total System Performance Assessment
TSPAI	Total System Performance Assessment and Integration
TSPA-LA	Total System Performance Assessment – License Application
TSPA-VA	Total System Performance Assessment – Viability Assessment
YMP	Yucca Mountain Project

## 1. PURPOSE

The purpose of this report is to document the screening of the cladding degradation features, events, and processes (FEPs) for commercial spent nuclear fuel (CSNF). This report also addresses the effect of some FEPs on both the cladding and the CSNF, DSNF, and HLW waste forms where it was considered appropriate to address the effects on both materials together (FEP 2.1.09.09.0A, 2.1.09.11.0A, 2.1.11.05.0A, 2.1.12.02.0A, and 2.1.12.03.0A). This report summarizes the work of others to screen clad degradation FEPs in a manner consistent with, and used in, the Total System Performance Assessment – License Application (TSPA-LA). This document was prepared according to *Technical Work Plan for Waste Form Degradation Modeling, Testing, and Analyses in Support of LA* (BSC 2004a [DIRS 167796]).

The development of a comprehensive list of FEPs potentially relevant to postclosure performance of a repository at Yucca Mountain is an ongoing, iterative process based on site-specific information, design, and regulations. The approach for developing an initial list of FEPs in support of Total System Performance Assessment for the Site Recommendation (CRWMS M&O 2000a [DIRS 153246]) was documented in The Development of Information Catalogued in REV00 of the YMP FEP Database (BSC 2001c [DIRS 154365]). The initial FEP list contained 328 FEPs, of which 176 were included in the TSPA-SR model (CRWMS M&O 2000a [DIRS 153246], Tables B-9 through B-17). To support the TSPA-LA model, the FEP list was re-evaluated in accordance with The Enhanced Plan for Features, Events, and Processes (FEPs) at Yucca Mountain (BSC 2002 [DIRS 158966], Section 3.2). This was supplemented by KTI Letter Report Response to Additional Information Needs on TSPA 2.05 and TSPA 2.06 (Freeze 2003 [DIRS 165394]). This re-evaluation resulted in an initial list of FEPs for TSPA-LA, documented in DTN: MO0307SEPFEPs4.000 [DIRS 164527].

Since the initial list was developed, some modifications have occurred. As noted above, FEPs 2.1.09.09.0A, 2.1.09.11.0A, 2.1.11.05.0A, 2.1.12.02.0A, and 2.1.12.03.0A were re-assigned to this report. FEP 2.1.02.07.0A was re-assigned from this report to a different FEP analysis report. The description for FEP 2.1.02.11.0A was modified for clarity. The description for FEP 2.1.02.15.0A was modified since H<sub>2</sub>O<sub>2</sub> was incorrectly identified as ions in solution. The description of FEP 2.1.02.19.0A was modified to reflect the current temperature limit for creep of 400°C. The description of FEP 2.1.02.24.0A was modified to add impact from waste package internals and to remove rockfall damage from seismic events, which is now addressed in FEP 1.2.03.02.0B.

Table 1-1 provides the modified list of cladding FEPs, including their screening decisions (include or exclude). The primary purpose of this report is to identify and document the analysis, screening decision, and TSPA-LA disposition (for included FEPs) or screening argument (for excluded FEPs) for these FEPs related to clad degradation. In some cases, where a FEP covers multiple technical areas and is shared with other FEP reports, this cladding FEP report may provide only a partial technical basis for the screening of the FEP. The full technical bases for these shared FEPs are addressed collectively by all of the sharing FEP reports. The screening decisions and associated TSPA-LA dispositions or screening arguments from all of the FEP reports will be cataloged in a project-specific FEPs database. This report, along with the other FEP reports, and the database are being used to document information related to the FEPs screening to assist reviewers during the license review process.

Table 1-2 summarizes the changes to the cladding FEPs from TSPA-SR (CRWMS M&O 2000g [DIRS 153947]) to the modified TSPA-LA list, including the changes in assignment and descriptions noted previously. Two major analysis changes have occurred. In TSPA-SR a creep model was included in the TSPA analysis although the temperatures of the fuel were sufficiently low that no cladding failures were predicted from this cause. The creep model included internal pressurization of cladding and thermally induced stress changes. Since no failures are predicted to occur because of creep, the FEPs dealing with creep (FEPs 2.1.02.19.0A, 2.1.02.20.0A, 2.1.11.05.0A) are now excluded from TSPA-LA. The SR model contained a non-mechanistic corrosion model that was used to include failure from various corrosion mechanisms. Since SR, a pitting model and an in-package chemistry model have been developed. When these models were combined, no cladding failure from corrosion was predicted and these FEPs (FEPs 2.1.02.14.0A, 2.1.02.15.0A, 2.1.02.16.0A, 2.1.02.27.0A) were excluded.

The four FEPs included in the TSPA-LA are described in detail in *Clad Degradation – Summary and Abstraction for LA* (BSC 2003a [DIRS 162153]) and summarized in this report. *Clad Degradation – Summary and Abstraction for LA* (BSC 2003a [DIRS 162153]) also describes one FEP (2.1.02.24.0A) Mechanical Impact on Cladding, as included. At that time it was included because the cladding is modeled to be damaged by rock overpressure after the drip shield and waste package deteriorates. This damage occurs well after the 10,000-year regulatory period and is now characterized as excluded. For excluded FEPs, the technical bases for their exclusion are documented here.

This analysis is limited to fuel exposed to normal operation and anticipated operational occurrences (i.e., events that are anticipated to occur within a reactor lifetime), and is not applicable to fuel that has been exposed to severe accidents. Fuel burnup projections have been limited to the current commercial reactor licensing environment with restrictions on fuel enrichment (5 percent for material shipment and fuel manufacturing, shipment, and storage), cladding oxide coating thickness, and rod plenum pressures. This is consistent with the projections for advanced reloads. The fuel considered has burnup up to 75 MWd/kgU and half of the fuel is above 44.7 MWd/kgU, today's typical PWR burnup range. Ranges and uncertainties have been defined in *Initial Cladding Condition* (CRWMS M&O 2000c [DIRS 151659], Section 6.2). Information provided in this FEPs screening will be used to evaluate which cladding degradation mechanisms are included in the postclosure performance of the repository in relation to waste form degradation.

The CSNF cladding performance is used to bound naval fuel cladding behavior. The Naval Nuclear Propulsion Program has demonstrated that the performance of naval spent nuclear fuel cladding is better than or equal to that of cladding on CSNF (BSC 2001a [DIRS 152059], p. 36 and Figure 6.1-2). Cladding degradation for defense spent nuclear fuel (DSNF), including aluminum-clad fuel, is not addressed in this report, but is addressed in a general waste form screening report *Miscellaneous Waste-Form FEPs* (CRWMS M&O 2001c [DIRS 153938]).

Table 1-1. FEPs Related to the CSNF Clad Degradation Component

Section	FEP Number	FEP Name	Screening Decision	Shared With
6.1	2.1.02.11.0A	Degradation of cladding from waterlogged rods	Excluded	
6.2	2.1.02.12.0A	Degradation of cladding prior to disposal	Included	
6.3	2.1.02.13.0A	General corrosion of cladding	Excluded	
6.4	2.1.02.14.0A	Microbially influenced corrosion (MIC) of cladding	Excluded	
6.5	2.1.02.15.0A	Localized (radiolysis enhanced) corrosion of cladding	Excluded	
6.6	2.1.02.16.0A	Localized (pitting) corrosion of cladding	Excluded	
6.7	2.1.02.17.0A	Localized (crevice) corrosion of cladding	Excluded	
6.8	2.1.02.18.0A	Enhanced corrosion of cladding from dissolved silica	Excluded	
6.9	2.1.02.19.0A	Creep rupture of cladding	Excluded	
6.10	2.1.02.20.0A	Internal pressurization of cladding	Excluded	
6.11	2.1.02.21.0A	Stress corrosion cracking (SCC) of cladding	Excluded	
6.12	2.1.02.22.0A	Hydride cracking of cladding	Excluded	
6.13	2.1.02.23.0A	Cladding unzipping	Included	
6.14	2.1.02.24.0A	Mechanical impact on cladding	Excluded	
6.15	2.1.02.25.0B	Naval SNF Cladding	Included	
6.16	2.1.02.26.0A	Diffusion-controlled cavity growth (DCCG) in cladding	Excluded	
6.17	2.1.02.27.0A	Localized (fluoride enhanced) corrosion of cladding	Excluded	
6.18	2.1.07.01.0A	Rockfall	Excluded	WP, EBS
6.19	2.1.09.03.0A	Volume increase of corrosion products impacts cladding	Included	
6.20	2.1.09.09.0A	Electrochemical effects in EBS	Excluded	WP
6.21	2.1.09.11.0A	Chemical effects of waste-rock contact	Excluded	
6.22	2.1.11.05.0A	Thermal expansion/stress of in-package EBS components	Excluded	
6.23	2.1.12.02.0A	Gas generation (He) from waste form decay	Excluded	EBS
6.24	2.1.12.03.0A	Gas generation (H <sub>2</sub> ) from waste package corrosion	Excluded	WP, EBS

NOTE: WP = waste package, EBS = engineered barrier system

Table 1-2. Changes to the Cladding FEPs from TSPA-SR to TSPA-LA

LA #	LA FEP Name	SR-#A	SR-NameA	Significant Scope and Screening Changes from TSPA-SRA to TSPA-LA
		2.1.02.07.00	Gap and Grain Release of Cs, I	Not a cladding FEP for LA. FEP now addressed by WF in BSC 2004c [DIRS 167321]
2.1.02.11.0A	Degradation of cladding from waterlogged rods	2.1.02.11.00	Waterlogged Rods	No change, both exclude
2.1.02.12.0A	Degradation of cladding prior to disposal	2.1.02.12.00	Cladding Degradation Before YMP Receives It	No change, both include
2.1.02.13.0A	General corrosion of cladding	2.1.02.13.00	General Corrosion of Cladding	No change, both exclude
2.1.02.14.0A	Microbially influenced corrosion (MIC) of cladding	2.1.02.14.00	Microbiologically Influenced Corrosion (MIC) of Cladding	LA: Excluded with new pitting model, SR: Included as part of non-mechanistic corrosion model
2.1.02.15.0A	Localized (radiolysis enhanced) corrosion of cladding	2.1.02.15.00	Acid Corrosion of Cladding From Radiolysis	LA: Excluded with new pitting model and in-package chemistry, SR: Included as part of non-mechanistic corrosion model
2.1.02.16.0A	Localized (pitting) corrosion of cladding	2.1.02.16.00	Localized Corrosion (Pitting) of Cladding	LA: Excluded with new pitting model, SR: Included as part of non-mechanistic corrosion model
2.1.02.17.0A	Localized (crevice) corrosion of cladding	2.1.02.17.00	Localized Corrosion (Crevice Corrosion) of Cladding	No change, both exclude
2.1.02.18.0A	Enhanced corrosion of cladding from dissolved silica	2.1.02.18.00	High Dissolved Silica Content of Waters Enhances Corrosion of Cladding	No change, both exclude
2.1.02.19.0A	Creep rupture of cladding	2.1.02.19.00	Creep Rupture of Cladding	LA: Exclude, SR: Included in creep model but no cladding failures when model was used
2.1.02.20.0A	Internal pressurization of cladding	2.1.02.20.00	Pressurization From He Production Causes Cladding Failure	LA: Exclude, SR: Included in creep model but no cladding failures when model was used
2.1.02.21.0A	Stress corrosion cracking (SCC) of cladding	2.1.02.21.00	Stress Corrosion Cracking (SCC) of Cladding	LA: Exclude, SR: Included assuming high iodine and stresses present
2.1.02.22.0A	Hydride cracking of cladding	2.1.02.22.00	Hydride Embrittlement of Cladding	No change, both exclude
2.1.02.23.0A	Cladding unzipping	2.1.02.23.00	Cladding Unzipping	No change, both include
2.1.02.24.0A	Mechanical impact on cladding	2.1.02.24.00	Mechanical Failure of Cladding	LA Scope expanded to address impact from waste package internals, reduced by having seismic rockfall now addressed as part of shared DE and EBS FEP 1.2.03.02.0B. LA: Exclude, SR: Included from rock overpressure after regulatory period
2.1.02.25.0B	Naval SNF Cladding			New FEP since SR, LA: Include
2.1.02.26.0A	Diffusion-controlled cavity growth (DCCG) in cladding	2.1.02.26.00	Diffusion-Controlled Cavity Growth	No change, both exclude

Table 1-2. Changes to the Cladding FEPs from TSPA-SR to TSPA-LA (Continued)

LA #	LA FEP Name	SR-#A	SR-NameA	Significant Scope and Screening Changes from TSPA-SRA to TSPA-LA
2.1.02.27.0A	Localized (fluoride enhanced) corrosion of cladding	2.1.02.27.00	Localized Corrosion Perforation from Fluoride	LA: Excluded, low Fluoride concentrations, pH>3.18 , SR: Included as part of non-mechanistic corrosion model
2.1.07.01.0A	Rockfall	2.1.07.01.00	Rockfall (Large Block)	LA Scope reduced by having seismic rockfall now addressed as part of shared DE and EBS FEP 1.2.03.02.0B , LA and SR both exclude
2.1.09.03.0A	Volume increase of corrosion products impacts cladding	2.1.09.03.00	Volume Increase of Corrosion Products	LA Scope reduced to address impacts on cladding only. Impacts on other EBS components are now addressed in WP FEP 2.1.09.03.0B and EBS FEP 2.1.09.03.0C, LA and SR both include
2.1.09.09.0A	Electrochemical effects in EBS	2.1.09.09.00 *	Electrochemical Effects (Electrophoresis, Galvanic Coupling) in Waste and EBS	No change, both exclude
2.1.09.11.0A	Chemical effects of waste-rock contact	2.1.09.11.00 *	Waste-Rock Contact	No change, both exclude
2.1.11.05.0A	Thermal expansion/stress of in-package EBS components	2.1.11.05.00 * 2.1.11.07.00	Differing Thermal Expansion of Repository Components Thermally-Induced Stress Changes in Waste and EBS	LA Scope addresses all in-package issues that were in the two SR FEPs. LA: Exclude, SR included as part of creep analysis
2.1.12.02.0A	Gas generation (He) from waste form decay	2.1.12.02.00 *	Gas generation (He) from fuel decay	No change, both exclude
2.1.12.03.0A	Gas generation (H <sub>2</sub> ) from waste package corrosion	2.1.12.03.00 *	Gas generation (H <sub>2</sub> ) from metal corrosion	No change, both exclude

\* These were not addressed as Cladding FEPs for SR, but were addressed elsewhere (WF and/or WP and/or EBS).

^ Source: CRWMS M&O 2000g [DIRS 153947]

## 1.1 SCOPE

This report addresses clad degradation FEPs, which represent the key phenomena that result in degradation of cladding and, in some cases, the CSNF pellets themselves. Clad degradation FEPs addressed in this report are provided in Table 1-1.

The repository design continues to evolve in preparation for the license application. In general, these design changes can directly influence the screening arguments for FEPs and their inclusion in or exclusion from the waste form degradation model. The elimination of backfill is an important design change that was made after the development of the current waste form degradation model. The primary effect of the elimination of backfill is the decrease of peak temperatures inside the waste package, which is beneficial to reducing uncertainty (CRWMS M&O 2001a [DIRS 151662], Section 6.2). However, the absence of backfill does not affect the cladding degradation FEPs included in the TSPA-LA analysis. The original screening (earlier version of this report) was performed with backfill temperatures and contained many of the same conclusions.

## 1.2 FEPS IDENTIFICATION AND ANALYSIS

To support the TSPA-LA model, the FEP list was reevaluated in accordance with *The Enhanced Plan for Features, Events, and Processes (FEPs) at Yucca Mountain* (BSC 2002 [DIRS 158966], Section 3.2) and supplemented by *KTI Letter Report Response to Additional Information Needs on TSPAI 2.05 and TSPAI 2.06* (Freeze 2003 [DIRS 165394]). The resulting 24 cladding FEPs are listed in Table 1-1.

The U.S. Nuclear Regulatory Commission (NRC) requires the consideration and evaluation of FEPs as part of the performance assessment activities. More specifically, the NRC regulations allow the exclusion of FEPs from the TSPA if they can be shown to be of low probability or consequence. The specified criteria can be summarized as follows.

1. The event has at least one chance in 10,000 of occurring over 10,000 years (see 10 CFR 63.114(d) [DIRS 156605]).
2. The magnitude and time of the resulting radiological exposure to the RMEI, or radionuclide release to the accessible environment, would be significantly changed by its omission (see 10 CFR 63.114 (e and f) [DIRS 156605]).

Additionally, the Acceptance Criterion in *Yucca Mountain Review Plan, Final Report* (NRC 2003 [DIRS 163274], Section 2.2.1.2.1.3) allows the exclusion of FEPs from TSPA if they are inconsistent with specifications within the NRC regulations. This criterion can be summarized in the form of a third FEP screening statement.

3. The FEP is not excluded by regulation.

Evaluating the FEPs against these screening statements may be done in any order. If there are affirmative conditions for all three screening criteria, a FEP is “Included” in the TSPA-LA model. If there is a negating condition in any of the three screening criteria, the FEP is “Excluded” from the TSPA-LA model.

For the cladding FEPs, all three screening criteria were considered, but only two (Criteria 1 and 2 above) were used. Consequence-based screening arguments can be established in a variety of ways, including TSPA-LA sensitivity analyses, modeling studies outside of the TSPA-LA, or reasoned arguments based on literature research. Probability-based screening arguments are based on a comparison of the FEP probability of occurrence with the regulatory probability criterion.

## 2. QUALITY ASSURANCE

The Quality Assurance program applies to the development of this document because this model will be part of the TSPA-LA safety analysis. This document was prepared in accordance with *Technical Work Plan for Waste Form Degradation, Modeling, Testing, and Analyses in Support of LA* (BSC 2004a [DIRS 167796]). This report does not directly impact structures, systems, or components classified in accordance with AP-2.22Q, *Classification Analyses and Maintenance of the Q-List*. The technical work plan contains the Process Control Evaluation used to evaluate the control of electronic management of data (BSC 2004a [DIRS 167796], Attachment I) during

modeling and documentation activities. This evaluation determined that the methods identified in the implementing procedures are adequate. There were no deviations from these methods. This report was prepared using AP-SIII.9Q, *Scientific Analyses*.

### 3. USE OF SOFTWARE

No software is used for analysis in this report. The analyses and arguments presented herein are based on regulatory requirements, results of analyses presented and documented in other reports, or technical literature. This report was documented using only commercially available software (Microsoft Word 97, SR2) for word processing, which is not required to be qualified or documented per AP-SI.1Q, *Software Management*. There were no additional applications (routines or macros) developed for documentation using this commercial software. SigmaPlot, Scientific Graphic Software, Version 2.0, Jandel Corporation is used to plot data. No calculations are performed with this software. This software is not required to be qualified or documented per AP-SI.1Q, *Software Management*, as specified in Section 2.1.2.

### 4. INPUTS

#### 4.1 DIRECT INPUTS

This section identifies input data, parameters, and other forms of analysis inputs used in this report. The data and technical information used in this report were obtained from controlled source documents and other appropriate sources.

##### 4.1.1 Data

No data were used as direct input.

##### 4.1.2 Parameters and Parameter Uncertainty

The analyses and arguments presented herein are based on guidance and regulatory requirements, results of analyses presented and documented in other reports or other technical literature. The sources for the detailed discussions of included FEPs are provided in Table 4-1. Sources for excluded FEPs are listed in Table 4-2. The justification for using the technical information listed in Table 4-2 is presented in Appendix C. Models developed in the supporting documents are cited for traceability and transparency purposes; however, they were not used directly in development of these analyses and arguments presented herein.

Table 4-1. Information Sources for FEPs Included in TSPA-LA

Section Used	FEP Number	FEP Name	Source
6.2	2.1.02.12.0A	Degradation of cladding prior to disposal	BSC 2003a [DIRS 162153], Sections 6.2.1, 6.2.2
6.13	2.1.02.23.0A	Cladding unzipping	BSC 2003a [DIRS 162153], Section 6.2.4
6.15	2.1.02.25.0B	Naval SNF Cladding	BSC 2003a [DIRS 162153], Section 6
6.19	2.1.09.03.0A	Volume increase of corrosion products impacts cladding	BSC 2003a [DIRS 162153], Section 6.2.4

Table 4-2. Information Sources for FEPs Excluded from TSPA-LA

Section Used	FEP Number	FEP Name	Source	Information
Through out	All	NA	10 CFR 63.114(d, e, f) [DIRS 156605].	FEP screening considerations
6.1	2.1.02.11.0A	Degradation of cladding from waterlogged rods	NRC 1997 [DIRS 101903], Section 8.V.1 BSC 2003a [DIRS 162153], Section 6.2.1	Waterlogging not a problem Fraction of failed rods
6.3	2.1.02.13.0A	General corrosion of cladding	Hillner et al. 1998 [DIRS 100455], Pourbaix 1974 [DIRS 100817], p. 226	Corrosion rate Stability of ZrO <sub>2</sub>
6.4	2.1.02.14.0A	Microbially influenced corrosion (MIC) of cladding	Wolfram et al. 1996 [DIRS 165268], pp. iii, iv Hillner et al. 1998 [DIRS 100455], p. 11	MIC and Zirconium alloys MIC and Zirconium alloys
6.5	2.1.02.15.0A	Localized (radiolysis enhanced) corrosion of cladding	BSC 2003f [DIRS 161962], Attachment III BSC 2003a [DIRS 162153] BSC 2003g [DIRS 164667]	In-package chemistry Pitting potential not met
6.6	2.1.02.16.0A	Localized (pitting) corrosion of cladding	BSC 2003f [DIRS 161962], Attachment III BSC 2003g [DIRS 164667], Section 8.2 CRWMS M&O 2000b [DIRS 151561]	In-package chemistry Pitting calculation for waste package MIC little effect on geochemistry
6.7	2.1.02.17.0A	Localized (crevice) corrosion of cladding	Yau and Webster 1987 [DIRS 100494], p. 717 Greene et al. 2000 [DIRS 145073], p. 7) Brossia et al. (2002 [DIRS 161988])	Resistance to Crevice corrosion Resistance to Crevice corrosion Resistance to Crevice corrosion
6.8	2.1.02.18.0A	Enhanced corrosion of cladding from dissolved silica	Hansson 1984 [DIRS 101676] Yau and Webster 1987 [DIRS 100494], Table 6	No accelerated corrosion No accelerated corrosion
6.9	2.1.02.19.0A	Creep rupture of cladding	NRC 2002 [DIRS 164593], p. 2	Little creep damage below 400°C
6.10	2.1.02.20.0A	Internal pressurization of cladding	Piron and Pelletier 2001 [DIRS 165318], Section 5.3	Helium pressurization
6.11	2.1.02.21.0A	Stress corrosion cracking (SCC) of cladding	Beckman 2001 [DIRS 156122], p. 103 BSC 2003a [DIRS 162153] BSC 2003g [DIRS 164667]	Iodine-induced SCC unlikely Passive layer preserved
6.12.0	2.1.02.22.0A	Hydride cracking of cladding (General)	Kreyns et al. 1996 [DIRS 100462], Figure 5	Fracture toughness vs. hydrogen content
6.12.1	2.1.02.22.0A	Hydride cracking of cladding (zirconium alloys corrosion)	Lanning et al. 1997 [DIRS 101704], Volume 1, p. 8.4, Figure 8.2	Hydrogen absorption from general corrosion
6.12.2	2.1.02.22.0A	Hydride cracking of cladding (galvanic corrosion)	Yau and Webster 1987 [DIRS 100494], p. 718, Table 15 Hansson 1984 [DIRS 101676], p. 6	Galvanic corrosion Rapid passivation

Table 4-2. Information Sources for FEPs Excluded from TSPA-LA (Continued)

Section Used	FEP Number	FEP Name	Source	Information
6.12.3	2.1.02.22.0A	Hydride cracking of cladding (delayed hydride cracking)	Peehs 1998 [DIRS 109219], pp. 5, 6 Cragnoilino et al. 1999 [DIRS 152354], p.4-21	DHC not expected DHC not expected
6.12.4	2.1.02.22.0A	Hydride cracking of cladding (hydride reorientation)	EPRI 2002 [DIRS 161421] Cragnoilino et al. 1999 [DIRS 152354], p. 4-22	No reorientation in dry storage No reorientation of $T_{max} < 290^{\circ}C$
6.12.5	2.1.02.22.0A	Hydride cracking of cladding (axial migration)	Cunningham et al. 1987 [DIRS 101591], Appendix C Cappelaere et al. 2002 [DIRS 164195], p. 5	Axial migration is minor Axial migration is minor
6.12.6	2.1.02.22.0A	Hydride cracking of cladding (fuel reaction)	Edsinger 2000 [DIRS 154433]	Hydrating of cladding requires reducing environment in BWRs
6.14	2.1.02.24.0A	Mechanical impact on cladding	CRWMS M&O 2001b [DIRS 153937].  BSC 2003c [DIRS 163935], Section 6.5.1.2.1.3.2	Rockfalls will not damage the waste package Volumes and dimensions for oxides
6.16	2.1.02.26.0A	Diffusion-controlled cavity growth (DCCG) in cladding	NRC 2000 [DIRS 147797] Hayes et al. 1999 [DIRS 164598], Figures 2, 5, 6, 8, and 11	Little creep damage under $400^{\circ}C$ DCCG is unlikely if $T < 330 - 400^{\circ}C$
6.17	2.1.02.27.0A	Localized (fluoride enhanced) corrosion of cladding	Pourbaix 1974 [DIRS 100817], p. 583 BSC 2003f [DIRS 161962], Attachment III)	Hydrofluoric acid exists for $pH < 3.18$ $pH > 3.5$
6.18	2.1.07.01.0A	Rockfall	CRWMS M&O 2001b [DIRS 153937].	Rockfalls will not damage the waste package
6.20	2.1.09.09.0A	Electrochemical effects in EBS	Yau and Webster 1987 [DIRS 100494], p. 718, Table 15 Hansson 1984 [DIRS 101676], p. 6	Zirconium is a noble metal Passive film forms in seconds
6.21	2.1.09.11.0A	Chemical effects of waste-rock contact	Adler, Flitton, et al. 2002 [DIRS 161991], p. 4 BSC 2003a [DIRS 162153]	Cladding/rock contact test
6.22	2.1.11.05.0A	Thermal expansion/stress of in-package EBS components	BSC 2004c [DIRS 167321], Section 6.2.1 BSC 2004d [DIRS 167619], Section 7.5.3	Fuel pellet fragmentation Glass temperatures
6.23	2.1.12.02.0A	Gas generation (He) from waste form decay	Piron and Pelletier 2001 [DIRS 165318], Section 5.3	Helium pressurization
6.24	2.1.12.03.0A	Gas generation ( $H_2$ ) from waste package corrosion	Clayton 1989 [DIRS 149208], Tables 1 through 4 IAEA 1998 [DIRS 150560], p. 92 Pourbaix 1974 [DIRS 100817], p. 226	$H_2$ not absorbed through passive layer $H_2$ not absorbed through passive layer Stability of Zr in water
App. A	NA	NA	BSC 2003b [DIRS 166463], Section 6.2	Temperature history of waste package surface

#### 4.1.3 Other Model / Analyses Inputs and Technical Information

The list of cladding degradation FEPs was extracted from the LA FEP list documented in DTN: MO0307SEPFEPS4.000 [DIRS 164527] and is considered as input for this analysis.

The low consequence requirements are stated in 10 CFR 63.114 (e and f) [DIRS 156605]:

(e) Provide the technical basis for either inclusion or exclusion of specific features, events, and processes in the performance assessment. Specific features, events, and processes must be evaluated in detail if the magnitude and time of the resulting radiological exposures to the reasonably maximally exposed individual, or radionuclide releases to the accessible environment, would be significantly changed by their omission.

(f) Provide the technical basis for either inclusion or exclusion of degradation, deterioration, or alteration processes of engineered barriers in the performance assessment, including those processes that would adversely affect the performance of natural barriers. Degradation, deterioration, or alteration processes of engineered barriers must be evaluated in detail if the magnitude and time of the resulting radiological exposures to the reasonably maximally exposed individual, or radionuclide releases to the accessible environment, would be significantly changed by their omission.

and supported by 10 CFR 63.342 [DIRS 156605]:

DOE's performance assessments need not evaluate the impacts resulting from any features, events, and processes or sequences of events and processes with a higher chance of occurrence if the results of the performance assessments would not be changed significantly.

Although NRC regulations do not define the terms "significantly changed" and "changed significantly," this report infers the absence of "significant change" to be equivalent to having no or negligible effect (i.e., inclusion of effect would have negligible effect on consequence).

The low-probability criterion is stated in 10 CFR 63.114(d)[DIRS 156605]:

Consider only events that have at least one chance in 10,000 of occurring over 10,000 years.

and supported by 10 CFR 63.342 [DIRS 156605]:

DOE's performance assessments shall not include consideration of very unlikely features, events, or processes, i.e., those that are estimated to have less than one chance in 10,000 of occurring within 10,000 years of disposal.

The low-probability criterion (i.e., very unlikely FEPs) is stated as less than one chance in 10,000 of occurring in 10,000 years ( $10^{-4}/10^4$  yr), a  $10^{-8}$  annual-exceedance probability.

## 4.2 CRITERIA

The low consequence and low probability requirements stated in 10 CFR 63.114 (d, e and f) [DIRS 156605] and supported by 10 CFR 63.342 [DIRS 156605] can be considered criteria, as discussed in Section 4.1.3.

## 4.3 CODES AND STANDARDS

American Society for Testing and Materials (ASTM) Standard C1174-97, *Standard Practice for Prediction of the Long-Term Behavior of Materials, Including Waste Forms, Used in Engineered Barrier Systems (EBS) for Geological Disposal of High-Level Radioactive Waste* (ASTM 1998 [DIRS 105725]), is used to support the degradation model development methodology, categorize the model developed with respect to its usage for long-term TSPA, and relate the information/data used to develop the model to the requirements of the standard.

For the repository, cladding is not an engineered barrier. It is not designed and controlled by the project to reduce release of radionuclides. The behavior can be modeled but the design characteristics are not within the project controls.

## 5. ASSUMPTIONS

There are no assumptions used in this report.

## 6. SCIENTIFIC ANALYSIS DISCUSSION

This section discusses each of the 24 FEPs dealing with cladding degradation (Table 6-1). The purpose of this report is to document the screening of the cladding degradation FEPs. For included FEPs, a summary of their implementation in TSPA-LA is presented here. As shown in Table 4-1, detailed documentation of their inclusion is presented in BSC 2003a [DIRS 162153]. BSC 2003c [DIRS 163935] provides additional support for FEP 2.1.09.03.0A. For excluded FEPs, the arguments for their exclusion are documented here. The excluded FEPs are listed in Table 4-2 with the sources for the technical information for their exclusion. Table 6-2 contains additional sources for corroborating models and information used to develop this report.

For cladding FEPs that are excluded from the TSPA, the screening arguments are based on low probability of occurrence or low consequence, in accordance with the criteria identified in Section 4.1.3. As appropriate, screening arguments cite work done outside this activity, such as in other scientific analyses.

In a few cases, a low-consequence argument, but based on probability, has been invoked. This is acceptable if a FEP can be defined in terms of its potential to affect the behavior (or response) of the disposal system (consequence), rather than solely in terms of the probability of the independent phenomenon. To evaluate this aspect one defines a threshold value at which a FEP has the potential to affect repository performance, and then defines the probability of the threshold being violated. This use of probability to support a low-consequence argument is particularly germane to FEPs involving potential breaching of containers. An example of this approach is FEP 2.1.02.16.0A, Localized (pitting) corrosion of cladding. The FEP is defined in terms of the consequence to the cladding from localized corrosion. The probability of localized

corrosion was determined to be low but could not be quantified for the purpose of comparison with the low probability criterion. However, it could be determined that the associated consequence would not be significant. In other words, under the range of expected repository conditions, the threshold value for localized corrosion (i.e., the value above which significant damage and resulting effects on behavior would occur) is not achieved. Therefore, localized (pitting) corrosion of cladding can be excluded based on low consequence, because it is not expected to occur at a magnitude sufficient to cause a significant effect on behavior.

For FEPs that are included in the TSPA, the TSPA Disposition section of each FEP discussion includes a short summary of how the FEP has been incorporated in the TSPA models. Details of the scientific analysis that describes the disposition are presented in *Clad Degradation – Summary and Abstraction for LA* (BSC 2003a [DIRS 162153]).

The output of this analysis (TSPA-LA dispositions for included FEPs and screening arguments for excluded FEPs) is intended to be used to support the project-specific FEP database and to promote traceability and transparency regarding FEP screening.

Table 6-1. LA FEP List for Cladding

Section	FEP Number	FEP Name	Screening Decision	Description
6.1	2.1.02.11.0A	Degradation of cladding from waterlogged rods	Excluded	Failed fuel rods (attributed to breaches caused by manufacturing defects and reactor operations) comprise a small fraction of the fuel rods that are currently being stored in commercial reactor spent fuel pools. Failed fuel contains water in the fuel rod void space that may promote degradation of the spent fuel cladding. Such fuel is referred to as "waterlogged." The moisture remaining in a "dried" fuel rod is used to determine the extent of degradation of spent fuel cladding.
6.2	2.1.02.12.0A	Degradation of cladding prior to disposal	Included	Certain aspects of cladding degradation occur before the spent fuel arrives at Yucca Mountain. Possible mechanisms include rod cladding degradation during reactor operation, degradation during wet spent fuel pool storage, degradation during dry storage, and rod degradation during shipping (from creep and from vibration and impact) and fuel handling.
6.3	2.1.02.13.0A	General corrosion of cladding	Exclude	General corrosion of cladding could expose large areas of fuel and produce hydrides.
6.4	2.1.02.14.0A	Microbially influenced corrosion (MIC) of cladding	Excluded	Microbially Influenced Corrosion (MIC) of cladding potentially may be a local cladding corrosion mechanism where microbes produce a local acidic environment that could produce multiple penetrations through the fuel cladding.
6.5	2.1.02.15.0A	Localized (radiolysis enhanced) corrosion of cladding	Excluded	Radiolysis in a nitrogen/oxygen gas mixture with the presence of water film results in the formation of nitric acid (HNO <sub>3</sub> ). Hydrogen peroxide (H <sub>2</sub> O <sub>2</sub> ) is formed in the water from radiolysis. These chemicals can enhance corrosion of the fuel cladding.
6.6	2.1.02.16.0A	Localized (pitting) corrosion of cladding	Exclude	Localized corrosion in pits could produce penetrations of cladding.
6.7	2.1.02.17.0A	Localized (crevice) corrosion of cladding	Excluded	Localized corrosion in crevices could produce penetrations of cladding.
6.8	2.1.02.18.0A	Enhanced corrosion of cladding from dissolved silica	Excluded	It must be determined if the high dissolved silica content of waters enhances corrosion of cladding.
6.9	2.1.02.19.0A	Creep rupture of cladding	Excluded	At high temperatures (>400°C) for sufficiently long time intervals, creep rupture of Zircaloy cladding on spent fuel can occur and produce small perforations in the cladding to relieve stress. After the waste package fails, the fuel can react with water and radioisotopes can thereby escape over time from the fuel rod.
6.10	2.1.02.20.0A	Internal pressurization of cladding	Excluded	Increased pressure within the fuel rod due to the production of helium gas could contribute to cladding failure.
6.11	2.1.02.21.0A	Stress corrosion cracking (SCC) of cladding	Excluded	Stress corrosion cracking mechanisms can contribute to cladding failure. These mechanisms can operate both from the inside out from the action of fission products, or from the outside in from the actions of salts or other chemicals within the waste package.

Table 6-1. LA FEP List for Cladding (Continued)

Section	FEP Number	FEP Name	Screening Decision	Description
6.12	2.1.02.22.0A	Hydride cracking of cladding	Excluded	Cladding contains hydrogen after reactor operation. The cladding might also pick up more hydrogen from cladding general corrosion (wet oxidation) after the waste package is breached. The hydrogen can exist both as zirconium hydride precipitates and as hydrogen in solid solution with zirconium. Hydrides might also form from UO <sub>2</sub> oxidation (after waste package and cladding perforation). In addition, hydrides may dissolve in warmer areas of the cladding and migrate to cooler areas. Hydrogen can also move from places of low stress to places of high stresses, causing hydride reorientation or delayed hydride cracking (DHC). The buildup of hydrides can cause existing cracks to propagate by DHC or hydride embrittlement.
6.13	2.1.02.23.0A	Cladding unzipping	Included	In either dry or wet oxidizing conditions and with perforated fuel cladding, the UO <sub>2</sub> fuel can oxidize. The volume increase of the fuel as it oxidizes can create stresses in the cladding that may cause gross rupture of the fuel cladding (unzipping).
6.14	2.1.02.24.0A	Mechanical impact on cladding	Exclude	Mechanical failure of cladding may result from external stresses such as rockfall or impact from waste package internals. Seismic induced impacts are addressed in a separate FEP.
6.15	2.1.02.25.0B	Naval SNF cladding	Included	DSNF to be disposed of in Yucca Mountain has a variety of fuel types that may not be similar to the CSNF to be disposed. Some of the fuel types may have initial cladding-degradation characteristics that are different from those for the CSNF. Therefore, the effectiveness of DSNF cladding as a barrier to radionuclide mobilization might be different from CSNF. This FEP addresses Naval SNF cladding only.
6.16	2.1.02.26.0A	Diffusion-controlled cavity growth (DCCG) in cladding	Excluded	Diffusion-Controlled Cavity Growth (DCCG) was once thought to be a possible creep rupture mechanism that could occur under the temperature and pressure conditions that prevailed during dry storage of spent fuel and might occur during disposal.
6.17	2.1.02.27.0A	Localized (fluoride enhanced) corrosion of cladding	Excluded	Fluoride is present in Yucca Mountain groundwater, and zirconium has been observed to corrode in environments containing fluoride. Therefore, fluoride corrosion of cladding may occur in waste packages.
6.18	2.1.07.01.0A	Rockfall	Excluded	Rockfalls may occur with blocks that are large enough to mechanically tear or rupture drip shields and/or waste packages. Seismic induced rockfall is addressed in a separate FEP.
6.19	2.1.09.03.0A	Volume increase of corrosion products impacts cladding	Included	Corrosion products have a higher molar volume than the intact, uncorroded material. Increases in volume during waste form and cladding corrosion could change the stress state in the material being corroded and lead to cladding unzipping.
6.20	2.1.09.09.0A	Electrochemical effects in EBS	Excluded	Electrochemical effects may establish an electric potential within the drift or between materials in the drift and more distant metallic materials. Migration of ions within such an electric field could affect corrosion of metals in the EBS and waste, and could also have a direct effect on the transport of radionuclides as charged ions.

Table 6-1. LA FEP List for Cladding (Continued)

Section	FEP Number	FEP Name	Screening Decision	Description
6.21	2.1.09.11.0A	Chemical effects of waste-rock contact	Excluded	Waste (CSNF, DSNF, and HLW) and rock are placed in contact by mechanical failure of the drip shields and/or waste packages. Chemical effects on the waste (e.g., dissolution) of waste may be enhanced or altered in a system where waste, rock minerals, and water are all in physical contact, relative to a system where only waste and water are in physical contact.
6.22	2.1.11.05.0A	Thermal expansion/stress of in-package EBS components	Excluded	Thermally induced stresses could alter the performance of the waste or EBS. For example, thermal stresses could cause the waste form to develop cracks and create pathways for preferential fluid flow and, thereby, accelerate degradation of the waste.
6.23	2.1.12.02.0A	Gas generation (He) from waste form decay	Excluded	Helium (He) gas production may occur by alpha decay in the waste. Helium production might cause local pressure buildup in cracks in the fuel and in the void between fuel and cladding, leading to cladding and waste-package failure.
6.24	2.1.12.03.0A	Gas generation (H <sub>2</sub> ) from waste package corrosion	Excluded	Gas generation can affect the mechanical behavior of the host rock and engineered barriers, chemical conditions, and fluid flow, and, as a result, the transport of radionuclides. Gas generation due to oxid corrosion of waste containers, cladding, and/or structural materials will occur at early times following closure of the repository. Anoxic corrosion may follow the oxid phase if all oxygen is depleted. The formation of a gas phase around the waste package may exclude oxygen from the iron, thus inhibiting further corrosion.

Appendix A of this report contains tables of mean and maximum temperatures expected for the cladding, which are needed to evaluate some of the FEPs. For FEPs included in the TSPA-LA, alternative conceptual models are discussed in the specific report for the included FEP (BSC 2003a [DIRS 162153]). For excluded FEPs, the discussions of alternative conceptual models, where appropriate, are included in this report. The output of this analysis (TSPA-LA dispositions for included FEPs and screening arguments for excluded FEPs) is intended to be used to support the project-specific FEP database and to promote traceability and transparency regarding FEP screening.

Table 6-2. Corroborating Models and Information Used to Develop This Report

Source	Information
Baker 1992 [DIRS 149104]	Solubility of oxygen in zirconium
Bradley, et al. 1981 [DIRS 101564]	Zircaloy-clad fuel rods before and after in-water spent fuel pool storage
Brossia et al. 2002 [DIRS 161988], Figure 3	Pitting experiments
Chan 1996 [DIRS 111876]	Hydride reorientation
Clayton 1984 [DIRS 131741]	Experiments with Zircaloy-4 fasteners
Coleman 1982 [DIRS 111999]	Hydride reorientation
Cox 1973 [DIRS 152920]	SCC and surface passivity
Cox 1990 [DIRS 152778]	Threshold Intensity Factors
Debes 1999 [DIRS 161193]	Fuel not damaged in transportation
Dieter 1961 [DIRS 147973]	Cladding degradation discussion
DOE 1996 [DIRS 100320]	Fuel assembly description
Einzigler and Kohli 1984 [DIRS 101605]	Creep rupture studies
Einzigler 1994 [DIRS 100442]	Oxidation of UO <sub>2</sub> is slower in steam than in air
Einzigler et al. 1982 [DIRS 101604]	Accelerated high temperature tests
Garde 1986 [DIRS 101651]	Fuel/Zirconium reaction, pressures
Garde 1989 [DIRS 113614]	hydride reorientation
Garde 1991 [DIRS 101652]	Fuel Temperatures
Garzarolli et al. 1979 [DIRS 149256]	Oxygen effects on corrosion of zirconium alloys and gas effects
Huang 1995 [DIRS 101683]	Threshold stress intensity properties
Jangg et al. 1978 [DIRS 110544], Tables 1, 6	Pitting experiments
Knoll and Gilbert 1987 [DIRS 123682]	Cask-drying
Kohli and Pasupathi 1986 [DIRS 131519]	Water-logged spent fuel storage rods
Little and Wagner 1996 [DIRS 131533]	Microbially influenced corrosion
Maguire (1984, Table 6)[DIRS 101717]	Pitting experiments
Mahmood et al. 2000 [DIRS 152241]	Delayed hydride cracking unlikely at temperatures above 260°C
Manaktala 1993 [DIRS 101719]	Pin degradation during reactor operation
Mardon et al. 1997 [DIRS 109213]	Figure of hydride concentration vs. burnup
McMinn et al. 2000 [DIRS 112149]	Precipitation and dissolution solubilities of hydrogen
McNeil and Odom 1994 [DIRS 131537]	Sulfate-reducing bacteria do not affect zirconium alloys
Peehs and Fleisch 1986 [DIRS 102065]	Water-logged spent fuel storage rods
Pescatore and Cowgill 1994 [DIRS 102066]	Comparison of creep models for Zircaloy

Table 6-2. Corroborating Models and Information Used to Develop This Report (Continued)

Source	Information
Pescatore et al.1990 [DIRS 101230]	Survey of all cladding failure modes, SSCs, creep, DHC, and others
Puls 1988 [DIRS 102067]	Series of strain tests on Zircaloy-2
Reed-Hill 1973 [DIRS 121838]	Stress intensity at crack tip
Riley and Covino 1982 [DIRS 161993], p. 11	Pitting experiments
Rothman 1984 [DIRS 100417]	General corrosion, helium pressure, and DHC
Seibold et al. 2001 [DIRS 164458]	Corrosion rates of alloys
Shi and Puls 1994 [DIRS 102084]	Threshold stress intensity factor
Simpson and Chow 1987 [DIRS 164483]	Hydride reorientation
Smith 1966 [DIRS 149107]	Hydrides, hydrogen absorption and oxygen dissolution in zirconium alloys
Soderman and Jonsson 1996 [DIRS 149441]	electrophoresis or electro-osmosis
Štefanić and LaVerne 2002 [DIRS 166303]	Half life of hydrogen peroxide
Tasooji et al. 1984 [DIRS 102093]	Iodine-induced SSC was not a major failure mechanism
Wallace et al. 1989 [DIRS 112344]	Hydride reorientation
Wolery and Daveler 1992 [DIRS 100097]	Description of EQ6
Yau 1983 [DIRS 149233]	General Corrosion, pitting
Yau 1984 [DIRS 102050]	General, crevice and SCC tests with zirconium alloys
Yau and Maguire, M. 1990 [DIRS 110761]	Fluorides and pitting

## 6.1 DEGRADATION OF CLADDING FROM WATERLOGGED RODS

### FEP Number:

2.1.02.11.0A

### YMP FEP Description:

Failed fuel rods (attributed to breaches caused by manufacturing defects and reactor operations) comprise a small fraction of the fuel rods that are currently being stored in commercial reactor spent fuel pools. Failed fuel contains water in the fuel rod void space that may promote degradation of the spent fuel cladding. Such fuel is referred to as “waterlogged.” The moisture remaining in a “dried” fuel rod is used to determine the extent of degradation of spent fuel cladding.

### Descriptor Phrases:

Residual moisture from storage enhances degradation of cladding

### Screening Decision:

Excluded – Low Consequence

### TSPA-LA Disposition:

NA

**Related FEPs:**

- 2.1.02.12.0A, Degradation of cladding prior to disposal
- 2.1.12.03.0A, Gas generation (H<sub>2</sub>) from waste package corrosion

**Screening Argument:** Degradation of cladding and waste form from waterlogged rods is excluded from the TSPA-LA because of low consequence.

Waterlogged rods are already failed, and further cladding failures of intact rods and waste form degradation are not expected because of the small amount of water present. Few rods are breached at the time they are received at the repository (FEP 2.1.02.12.0A; BSC 2003a [DIRS 162153], Section 6.2.1). The supply of water that remains in the fuel after cask drying will not be sufficient to oxidize the fuel to an unacceptable level (NRC 1997 [DIRS 101903], Section 8.V.1; Knoll and Gilbert 1986 [DIRS 123682], p. iii). Moisture is effectively removed from defective rods during the cask drying operations. The residual moisture of the cask atmosphere can be estimated based on the drying conditions where the cask or waste package is vacuum dried at 5 mbars (maximum water vapor pressure, equivalent to 7.7 g or 0.43 moles of water). The consequence of a small amount of remaining moisture on the waste form, waste package, and cladding is negligible.

The fraction of fuel rods with breached cladding is currently estimated to be 0.01 to 1 percent (FEP 2.1.02.12.0A; BSC 2003a [DIRS 162153], Section 6.2.1), or about 5.6 rods in an average pressurized water reactor waste package.

Since cask drying operations will remove most of the water from the fuel rods, it is reasonable to expect that the supply of water that remains in the fuel after cask drying will not be sufficient to oxidize the fuel. *Standard Review Plan for Dry Cask Storage Systems* (NRC 1997 [DIRS 101903], Section 8.V.1) describes the cask drying criteria with reference to Knoll and Gilbert 1987 [DIRS 123682]. Less than 0.43 mole (7.7 g) of H<sub>2</sub>O is expected to be present in a 7-m<sup>3</sup> cask after drying. This amount of water produces an insignificant potential for corrosion of the cladding during dry storage or during disposal (CRWMS M&O 1995 [DIRS 102829], p. 16).

A PWR waste package contains approximately 2,500 kg ( $3.4 \times 10^5$  moles) of zirconium alloys (CRWMS M&O 2000 [DIRS 151659], Table 2). Less than 0.43 mole (7.7 g) of H<sub>2</sub>O is expected to be present (Knoll and Gilbert 1987 [DIRS 123682]) and general corrosion of the zirconium alloys from the water would only degrade a small fraction (0.2 mole). Hydrogen uptake would be insignificant compared to existing hydrides on the cladding.

Kohli and Pasupathi (1986 [DIRS 131519], p. iii) discuss removal of water from waterlogged fuel rods. Two reactor-breached fuel rods were tested, along with two fuel rods that were intentionally defected after irradiation. A predetermined amount of moisture was added to the intentionally defected rods to enable the extent of the moisture released during the drying to be determined. The rods were dried in flowing argon at atmospheric pressure while being heated in a furnace. The center 1.8 m of the furnace was heated to 400°C; the remainder was heated to 200°C. The reactor operations breached rods were dried in the as-received condition, then a hole was drilled in the cladding, water was injected, and the experiment was repeated. In the reactor breached rods, the bulk of the uncombined water was removed in 1 to 1.3 hours and all

measurable releases ended after 3.7 hours. This set of experiments demonstrated that standard cask drying procedures would remove water from failed rods.

Peehs and Fleisch (1986 [DIRS 102065], pp. 199 to 202) described the behavior of waterlogged PWR fuel rods on heating at 400°C in a hot cell. The bulk of the water was released during the cask drying operation. Testing results showed that the moisture can be removed from defective rods during the cask drying operations and the residual moisture of the cask atmosphere can be minimized.

An alternative conceptual model for waterlogged rods would be that the failed rods contain water, which is then released into the waste package to be consumed by the carbon steel rack inside the waste package. This alternative conceptual model is possible because of the rate at which carbon steel racks react with water vapor to form rust is faster than that for zirconium and UO<sub>2</sub>. The hydrogen that is produced tends not to be absorbed by the zirconium alloys (FEP 2.1.12.03.0A). It would lead to no significant damage because of the limited amount of water and large volume of steel in a waste package.

In conclusion, cladding and waste form degradation from waterlogged fuel rods is excluded from TSPA-LA. There are few failed rods in any waste package that could be waterlogged and the volume of water inside a rod is quite limited. Because the drying procedure is effective, the quantity of water is limited could only affect a small amount of fuel. Cladding failure due to rod waterlogging has a low consequence, and is excluded from further consideration. The magnitude and time of the resulting radiological exposures to the reasonably maximally exposed individual, or radionuclide releases to the accessible environment, would not be significantly changed by the omission of this FEP (degradation from waterlogged rods) from the performance assessment (TSPA-LA) model.

## **6.2 DEGRADATION OF CLADDING PRIOR TO DISPOSAL**

### **FEP Number:**

2.1.02.12.0A

### **YMP FEP Description:**

Certain aspects of cladding degradation occur before the spent fuel arrives at Yucca Mountain. Possible mechanisms include rod cladding degradation during reactor operation, degradation during wet spent fuel pool storage, degradation during dry storage, and rod degradation during shipping (from creep and from vibration and impact) and fuel handling.

### **Descriptor Phrases:**

Degradation of cladding during dry storage  
Degradation of cladding during reactor operation  
Degradation of cladding during shipment and handling  
Degradation of cladding during wet (pool) storage

### **Screening Decision:**

Included

**TSPA-LA Disposition:** Degradation of cladding prior to disposal is included in TSPA-LA cladding degradation abstraction. The failure rate from prior degradation is based on historical data on reactor operation. It also includes failure from wet pool storage and transportation (negligible), dry storage, and handling (including spent pool events). In the TSPA, this percentage of rods is available for radionuclide release through fast release and axial splitting when the waste package fails. It is specified as a 0.01 to 1 percent log uniform distribution (0.1 percent median). The TSPA abstraction models that all stainless steel cladding has failed and places the stainless steel cladding into waste packages as it arrives at the repository. This results in 3.5 to 7 percent (uniform distribution) of the waste packages containing stainless-steel-clad fuel rods. These waste packages contain 15 to 30 percent stainless-steel-clad fuel rods that are failed and available for fast release and unzipping upon waste package failure. In the TSPA-LA, waste packages containing stainless-steel-clad fuel rods are considered a different fuel type group with a high initial cladding failure percent. The scientific analysis that describes the disposition in greater detail is presented in *Clad Degradation – Summary and Abstraction for LA* (BSC 2003a [DIRS 162153]).

**Related FEPs:**

- 2.1.02.11.0A, Degradation of cladding from waterlogged rods
- 2.1.02.19.0A, Creep rupture of cladding

### 6.3 GENERAL CORROSION OF CLADDING

**FEP Number:**

- 2.1.02.13.0A

**YMP FEP Description:**

General corrosion of cladding could expose large areas of fuel and produce hydrides.

**Descriptor Phrases:**

- Dry oxidation of cladding
- General (uniform) corrosion of cladding
- Thermal effects on corrosion of cladding
- Wet oxidation (aqueous corrosion) of cladding
- Zirconium oxidation of cladding

**Screening Decision:**

Excluded – Low Consequence

**TSPA-LA Disposition:**

NA

**Related FEPs:**

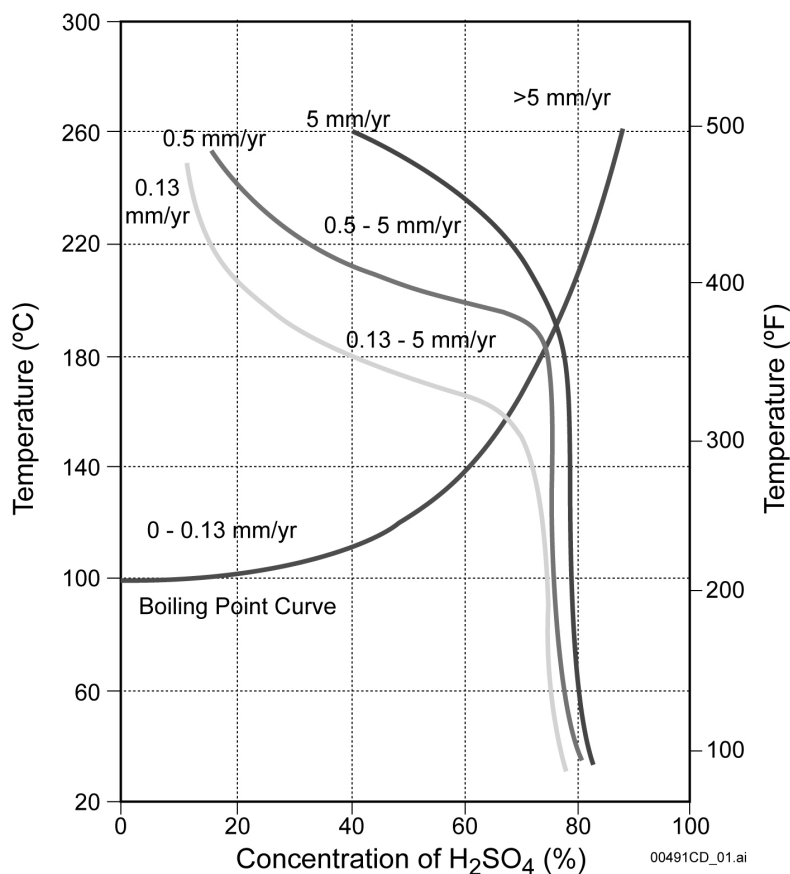
- 2.1.02.15.0A, Localized (radiolysis enhanced) corrosion of cladding
- 2.1.02.16.0A, Localized (pitting) corrosion of cladding
- 2.1.02.17.0A, Localized (crevice) corrosion of cladding
- 2.1.02.22.0A, Hydride cracking of cladding

**Screening Argument:** General corrosion of cladding has been excluded from the TSPA-LA on the basis of low consequence.

The in-package chemistry model predicts that in most cases the pH remains above 3.5. When uncertainties are added, minimum pHs in the range of 2.5 to 3 are possible. These low pHs are caused by sulfur in the carbon steel rack being released and forming sulfuric acid ( $\text{H}_2\text{SO}_4$ ). This period of low pH lasts for the time period when the carbon steel is corroding (see Figure 6.5-1 for pH profile). Yau and Webster (1987 [DIR 100494], pp. 709 – 710, Figs. 5, 7, and Table 6) review the corrosion potential for zirconium alloys in sulfuric acid. They note that zirconium alloys resist attack from  $\text{H}_2\text{SO}_4$  at all concentrations up to 70 percent and at temperatures to boiling (their Figure 5, reproduced in this report as Figure 6.3-1). A concentration of 70 percent  $\text{H}_2\text{SO}_4$  represents a theoretical pH of about  $-1.15$ , well below anything expected in the waste package. In the range that zirconium alloys show corrosion resistance in  $\text{H}_2\text{SO}_4$ , a protective film is formed on the zirconium that is predominantly cubic zirconium oxide ( $\text{ZrO}_2$ ) with only traces of monoclinic phases. At higher concentrations than 70 percent, zirconium corrodes because loose films form that are zirconium disulfate tetrahydrate and partially zirconium hydrides. In concentrations of less than 65 percent  $\text{H}_2\text{SO}_4$ , zirconium can tolerate some amounts of strong oxidizing agents such as 200 ppm  $\text{Fe}^{3+}$  and 200 ppm  $\text{NO}_3^-$  (Yau and Webster (1987 [DIR 100494], Fig. 7). Moreover, in 20 percent or less  $\text{H}_2\text{SO}_4$  ( $\text{pH} > -0.61$ ), zirconium can tolerate a great amount of strong oxidizing agents. Consequently, zirconium equipment is often used in steel pickling. Zirconium alloys are used in the chemical industry under low pH conditions. In the manufacturing of  $\text{H}_2\text{O}_2$ , zirconium alloys are used to contain up to 65 percent  $\text{H}_2\text{SO}_4$  at up to  $150^\circ\text{C}$ . In the manufacturing of  $\text{HNO}_3$  zirconium alloys are used to contain the acid up to 65 percent concentrations and temperatures to  $204^\circ\text{C}$ . A pH of 1.5 (minimum in waste package with uncertainties) represents only 0.15 weight percent of  $\text{H}_2\text{SO}_4$  and is not expected to cause accelerated corrosion.

At low pHs (below  $-0.6$ ), the  $\text{ZrO}_2$  film will start to slowly dissolve. This is shown in Figure 6-2 of *Pitting Model for Zirconium-Alloyed Cladding at YMP* (BSC 2003g [DIRS 164667]), where there is discontinuity in the corrosion potential at about  $\text{pH} = -0.6$ ; below this pH, the corrosion potential starts to rapidly decrease. This change in behavior is attributed to dissolution of the general oxide surface. Since the in-package chemistry model predicts pHs above  $-0.6$ , accelerated general corrosion is excluded from TSPA-LA performance models. The Pourbaix diagram for zirconium (Pourbaix 1974 [DIRS 100817], p. 226) shows that  $\text{ZrO}_2$  could start to dissolve at a pH of 4. In the text describing the diagram, the author (Pourbaix 1974 [DIRS 100817], pp. 228, 229) recognizes that the solubility is much too high ( $1.2 \times 10^{-3}$  moles/liter) and not consistent with experimental observations of solubility ( $10^{-7}$  moles/liter). He attributes these high solubilities to not having modeled the dominant form of oxide (such as cubic  $\text{ZrO}_2$ ), which controls the dissolution.

General corrosion is synonymous with zirconium oxidation for this repository application. The outer surface of the cladding becomes oxidized with a  $\text{ZrO}_2$  film, which adheres to the surface and slows down further oxidation (IAEA 1998 [DIRS 150560], Section 4.2.4). The oxidation could be from  $\text{O}_2$  consumption (dry oxidation) or  $\text{H}_2\text{O}$  consumption (wet oxidation). For the fuel in the repository, this corrosion does not occur until the waste package is penetrated.



Source: Yau and Webster, 1987 [DIR 100494], Figure 5

Figure 6.3-1. The Iso-Corrosion Diagram for Zirconium in Sulfuric Acid ( $H_2SO_4$ )

There are three possible effects of surface oxidation:

1. The oxidation could thin the cladding, contributing to cladding failure by creep rupture (see FEP 2.1.02.19.0A). Wet oxidation generates hydrogen, and some of the hydrogen is absorbed into the cladding to form hydrides.
2. This hydrogen pick up could lead to delayed hydride cracking (DHC), or general hydride embrittlement (see FEP 2.1.02.22.0A).
3. In the extreme, the oxidation could lead to cladding failure and expose the fuel pellets to the waste package environment.

The in-package chemistry model predicts that in most cases the pH remains above 3.5. Under these nominal chemical conditions (pH is greater than 3.5) in the repository, general corrosion failures of the cladding are unlikely. *Waterside Corrosion of Zirconium Alloys in Nuclear Power Plants* (IAEA 1998 [DIRS 150560]) summarizes much of the research on zirconium corrosion. Hillner et al. (1998, p. 9) [DIRS 100455] studied corrosion of Zircaloy and published a Zircaloy corrosion correlation based on Bettis Atomic Power Laboratory experiments. Bettis developed Zircaloy for naval reactors in the early 1950s and has an extensive database on Zircaloy performance, including continuous autoclave corrosion tests on some samples for 30 years.

Some samples have developed oxide thickness as great as 110  $\mu\text{m}$ , greater than those expected during repository corrosion based on Hillner et al. calculations. The experiments are consistent with diffusion of oxygen ions through the corrosion film being the rate-limiting phenomenon. This corrosion film is generated in layers, with the physical characteristics of lower layer staying consistent (uniform). The consistency of the lower 2  $\mu\text{m}$  of oxide film leads to a steady corrosion rate after a transition period. The recommended post-transition rate equation is:

$$\Delta Th = 1.72 \times 10^9 \times \exp(-11452/T) \quad (\text{Eq. 6.3-1})$$

where

$$\begin{aligned} \Delta Th &= \text{oxide growth rate, } \mu\text{m/yr} \\ T &= \text{temperature, K} \end{aligned}$$

This corrosion rate equation is similar to the equations developed by others, but predicts a slightly higher corrosion rate. This rate for unirradiated metal, from Equation 7 of Hillner et al. (1998 [DIRS 100455]), is doubled to represent the effect of irradiation (Hillner et al. 1998 [DIRS 100455], pp. 6, 9). The correlation is converted to micrometers per year ( $1\mu\text{m} = 14.7 \text{ mg/dm}^2$ ) (IAEA 1998 [DIRS 150560], p. 178). The pretransition rate is slower than the posttransition rate. The effect of irradiation conditioning before corrosion is to accelerate the corrosion rate for a few micrometers. To be conservative, Hillner et al. (1998 [DIRS 100455]) doubled the corrosion rate for the full thickness of the metal. The correlation shows a strong Arrhenius temperature relationship with the corrosion rate becoming small below 200°C. The Arrhenius temperature relationship is consistent with the low temperature data from Hillner et al. (1998 [DIRS 100455]). Corrosion tests at 270°C for 8.2 years have produced approximately 4  $\mu\text{m}$  of oxide, while corrosion tests at 360°C have produced films 88  $\mu\text{m}$  thick in 7.8 years (Hillner et al. 1998 [DIRS 100455], p. 25). Using this equation, one predicts an oxide thickness of only 0.22  $\mu\text{m}$  at a long term repository temperature of 40°C for a million years. At 80°C, in one million years, the loss would be 14  $\mu\text{m}$ , a small fraction of the cladding thickness (570  $\mu\text{m}$  for a Westinghouse 17×17 design). Hillner et al. also address other corrosion mechanisms, such as the instability of second-phase particles (or intermetallics), and identify no corrosion mechanism that is expected to fail the cladding.

If the waste package fails at repository closure, the cladding will be exposed to the high temperature profiles shown in Figures A-4, A-5, and A-6 in the presence of oxygen. At these elevated temperatures some oxidation of the cladding will occur. The amount of oxide film from general cladding corrosion has been calculated with failure at closure and extending the calculation out to the end of the regulatory period (10,000 years). The amount of cladding that is consumed is approximately 57 percent of the oxide thickness (Eq. 6.3-1), a portion due to the volume increase associated with Zircaloy oxidation. The cladding oxidation calculation was done for the design basis (hot) rod in the hottest waste package, average rod in average waste package and average rod in a cool waste package. Three rod locations were considered: the center rod (hottest), an interior rod at a radius of 60 percent of the outer fuel radius, and the outer rod. Table 6.3-1 provides the cladding thickness for the nine rods considered. The hottest rod loses less than 10 percent of its wall thickness and is not expected to fail. All other rods have very little thinning (approximately 2 percent or less). If the waste package fails after the thermal peak (after 100 years; see Figures A-4, A-5, and A-6), little or no corrosion occurs.

Table 6.3-1. Percent of Cladding Remaining in Waste Packages that Fail at Closure

	Center Rod (%)	Rod, 60% R <sub>OD</sub> %	Outer Rod (%)
Hot Waste Package, Hottest Fuel Loading	90.41	97.98	99.14
Mean Waste Package, Uniform Fuel Loading	98.42	99.08	99.68
Cool Waste Package, Uniform Fuel Loading	99.59	99.78	99.93

Hillner et al. (1998 [DIRS 100455], Figure 5) compare the weight gain of the samples in water, which correlates to the corrosion rate in water (the correlation used here) with that of steam. The steam corrosion rate is about 30 to 40 percent slower. A humid-air environment is expected to last for 470 to 3,500 years (Table A-4). Einziger (1994 [DIRS 100442], p. 556, Equation 14) states that dry oxidation of zirconium is slightly slower than the wet corrosion rate.

There are experimental corroborating observations about the slow corrosion rates of zirconium alloys near ambient temperature (27°C). Bradley et al. (1981 [DIRS 101564], p. 38) performed metallurgical examinations of Zircaloy-clad fuel rods from two assemblies (0551 and 0074) of the Shippingport PWR Core 1 “blanket” fuel after extended in-water spent fuel pool storage (21 years for 0551, and 16 years for 0074). The oxide film thickness on the Shippingport fuel rods after reactor operation was reported to be an average cladding oxide film thickness of 1.8 μm (0551) and 2.4 μm (0074). After extended in-water spent fuel pool storage, the average cladding oxide film thickness was found to be 1.7 μm (0551) and 2.3 μm (0074) (Bradley et al. 1981 [DIRS 101564], p. 38). The slight disagreement in these values is attributed to differences in measurement technique and experimental error. These results led to the conclusion that no significant change in oxide thickness occurred even after 16 to 21 years of pool storage. This conclusion is further supported by the observation that Zircaloy tube sheets (that had been cut to remove assembly 0551 fuel rods in 1960) stored in water for over 20 years were unblemished and showed no evidence of reaction with water.

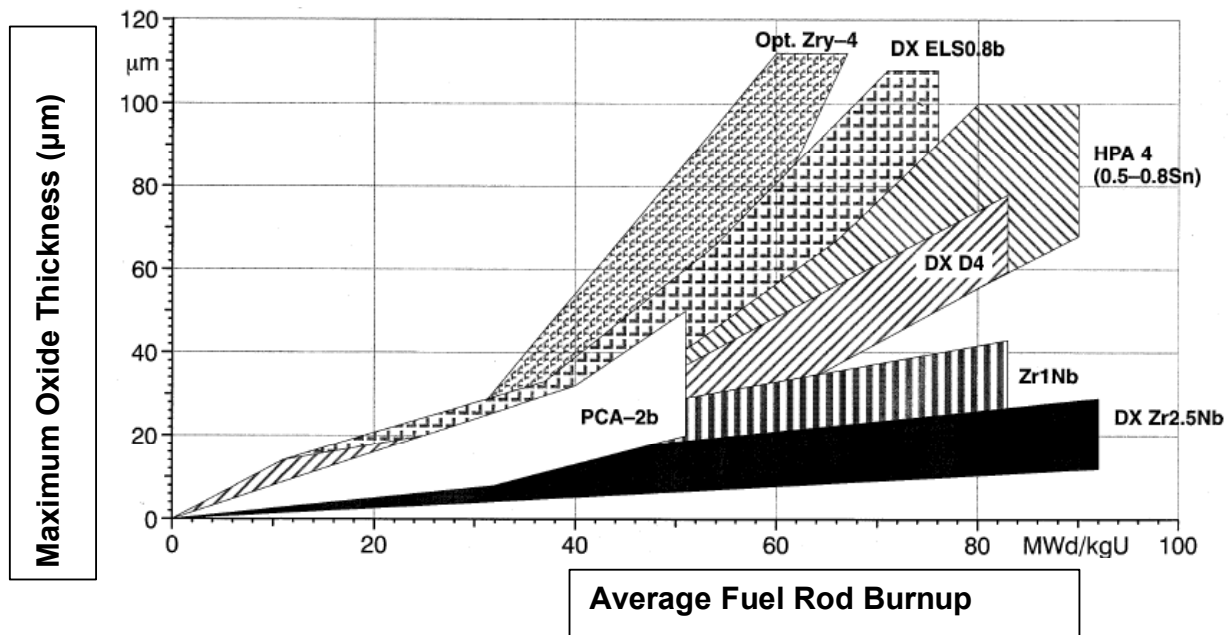
Rothman (1984 [DIRS 100417], pp. 6 to 13, Table 3) discusses cladding oxidation in repository conditions in great detail and compares the predicted cladding loss using six different oxidation correlations and predicts cladding thinning of 4 to 53 μm after 10,000 years at 180°C (a conservative temperature condition since the repository cools after a few hundred years) which would not lead to rod failure.

The cladding corrosion analyses (Hillner et al. 1998 [DIRS 100455], Rothman 1984 [DIRS 100417]) are based on the performance of Zircaloy-4 (Zirc-4), the cladding used in most PWRs before the year 2000. Today, most American PWRs use zirconium-niobium alloys for their reloads. Fuel supplied by Westinghouse (including some Combustion Engineering designs) is clad with ZIRLO (a 1 percent niobium alloy) and most fuel supplied by Framatome ANP uses M5™ (trademark of Framatome ANP, also 1 percent niobium). Seibold et al. (2001 [DIRS 164458], Figure 2, reproduced here as Figure 6.3-2) compare the oxidation rate of various cladding alloys as a function of burnup. In Figure 6.3-2, the HPA 4 alloys include ZIRLO and M5™ is represented in the group Zr-1Nb. Current NRC guidance requires fuel oxide thickness to be less than 100 μm at end of life. The figure shows that Zirc-4 is limited to fuel cycles less than about 54 MWd/kgU and that advanced alloys are required for higher burnups. ZIRLO has

an oxidation rate of about half that of Zirc-4. In PWR environments, M5™ has an oxidation rate of about one fifth that of Zirc-4. The hydride content of the cladding is directly proportional to the oxide thickness. At a given burnup, ZIRLO will have about half of the hydrides and M5™ will have one fifth of the hydrides as Zirc-4. Therefore, the new cladding is less likely to fail from general corrosion or hydride embrittlement (FEP 2.1.02.22.0A). The thinner oxide thickness produces lower fuel pellet temperatures and, thus, lowers fission gas release fractions. The remaining metal thickness is also greater. Therefore, cladding stresses are lower in advanced alloys and less creep is expected (FEP 2.1.02.19.0A).

As alternative conceptual models for general corrosion, Hillner et al. (1998 [DIRS 100455], Table 4) provides the expected corrosion for cladding after 10,000 years at 180°C using eight different corrosion equations developed by others. These alternative models show that Hillner’s equation is conservative and general corrosion is not expected to be significant in the repository.

In conclusion, cladding degradation from general corrosion is excluded from TSPA-LA. The small amount of corrosion that will occur during the regulatory period will not penetrate the cladding and therefore will not affect the release of radionuclides. Cladding failure due to general corrosion has a low consequence, and is excluded from further consideration. The magnitude and time of the resulting radiological exposures to the reasonably maximally exposed individual, or radionuclide releases to the accessible environment, would not be significantly changed by the omission of this FEP (general corrosion of cladding) from the performance assessment (TSPA-LA) model.



Source: Seibolt et al. 2001 [DIRS 164458], Figure 2

Figure 6.3-2. A Comparison of Oxide Thicknesses for Different Zirconium Alloys

## 6.4 MICROBIALLY INFLUENCED CORROSION (MIC) OF CLADDING

**FEP Number:**

2.1.02.14.0A

**YMP FEP Description:**

Microbially Influenced Corrosion (MIC) of cladding potentially may be a local cladding corrosion mechanism where microbes produce a local acidic environment that could produce multiple penetrations through the fuel cladding.

**Descriptor Phrases:**

Microbial induced pH change enhances localized corrosion of cladding  
Microbiologically influenced corrosion (MIC) of cladding

**Screening Decision:**

Excluded – Low Consequence

**TSPA-LA Disposition:**

NA

**Related FEPs:**

2.1.02.15.0A, Localized (radiolysis enhanced) corrosion of cladding  
2.1.02.16.0A, Localized (pitting) corrosion of cladding  
2.1.02.17.0A, Localized (crevice) corrosion of cladding

**Screening Argument:** Microbially influenced corrosion (MIC) activity is excluded as a cladding failure mechanism because of low consequence. Microbes are expected to be present in the repository, but MIC of cladding is not expected to cause cladding failure and, therefore, not have a significant effect on radionuclide exposures to the RMEI.

The term microbially influenced corrosion (MIC) is commonly used to designate corrosion caused by the presence and activities of microorganisms at the surfaces of metals.

Two studies of MIC on spent nuclear fuel have been performed. Wolfram et al. (1996 [DIRS 165268], pp. iii, iv) measured microbial activity in spent fuel pools. They concluded that all spent fuel pools tested contained microbial colonies. They also performed a literature search and concluded that “There was no evidence in the literature that zirconium or its alloys are susceptible to MIC.”

Hillner et al. (1998 [DIRS 100455], p. 11) studied the corrosion of Zircaloy-clad fuels under repository conditions. They indicate that there are two major forms of MIC for materials being considered for waste packages. They are (1) sulfide attack through the action of sulfate reducing bacteria (SRB) and (2) corrosion induced by organic acids secreted from certain bacteria. With respect to attack by SRB, Hillner et al. (1998 [DIRS 100455]) reference the work of McNeil and Odom (1994 [DIRS 131537], p. 176), which indicates by thermodynamic calculations that SRB do not affect zirconium alloys. With respect to corrosion induced by organic acids, Hillner et al. (1998 [DIRS 100455], p. 11) noted that it is most unlikely because of zirconium’s tolerance of a wide range of pHs and it is unlikely that production of weak organic acids will have an adverse

effect on the passivation of Zircaloy by a  $ZrO_2$  film. Yau and Webster (1987 [DIRS 100494], p. 717) also note that zirconium alloy resists a wide range of organic compounds, including acetic acid, acetic anhydride, formic acid, urea, ethylene dichloride, formaldehyde, citric acid, lactic acid, oxalic acid, tannic acid, and trichloroethylene. This supports the concept that organic solutions produced by MIC are unlikely to cause significant acceleration of the corrosion of zirconium alloys. *In-Drift Microbial Communities* (CRWMS M&O 2000b [DIRS 151561], p. 154) evaluated in-drift microbial communities and concluded that the estimates of microbial masses growing in the potential repository system suggest that the effect to the in-drift geochemistry should be small.

Little and Wagner (1996 [DIRS 131533], p. 367) corroborate this information in an overview of MIC of metals and alloys used in the storage of nuclear wastes. They indicate that MIC is a form of localized corrosion that results in pitting, selective leaching, crevice corrosion, under-deposit corrosion, and enhanced erosion and corrosion. Little and Wagner (1996 [DIRS 131533], pp. 367 and 368) describe several mechanisms for MIC. In addition, various case studies are presented that document MIC of alloys of iron, nickel, and copper. However, it should be noted that there is no indication in the literature of MIC occurring on zirconium metal or alloys. Yau and Webster (1987 [DIRS 100494], p. 709) report no corrosion of zirconium alloy from marine organisms was found during sea water corrosion tests for 129 days.

MIC is excluded as a component of the localized (pitting) corrosion model where MIC could cause a localized suppression of the water pH and permit other aggressive species to attack cladding. The zirconium alloy pitting model (BSC 2003g [DIRS 164667], Section 8) shows that pitting is dependent on the concentration of chlorides, ferric ions, and hydrogen peroxide (from radiolysis).

One U.S. commercial nuclear plant spent fuel pool experienced a significant MIC event that lasted for about four years (Ralph et al. 2002 [DIRS 161992]). After an extended lay-up period, the spent fuel pool water was found to contain a significant amount of algae and bacteria. Biological agents were purged using controlled additions of chlorine and hydrogen peroxide before the pool was returned to normal operating chemistries.

The assessment revealed that the steel rack corrosion products were up to 2.5 cm thick, and they had started to engulf the individual fuel rods or flow channels of the stored assemblies in the region where the rack and plates contacted the fuel assemblies. The corrosion product had adhered to the fuel. The iron oxide was composed of  $FeO$ ,  $Fe_2O_3$ , and  $Fe_3O_4$ . Ralph et al. (2002 [DIRS 161992], p. 6) states:

One fuel assembly was removed from its storage location and its channel was removed. The oxide from contact with the carbon steel rack was removed with a water lance utilizing 350 to 700  $kg/cm^2$  of water pressure. A camera with resolution of 0.025 mm was used to inspect the channel. The channel surface appeared uniform and smooth. No pitting, white discoloration or surface anomalies were observed.

The paper concluded: “The fuel cladding was not affected through any type of corrosion. Therefore, the corrosion did not change the classification of the fuel as intact or damaged.” As

with the experiments by Yau (1983 [DIRS 149233]), the lack of pitting or stress corrosion cracking implies that the corrosion potential ( $E_{cor}$ ) was not elevated to exceed  $E_{tp}$ , even with  $Fe_3O_4$  present and adhering to the zirconium oxide film. MIC colonies could also have locally suppressed the pH but, again, no localized corrosion was observed.

Adler Flitton et al. (2002 [DIRS 161991], p. 4) buried various metal samples in an arid vadose zone environment for three years. They reported indications of pitting from MIC on some of the metals, but observed no pitting on the zirconium alloy samples.

In summary, microbes are expected to be present in the repository, but MIC of cladding is not expected to cause cladding failure. The NRC requirements in 10 CFR 63.114 (e and f) allow the exclusion of MIC from the TSPA-LA because the omission would not significantly change the magnitude and time of the resulting radiological exposures to the reasonably maximally exposed individual (RMEI), or radionuclide releases to the accessible environment.

## **6.5 LOCALIZED (RADIOLYSIS ENHANCED) CORROSION OF CLADDING**

### **FEP Number:**

2.1.02.15.0A

### **YMP FEP Description:**

Radiolysis in a nitrogen/oxygen gas mixture with the presence of water film results in the formation of nitric acid ( $HNO_3$ ). Hydrogen peroxide ( $H_2O_2$ ) is formed in the water from radiolysis. These chemicals can enhance corrosion of the fuel cladding.

### **Descriptor Phrases:**

Localized corrosion of cladding enhanced by radiolysis induced pH change

### **Screening Decision:**

Excluded – Low Consequence

### **TSPA-LA Disposition:**

NA

### **Related FEPs:**

- 2.1.02.16.0A, Localized (pitting) corrosion of cladding
- 2.1.02.17.0A, Localized (crevice) corrosion of cladding
- 2.1.13.01.0A, Radiolysis

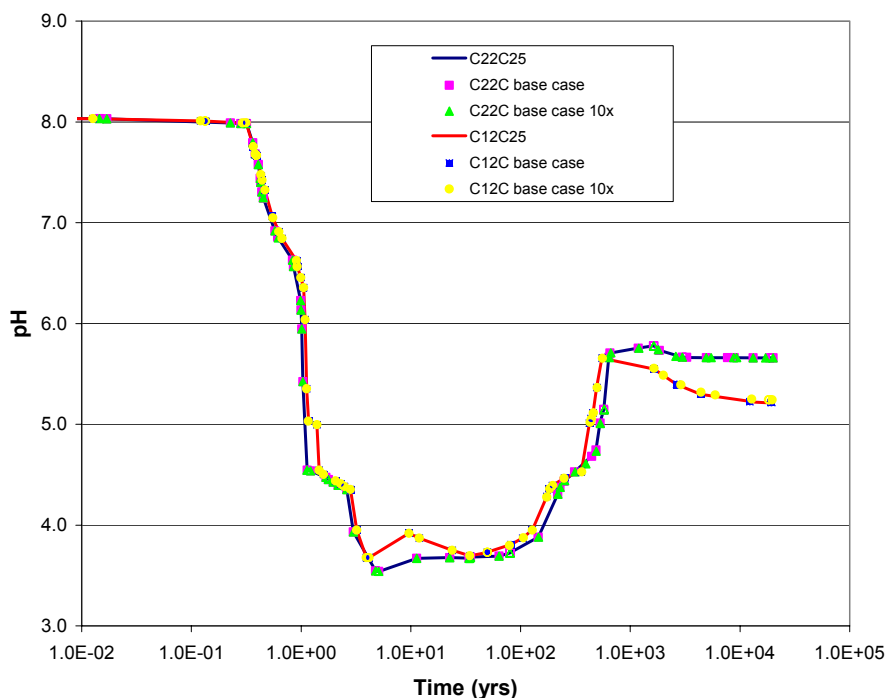
**Screening Argument:** Radiolysis, as a cladding failure mechanism, is excluded from the TSPA-LA on the basis of low consequence.

The in-package chemistry model (BSC 2003f [DIRS 161962], Attachment III) addressed the change of water chemistry with the inclusion of nitric acid and hydrogen peroxide production from radiolysis. In the analysis, all of the nitric acid that can be produced in a moist waste package was absorbed into the water film on the cladding surface. The radiation field was modeled as being constant at the dose at 500 years although it decreases with time.

The effect of radiolysis on the in-package chemistry was handled in a nonmechanistic manner (i.e., EQ6 does not have the facility to model the radiolysis process directly), therefore, only the products of radiolysis were included as inputs in EQ6 simulations. EQ6 is a reaction path code which models water, rock or other material interactions or fluid mixing in either a pure reaction progress mode or a time mode (Wolery and Daveler 1992 [DIRS 100097]). A series of runs was performed where nitric acid and hydrogen peroxide were included as inputs in EQ6 runs and the results of these simulations were compared to their non-radiolysis counterparts. Two base case runs (C12C25 and C22C25, BSC 2003f [DIRS 161962], Section 6.5.4) were used to test the effects of radiolysis. These runs were chosen because they represent the median fuel exposure value and the low and median water flux values. It would be expected that the effects of nitric acid and hydrogen peroxide additions would be greater at the low end of the flux range. Two simulations were performed for each file, the first using the base case nitric acid and hydrogen peroxide rates and the second multiplying the  $\text{HNO}_3$  and  $\text{H}_2\text{O}_2$  rates by a factor of ten.

The results of the simulations are displayed in Figure 6.5-1, where the pH profiles for the various runs are displayed versus time. These results show that neither the base case nor the 10× base case generation rates of  $\text{HNO}_3$  and  $\text{H}_2\text{O}_2$  had an impact on the in-package pH. Therefore, it may be concluded that if radiolysis only affects the chemistry via  $\text{HNO}_3$  and  $\text{H}_2\text{O}_2$  generation, then it will not be a significant process with regard to influencing the in-package chemistry. The radiolysis did not significantly affect the concentrations of  $\text{Cl}^-$ ,  $\text{Fe}^{3+}$ , or  $\text{H}_2\text{O}_2$  and therefore did not change the corrosion potential of the passive film on the zirconium alloy.

Table 6.5-1 provides the ferric iron, chloride, and hydrogen peroxide maximum concentrations for the simulations. Again, runs with  $\text{HNO}_3$  and  $\text{H}_2\text{O}_2$  input show little deviation compared to the runs without.



Source: BSC 2003f [DIRS 161962], Attachment III

Figure 6.5-1. pH Profiles Showing How the Radiolysis Inputs Affect the pH

Table 6.5-1. Chloride, Ferric Iron, and Hydrogen Peroxide Molality

EQ6 Input File	Maximum Molalities		
	Cl <sup>-</sup>	Fe <sup>+++</sup>	H <sub>2</sub> O <sub>2</sub> (aq)
C22C25	6.6E-04	8.8E-11	3.7E-19
C22CBC	6.6E-04	8.8E-11	3.7E-19
C22BC10x	6.5E-04	8.8E-11	3.7E-19
C12C25	9.7E-04	5.3E-11	3.7E-19
C12CBC	9.6E-04	5.3E-11	3.7E-19
C12BC10x	9.2E-04	5.4E-11	3.7E-19

Source: BSC 2003f [DIRS 161962]

The Center for Nuclear Waste Regulatory Analysis (CNWRA) performed a series of corrosion tests where hydrogen peroxide was added to the ongoing test while the corrosion potential was being measured. Greene et al. (2000 [DIRS 145073], Figure 8) shows two experiments where H<sub>2</sub>O<sub>2</sub> was added and the corrosion potential was measured. In one test, the H<sub>2</sub>O<sub>2</sub> was added two different times. In the three cases where H<sub>2</sub>O<sub>2</sub> was added, the effect of the hydrogen peroxide rapidly died out. In another test (Greene et al. 2000 [DIRS 145073], Figure 11), a sample that was oxidized in air at 200°C was exposed to a solution of 1M NaCl. When 5 mM H<sub>2</sub>O<sub>2</sub> was added, the corrosion potential increased by 0.275 V<sub>SCE</sub> (Volts, Standard Calomel Electrode scale) and pitting was observed. In this experiment the corrosion potential normally is nominally -0.07 V<sub>SCE</sub>, and the repassivation potential is 0.04 V<sub>SCE</sub>, so the increase in corrosion potential is significant. The concentrations of chloride and hydrogen peroxide in this experiment are many orders of magnitude higher than expected in the waste package (see concentrations in Table 6.5-1).

Brossia et al. (2002 [DIRS 161988], Figure 3) report two experiments where H<sub>2</sub>O<sub>2</sub> was added to ongoing corrosion potential tests. The metal samples had oxide coatings of 1.7 μm and 3.4 μm thick. The initial solution contained 0.1 M NaCl at 95°C and 5 mM H<sub>2</sub>O<sub>2</sub> was added. In both tests the corrosion potential initially increased, but later one test showed decreasing corrosion potentials. Pitting was not observed in either experiment. Again, these concentrations are higher than expected in the in-package chemistry.

The experiments by Greene et al. (2000 [DIRS 145073], Figure 8) discuss the stability of H<sub>2</sub>O<sub>2</sub>. IAEA (1998 [DIRS 150560], p. 220) and suggest that H<sub>2</sub>O<sub>2</sub> is known to decompose catalytically on the surfaces of various types of materials at ambient temperatures, and that zirconium oxides enhance decomposition. H<sub>2</sub>O<sub>2</sub> decomposes in bulk solutions at elevated temperatures (Štefanic and LaVerne 2002, [DIRS 166303], Abstract). Table 6.5-2 provides the half-life of H<sub>2</sub>O<sub>2</sub> at various temperatures and shows that bulk decomposition during the regulatory period will be significant.

The in-package model, coupled with the pitting experiments and pitting model (see FEP 2.1.02.16.0A and Table 6.6-1), shows that radiolytic production of nitric acid and hydrogen peroxide is not sufficient to influence the corrosion potentials significantly at the steady state concentrations expected in the repository and produce pitting. Zirconium alloys have been shown to be relatively inert in both nitric acid and hydrogen peroxide as discussed by Yau and Webster (1987 [DIRS 100494]) and in *Clad Degradation—Local Corrosion of Zirconium and Its*

*Alloys Under Repository Conditions* (CRWMS M&O 2000d [DIRS 136058], Sections 6.1.6 and B.4). For example, the chemical processing industry uses peroxide strengths of 90 percent with zirconium equipment. The service life has been increased by an order of magnitude compared to graphite components previously used, which were generally considered to be inert. In nitric acid, zirconium and its alloys are inert up to acid concentrations of 65 weight percent. Since radiolysis does not produce nitric acid and hydrogen peroxide at greater concentrations, there will be no impact (low consequence) on the uniform corrosion rate as a result of radiolysis.

Table 6.5-2. Half-Life of Hydrogen Peroxide at Various Temperatures

Temperature (°C)	Half-Life (Days)
25	46
50	4.9
73	0.83
95	0.19
100	0.14

Source: Štefanic and LaVerne 2002 [DIRS 166303], Abstract

In conclusion, cladding degradation from radiolysis enhanced corrosion is excluded from TSPA-LA. Radiolytic production of nitric acid and hydrogen peroxide was included in the in-package chemistry model (BSC 2003f [DIRS 161962], Attachment III) and this analysis showed that radiolysis had a small effect on the chemistry. Experiments where hydrogen peroxide was added to tests show that in many cases the effect of the hydrogen peroxide quickly becomes negligible. Radiolysis by itself is not expected to damage the cladding (low consequence). Cladding failure due to radiolysis enhanced corrosion has a low consequence, and is excluded from further consideration. The magnitude and time of the resulting radiological exposures to the reasonably maximally exposed individual, or radionuclide releases to the accessible environment, would not be significantly changed by the omission of this FEP (radiolysis enhanced corrosion) from the performance assessment (TSPA-LA) model.

## 6.6 LOCALIZED (PITTING) CORROSION OF CLADDING

### FEP Number:

2.1.02.16.0A

### YMP FEP Description:

Localized corrosion in pits could produce penetrations of cladding.

### Descriptor Phrases:

Pitting corrosion of cladding

### Screening Decision:

Excluded - Low Consequence

### TSPA-LA Disposition:

NA

**Related FEPs:**

- 2.1.02.15.0A, Localized (radiolysis enhanced) corrosion of cladding
- 2.1.02.17.0A, Localized (crevice) corrosion of cladding
- 2.1.02.13.0A, General corrosion of cladding

**Screening Argument:** Localized corrosion of the cladding from pitting has been excluded on the basis of low consequence. A comparison of the expected in-package chemistry to the chemical composition where pitting is observed shows that pitting is not expected. Therefore, the inclusion of a pitting model in TSPA-LA would not have a significant effect on the magnitude and time of radiological exposures or radionuclide releases (low consequence).

A zirconium-pitting model (BSC 2003g [DIRS 164667]) was developed to investigate the chemical conditions at which pitting occurs. Zirconium alloys are susceptible to pitting in a particularly aggressive combination of chloride (Cl<sup>-</sup>) ions, ferric ions (Fe<sup>+3</sup>), or hydrogen peroxide (H<sub>2</sub>O<sub>2</sub>). In order to predict cladding failure from chloride pitting, a review of the literature for pitting rates and electrochemical data for various zirconium alloys was conducted. Based on this review of the literature, failure criteria were constructed based on an electrochemical definition of pitting as the condition at which the corrosion potential for as-polished metal exceeds repassivation potential (i.e.,  $E_{cor} > E_{rp}$ ). Corrosion potential and repassivation potential values were obtained for as-polished zirconium alloys in various solution concentrations of Cl<sup>-</sup>, Fe<sup>+3</sup>, and H<sub>2</sub>O<sub>2</sub> using measurements obtained from various experiments. The model to predict repassivation potential depends only on chloride concentration in the solution. The corrosion potential for as-polished metal ( $E_{cor}$ ) was modeled by performing a regression analysis to fit experimental data with varying molar concentrations of Cl<sup>-</sup>, Fe<sup>+3</sup>, and H<sub>2</sub>O<sub>2</sub>. The model describes the conditions where pitting was observed in experiments. High concentrations of chlorides at extremely low pH (below -0.6) can lead to the general dissolution of the protective zirconium oxide film.

This model was evaluated using in-package chemistry, including the production of nitric acid and hydrogen peroxide from radiolysis (see FEP 2.1.02.15.0A and Table 6.5-1). Table 6.6-1 provides the corrosion potential for as-polished metals, repassivation potential, and potential differences for the cases described in Table 6.5-1. Table 6.6-1 shows that pitting is not expected because the repassivation potential exceeds the corrosion potential for as-polished metal. Figure 6.6-1 shows the chemical conditions where pitting would occur and the chemical regions predicted. No pitting was predicted to occur for any conditions that were associated with Zircaloy cladding in the repository. In a sensitivity study with acid production from radiolysis increased by a factor of ten, no pitting was predicted to occur.

The in-package chemistry model predicts that in most cases the pH remains above 3.5. When additional uncertainties are added, minimum pHs in the range of 2.5 are possible. To address the potential for pitting at low pHs, an in-package chemistry sensitivity study was performed. The radiolytic production of nitric acid and hydrogen peroxide was 10 times nominal (case C12BC10x in Table 6.6-1) but the amount of sulfur in the carbon steel rack was increased by a factor of 20. Sulfur in the steel suppresses pH, as shown in Figure 6.5-1. Increasing the amount of sulfur by a factor of 20 reduces the pH to a minimum of 2.2. At this pH, the concentration of Fe<sup>3+</sup> to  $3.8 \times 10^{-6}$  molality and chloride is  $9.7 \times 10^{-4}$  molality. Hydrogen peroxide is less than  $10^{-12}$  molality. For this chemical composition, the pitting model predicts a corrosion potential of

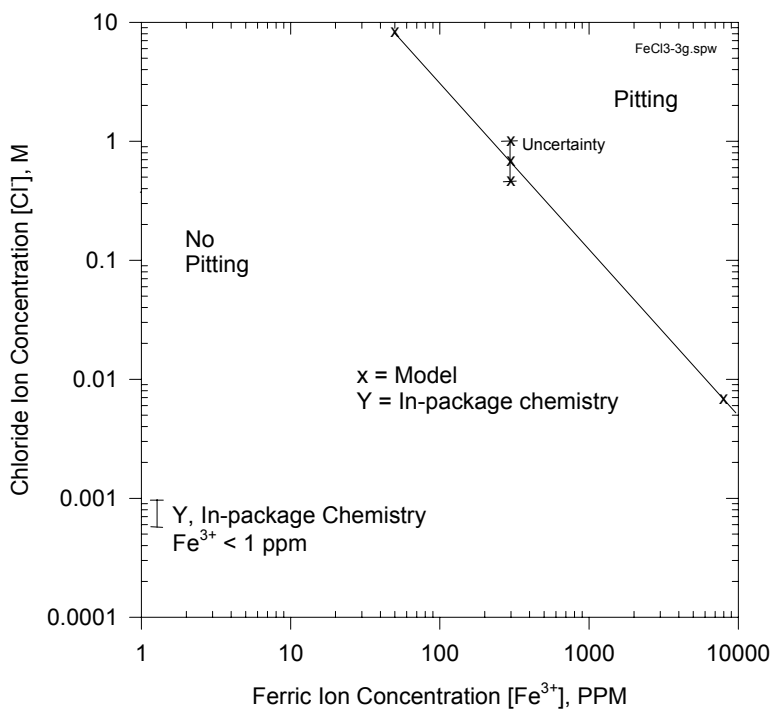
-0.2  $V_{SCE}$  and a repassivation potential of +0.29  $V_{SCE}$ . Since the repassivation potential exceeds the corrosion potential, no pitting is predicted. At the minimum pHs predicted in the in-package chemistry model, no pitting is predicted to occur.

Table 6.6-1. Corrosion and Repassivation Potentials for In-Package Chemistry Condition

Case #	$E_{cor}$ $V_{SCE}$	$E_{rp}$ $V_{SCE}$	Difference <sup>a</sup> ( $E_{rp}-E_{cor}$ ) $V_{SCE}$
C22C25	-0.20	0.30	0.50
C22CBC	-0.20	0.30	0.50
C22BC10x	-0.20	0.30	0.50
C12C25	-0.20	0.29	0.49
C12CBC	-0.20	0.29	0.49
C12BC10x	-0.20	0.29	0.49

Source: BSC 2003g [DIRS 164667]

NOTE: <sup>a</sup> Negative difference implies pitting is possible.



Source: BSC 2003g [DIRS 164667]

Figure 6.6-1. Comparison of In-Package Chemistry with Chemical Conditions Necessary for Pitting

The pitting model was generated with data for as-polished samples, but CSNF is coated with thick oxides (54  $\mu\text{m}$  mean, 5 to 95 percent  $\mu\text{m}$  range = 112  $\mu\text{m}$  to 5.3  $\mu\text{m}$ , CRWMS M&O 2000c [DIRS 151659], Section 6.4). These oxides will affect the measured corrosion potential (open circuit potential) because of the high electrical resistance of the coating, but will not increase susceptibility to pitting corrosion. This sensitivity to oxide thickness was demonstrated in a series of four tests performed on zirconium samples at the Center for Nuclear Waste Regulatory

Analyses. Two tests had oxide thickness of 1.7  $\mu\text{m}$  and 2 tests had 3.4  $\mu\text{m}$  coatings (Brossia et al. 2002 [DIRS 161988], Figure 3). These samples were exposed to 0.1M of NaCl. Prior to addition of oxidants to the solution, the highest corrosion potential was 0.67  $V_{\text{SCE}}$ , well above the repassivation potential of 0.12  $V_{\text{SCE}}$ . Two other samples also had potentials above the repassivation potential. No pitting was observed in the samples. Yau and Maguire (1990 [DIRS 110761], Fig. 4) showed that zirconium annealed in air (air oxidized) also had a corrosion potential that was both above the as-polished value and the repassivation potential. Again, no pitting was observed. These observations show that the corrosion potential for oxide coated material can exceed the repassivation potential and pitting will not occur.  $E_{\text{cor}} > E_{\text{rp}}$  is a necessary but not sufficient condition for pitting. For the case where the corrosion potential is raised above the repassivation potential only due to oxide formation, pitting will not occur, as discussed below.

When pitting occurs on metal surfaces, the pit behaves as an anode and the surrounding metal surface behaves as a cathode. The metal in the pit gives up electrons, becomes oxidized, and goes into solution. To support pitting, the electrons must be conducted to the free surface of the surrounding metal and be accepted by an oxidizing agent (e.g.,  $\text{H}_2\text{O}$ ,  $\text{Fe}^{3+}$ , or  $\text{O}_2$ ). The potential for pitting starts when some event creates a site with less protection than the surrounding metal. For pitting to then occur, three conditions must be satisfied:

1. The surface of the surrounding metal must be able to transport the electrons into the solution
2. Oxidizing agents in the solution must be present to accept the electrons
3. The pit site must support transport of the metal ions into solution.

Zirconium oxide is a poor conductor and a thick oxide coating restricts the current of electrons from the metal into the solution (Condition 1 above). This insulation results in the measured corrosion potential increasing from the Zircaloy corrosion potential toward the oxide-surface redox-reaction potential as the oxide insulation increases. The redox potential is not relevant to pitting susceptibility but is a consequence of inerting of the Zircaloy metal. If the oxide is defected, the metal corrosion potential decreases to that of the bare metal, and pitting occurs only if oxidizing species in solution or an applied potential forces the bare-metal Zircaloy corrosion potential above the repassivation potential. If there are insufficient oxidizing agents in the solution to support a critical current (Condition 2 above), then a new protective oxide surface will form on the potential pit surface and prevent dissolution of the metal (Condition 3 above).

In summary, although the corrosion potential ( $E_{\text{cor}}$ ) is greater than the repassivation potential ( $E_{\text{rp}}$ ) for zirconium with thick oxide layers, both empirical evidence and understanding of the response to local breakdown of the protective oxide layer (e.g., due to oxide layer cracking) indicate that pitting does not occur. The empirical evidence discussed in the above paragraph (Brossia et al. 2002, [DIRS 161988] Figure 3, Yau and Maguire 1990 [DIRS 110761], Fig. 4) showed that zirconium with thick oxide layers did not pit. The oxide layer on the zirconium surrounding the breakdown region prevents sufficient cathodic current to support pitting. Therefore, both the anodic and cathodic reactions supporting corrosion occur in the breakdown region, a condition that can not occur for pitting. In addition, upon breakdown of the oxide, the

corrosion potential drops to about the corrosion potential of the as-polished zirconium. In effect, the breakdown region will not be influenced by the surrounding oxidized zirconium surface and will behave as as-polished zirconium. Therefore, results obtained using as-polished zirconium coupons apply in assessing the corrosion behavior in the breakdown region. For the experiments described by Brossia et al. (2002, [DIRS 161988], Figure 3), the corrosion potential for an as-polished surface ( $-0.11 V_{SCE}$ ) is significantly less than the repassivation potential ( $0.12 V_{SCE}$ ), and pitting was neither observed nor expected to occur.

As further validation of the pitting model and results, a review of the literature for pitting observations for various zirconium alloys was conducted. Figure 6.6-2 provides the chemical environment where pitting is observed. Figure 6.6-2 contains experimental results by Yau (CRWMS M&O 2000d [DIRS 136058], Table 4), Maguire (1984 [DIRS 101717], Table 6), Riley and Covino (1982 [DIRS 161993], p. 11), Jangg et al. (1978 [DIRS 110544], Tables 1 and 6), Greene et al. (2000 [DIRS 145073], Figure 8) and Brossia et al. (2002 [DIRS 161988], Figure 3). Each experiment is shown with a different symbol and whether pitting is observed (symbols q, r, s, u). Yau's data (symbols a, q) show that pitting does not always occur under similar conditions.

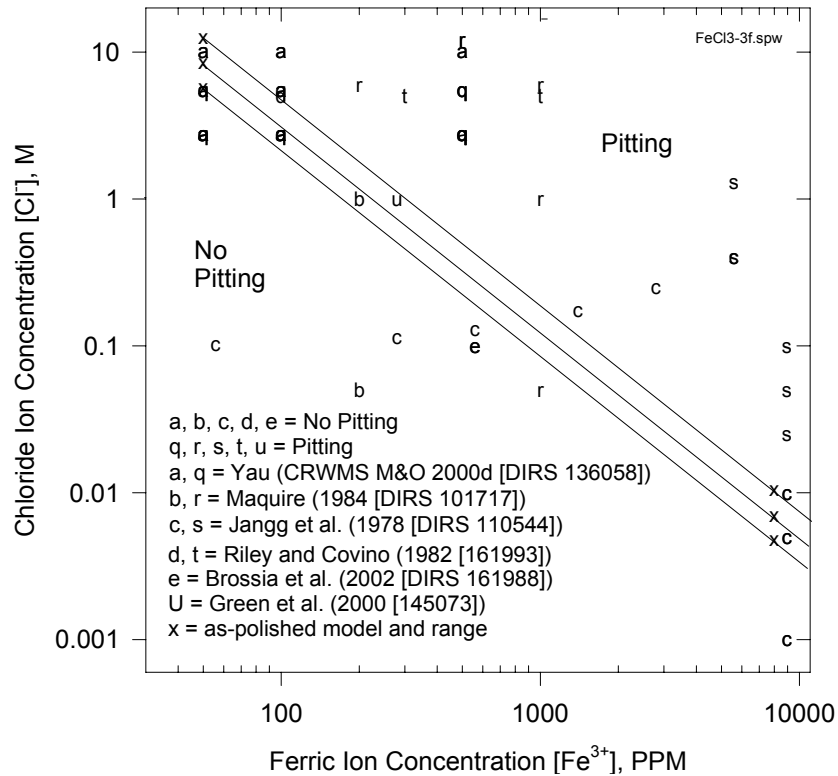
The in-package chemistry model (BSC 2003f [DIRS 161962], Attachment III) calculated the expected concentrations of chemicals in a thin film of water on the fuel. Table 6.5-1 provides the maximum concentrations of  $Cl^-$ ,  $Fe^{3+}$ , and  $H_2O_2$  expected with the inclusion of radiolysis. Figure 6.5-1 provides the evolution of the pH over time for the thin film of water. The pH stays above 3.5, which means few, if any, ferric ions ( $Fe^{3+}$ ) would exist. The concentrations of  $Cl^-$  and  $Fe^{3+}$  (Table 6.5-1) are not shown in Figure 6.6-2 because they are well to the bottom and left of the scales shown. A comparison of the chemistry and the regions where pitting is observed shows that cladding failure from pitting is unlikely.

Most of the tests shown in Figure 6.6-2 were performed on as-polished metal samples while CSNF cladding is coated with thick oxides (mean value =  $54 \mu m$ , CRWMS M&O 2000c [DIRS 151659], p. 30). Two tests were performed on zirconium samples with oxide thickness of 1.7 and  $3.4 \mu m$  (Brossia et al. 2002 [DIRS 161988], Figure 3). These samples were exposed to 0.1M of NaCl and either 5 mM  $FeCl_3$  or 5 mM  $H_2O_2$ . Pitting was not observed in any of these four tests (see symbol "e" in Figure 6.6-2 for the two ferric chloride tests).

Application of the pitting model (BSC 2003g [DIRS 164667]) to predict the pitting/no-pitting boundary is also illustrated in Figure 6.6-2. The lines (with uncertainty) where the model predicts the onset of pitting are shown as straight lines in log/log scale. Each line represents the chemical composition ( $Cl^-$  and  $Fe^{3+}$ ) where  $E_{cor} = E_{tp}$ . A straight line is expected since both  $E_{tp}$  and  $E_{cor}$  linearly depend on the log of the  $Cl^-$  and  $Fe^{3+}$  concentrations. The application of the as-polished pitting model to CSNF (with thick oxides) is expected to be conservative based on increased difficulty to provide the cathodic currents needed to support pitting.

In conclusion, cladding degradation from localized (pitting) corrosion of the cladding is excluded from TSPA-LA. A comparison of the expected in-package chemistry to the chemical composition where pitting is observed shows that pitting is not expected. Cladding failure due to pitting has a low consequence, and is excluded from further consideration. The magnitude and time of the resulting radiological exposures to the reasonably maximally exposed individual, or

radionuclide releases to the accessible environment, would not be significantly changed by the omission of this FEP (localized (pitting) corrosion of the cladding) from the performance assessment (TSPA-LA) model.



Source: This report.

Figure 6.6-2. Chemistry Where Pitting of Zirconium Has Been Observed

## 6.7 LOCALIZED (CREVICE) CORROSION OF CLADDING

### FEP Number:

2.1.02.17.0A

### YMP FEP Description:

Localized corrosion in crevices could produce penetrations of cladding.

### Descriptor Phrases:

Crevice corrosion of cladding

### Screening Decision:

Excluded – Low Consequence

### TSPA-LA Disposition:

NA

**Related FEPs:**

- 2.1.02.13.0A, General Corrosion of Cladding
- 2.1.02.14.0A, Microbially influenced corrosion (MIC) of cladding
- 2.1.02.15.0A, Localized (radiolysis enhanced) corrosion of cladding
- 2.1.02.16.0A, Localized (pitting) corrosion of cladding

**Screening Argument:** Localized (crevice) corrosion of the cladding is excluded from the TSPA-LA on the basis of low consequence.

Yau and Webster (1987 [DIRS 100494], p. 717) report: “Of all the corrosion-resistant structural metals, zirconium and tantalum are the most resistant to crevice corrosion. In low-pH chloride solutions or chlorine gas, for example, zirconium is not subject to crevice attack.” Greene et al. (2000 [DIRS 145073]) and Brossia et al. (2002 [DIRS 161988]) performed pitting and crevice corrosion tests on Zircaloy-4. They covered temperatures from 25 to 95°C, chloride concentrations from 0.001 to 4.0 M, and pH from 2.1 to 10.7. The solutions also contained the predominant anions in the groundwater. Some of their tests had sufficiently aggressive solutions to cause pitting on exposed surfaces. Other tests had voltages applied to the sample to raise the corrosion potential above the repassivation potential and cause pitting on exposed surfaces. They report that no crevice corrosion is observed under the same environment and electrochemical conditions that promote pitting corrosion on exposed surfaces. In summary, crevice corrosion is not observed under severe conditions that promote pitting on the exposed surfaces.

Additional corroborating information is also available. More detailed information is provided by Yau (1983 [DIRS 149233]) showing that zirconium and Zr-1.5 percent Sn were resistant to crevice corrosion after 14 days exposed to boiling (107°C), saturated NaCl solution with the pH adjusted to 0 by the addition of HCl. *Clad Degradation-Local Corrosion of Zirconium and its Alloys Under Repository Conditions* (CRWMS M&O 2000d [DIRS 136058]) shows that zirconium is not susceptible to crevice corrosion. Section 4.1.3 of that report (CRWMS M&O 2000d [DIRS 136058]) discusses the crevice corrosion resistance of zirconium in various chemical solutions, summarizes seven crevice corrosion tests, and reports that crevice corrosion was not observed. The U-bend tests discussed in Section 4.1.4 of *Clad Degradation-Local Corrosion of Zirconium and Its Alloys Under Repository Conditions* (CRWMS M&O 2000d [DIRS 136058]) are also designed to produce crevice corrosion under the U-bend test washers. In these tests, no crevice corrosion was reported. Section 6.1.10 of *Clad Degradation-Local Corrosion of Zirconium and Its Alloys Under Repository Conditions* (CRWMS M&O 2000d [DIRS 136058]) discusses the theoretical reasons why zirconium is immune to this type of corrosion.

In conclusion, cladding degradation from localized (crevice) corrosion is excluded from TSPA-LA. Crevice corrosion of zirconium under repository in-package chemistry conditions is not expected. NRC requirements in 10 CFR 63.114 (e and f) allow the omission because crevice corrosion is not expected under repository conditions and therefore will not significantly change the magnitude and time of the resulting radiological exposures to the reasonably maximally exposed individual (RMEI), or radionuclide releases to the accessible environment.

## 6.8 ENHANCED CORROSION OF CLADDING FROM DISSOLVED SILICA

**FEP Number:**

2.1.02.18.0A

**YMP FEP Description:**

It must be determined if the high dissolved silica content of waters enhances corrosion of cladding.

**Descriptor Phrases:**

Enhanced corrosion of cladding from dissolved silica

**Screening Decision:**

Excluded – Low Consequence

**TSPA-LA Disposition:**

NA

**Related FEPs:**

- 2.1.02.14.0A, Microbially influenced corrosion (MIC) of cladding
- 2.1.02.15.0A, Localized (radiolysis enhanced) corrosion of cladding
- 2.1.02.16.0A, Localized (pitting) corrosion of cladding
- 2.1.02.27.0A, Localized (Fluoride enhanced) corrosion of cladding

**Screening Argument:** Enhanced corrosion of cladding due to high dissolved silica content in waters is excluded from the TSPA-LA on the basis of low consequence.

Silicon dioxide reacts with hydrofluoric acid to form fluorosilicic acid, which is highly corrosive to zirconium in high concentrations (10 weight percent) (Yau and Webster 1987, p. 712). This reaction is not expected to occur because the pH is generally too high (pH>3.18) for hydrofluoric acid to exist and fluoride concentrations are too low (J13 well water contains only 2.2 ppm) to form significant concentrations of fluorosilicic acid. The fluoride corrosion itself is addressed in another FEP (2.1.02.27.0A) and is excluded. The potential for silica itself degrading the cladding is negligible. Hansson (1984 [DIRS 101676]) reports corrosion tests with concrete pore fluids which normally contain silica. Yau (1983 [DIRS 149233]) reports corrosion tests in sea water which also contains silica. Neither experimenter reports significant corrosion. Yau and Webster (1987 [DIRS 100494], Table 6) review the corrosion potentials for zirconium and report no corrosion with sodium silicate concentrations from 0 to 100 weight percent at ambient temperature to 100°C.

In conclusion, enhanced cladding degradation from dissolved silica is excluded from TSPA-LA. The NRC requirements in 10 CFR 63.114 (e and f) allow the omission because silica will not degrade cladding and therefore will not significantly change the magnitude and time of the resulting radiological exposures to the reasonably maximally exposed individual (RMEI), or radionuclide releases to the accessible environment.

## 6.9 CREEP RUPTURE OF CLADDING

**FEP Number:**

2.1.02.19.0A

**YMP FEP Description:**

At high cladding temperatures (>400°C) for sufficiently long time intervals, creep rupture of Zircaloy cladding on spent fuel can occur and produce small perforations in the cladding to relieve stress. After the waste package fails, the fuel can react with water and radioisotopes can thereby escape over time from the fuel rod.

**Descriptor Phrases:**

Thermally induced cladding creep (rupture)

**Screening Decision:**

Excluded – Low Consequence

**TSPA-LA Disposition:**

NA

**Related FEPs:**

2.1.02.26.0A, Diffusion-controlled cavity growth (DCCG) in cladding

**Screening Argument:** Creep rupture of cladding is excluded from the TSPA-LA on the basis of low consequence.

The Spent Fuel Project Office of the NRC issued Interim Staff Guidance – 11, Revision 2 (NRC 2002 [DIRS 164593], p. 2), which set a maximum temperature limit for the cladding (400°C) to prevent damage from creep or hydride reorientation during dry storage (similar temperature histories as repository closure). Since peak cladding temperatures in the repository are expected to be less than 268°C (Appendix A), damage from creep is expected to be minimal. Figure 6.9-2 compares cladding damage for dry storage and repository emplacement as a function of peak cladding temperatures, and shows that similar temperature limits apply to both environments and the analysis presented in *Clad Degradation – Summary and Abstraction* (CRWMS M&O 2001a [DIRS 151662], Section 6.2).

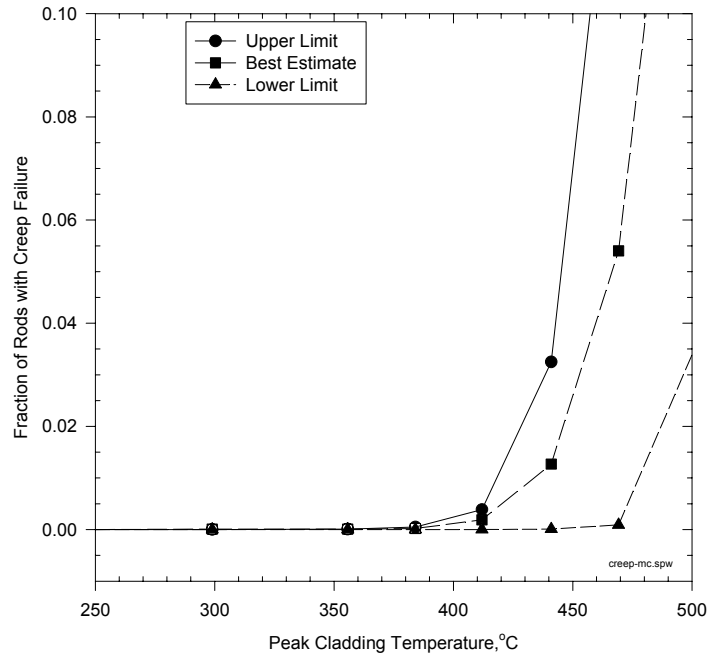
Additional corroborating information is available. A statistical analysis of creep failure was performed (CRWMS M&O 2001a [DIRS 151662], Section 6.2), in which a burnup distribution (rod average = 44 MWd/kgU, range = 2 to 75 MWd/kgU) was used and a distribution of rod properties (including stress) was developed. The Murty creep correlation was selected after comparing six different correlations with results from five different experiments. It was then modified to better predict irradiated cladding creep data. The fuel rods were exposed to two consecutive temperature histories before being placed in the repository. They were exposed to 24 hours of vacuum drying with a peak temperature of 430°C, followed by 20 years dry storage with a peak temperature of 350°C.

The sensitivity study considered creep strain for only 1,000 years of repository thermal history because after that time, the fuel is too cool for creep to occur. Uncertainties in the temperatures and strain rate were included. The radial temperature distribution across the waste package was also modeled. The waste package surface temperature was shifted upward or downward and the fraction of rods that fail from creep was calculated. Failure was predicted when the creep strain of a rod exceeds a creep failure criterion. The upper limit was a 1 percent strain failure criterion and lower limit was 6 percent strain. The best estimate creep failure criterion was a complementary cumulative distribution function (CCDF) based on 52 failure tests. Figure 6.9-1 shows the results of this sensitivity study. Rod failures started to occur during repository closure at a peak cladding temperature of 400°C. Cladding failure reached 1 percent at a peak temperature of about 430°C (best estimate). In the current repository design, the cladding temperatures are below 268°C (Table A-2) and rod failures from creep are not expected.

The Dry Storage Characterization Project (EPRI 2002 [DIRS 161421], p. xii) studied the condition of fuel assemblies that were exposed to various thermal transients (peak temperatures to 415°C) followed by 15 years of dry storage (peak temperature at 342°C and slowly decreasing). These temperatures are higher than expected at the repository (Appendix A of this report). The Project concluded “little or no cladding creep occurred during the thermal benchmark testing and dry storage. It is anticipated that the creep would not increase significantly during additional storage due to the low temperature after 15 years, the continual decrease in temperature from the reduction of decay heat, and the concurrent reduction in pressure and stress.”

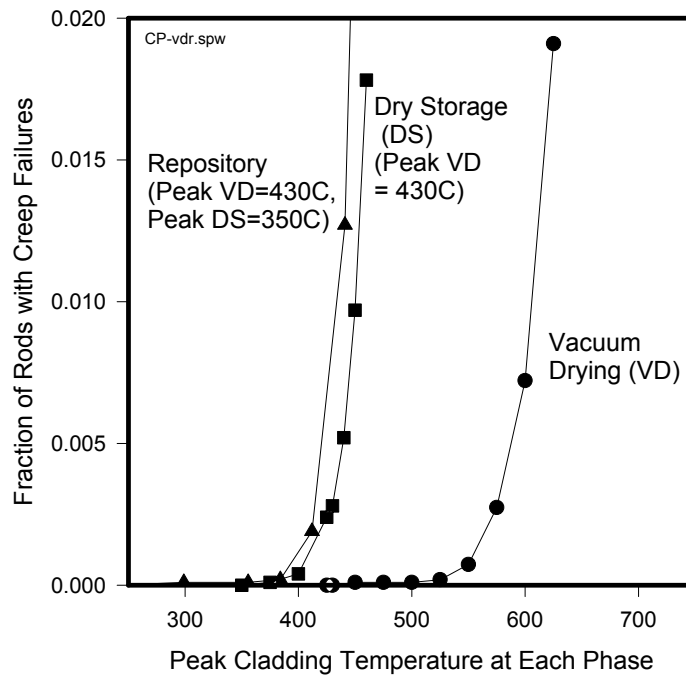
Over time, helium production from alpha decay could generate pressures that exceed the pressure at the peak temperature (see FEP 2.1.02.20.0A). The creep rate has a strong temperature dependency (Figures 6.9-1 and 6.9-2) and the slightly higher stress that occurs at 10,000 years does not change the creep results because the temperatures are less than 73°C and no observable creep occurs at these temperatures and strains.

In conclusion, creep rupture of cladding is excluded from the TSPA-LA on the basis of low consequence. Repository temperatures are too low to have any significant creep. The NRC requirements in 10 CFR 63.114 (e and f) allow the omission because the small amount of creep that will occur during the regulatory period will not significantly change the magnitude and time of the resulting radiological exposures to the reasonably maximally exposed individual (RMEI), or radionuclide releases to the accessible environment.



Source: CRWMS M&O 2001a [DIRS 151662]

Figure 6.9-1. Creep Failure Fraction as a Function of Peak Cladding Temperature



Source: CRWMS M&O 2001a [DIRS 151662]

Figure 6.9-2. Comparison of Creep Damage in Dry Storage and Repository Emplacement

## 6.10 INTERNAL PRESSURIZATION OF CLADDING

**FEP Number:**

2.1.02.20.0A

**YMP FEP Description:**

Increased pressure within the fuel rod due to the production of helium gas could contribute to cladding failure.

**Descriptor Phrases:**

Internal gas pressure from He (cladding damage)

**Screening Decision:**

Excluded – Low Consequence

**TSPA-LA Disposition:**

NA

**Related FEPs:**

- 2.1.02.19.0A, Creep Rupture of Cladding
- 2.1.02.21.0A, Stress corrosion cracking (SCC) of cladding
- 2.1.02.22.0A, Hydride cracking of cladding
- 2.1.12.02.0A, Gas generation (He) from waste form decay

**Screening Argument:** Internal pressurization of the cladding is excluded from the TSPA-LA on the basis of low consequence.

Piron and Pelletier (2001 [DIRS 165318], Section 5.3) investigated the pressurization of the fuel rods from helium production (alpha decay). They concluded that fuel (47.5 MWd/kgU) would produce 1,171 cm<sup>3</sup> (STP) of helium in a rod after 10,000 years. Piron and Pelletier's (2001 [DIRS 165318], Section 5.3) values are based on having all of the helium released. Piron and Pelletier's values were adjusted for burnup (36 MWd/kgU) and temperature to be consistent with the earlier analysis reported in *Initial Cladding Condition* (CRWMS M&O 2000c [DIRS 151659], Section 6.3). The resulting values are presented in Table 6.10-1. Their analysis produced a total rod pressure 30 to 50 percent higher than predicted in *Initial Cladding Condition* (CRWMS M&O 2000c [DIRS 151659], Section 6.3.4). Also given in this table are the pressures for the average burnup rod (44.1 MWd/kgU). This is shown in the last three lines of Table 6.10-1. The peak pressure (13.3 MPa) would have to be significantly higher (about 33 MPa to produce the necessary stress intensity for crack propagation) for the cladding to fail from delayed hydride cracking (FEP 2.1.02.22.0A, see Section 6.12.3). Even when using values provided by Piron and Pelletier (2001 [DIRS 165318]), the change in pressure is not significant and no cladding failure from helium production is expected.

Table 6.10-1. Effect of Helium Production on Rod Pressure

Time (years)	Temperature (°C)	Helium Pressure (MPa)	Fission Gas Pressure (MPa) <sup>a</sup>	Total Pressure (MPa)	He % of total Pressure (%)
0	135	0.03	5.4	5.5	0.46
10	268	0.13	7.2	7.3	1.8
90	212	0.52	6.5	7.0	7.4
950	131	1.9	5.4	7.3	26.4
10,000	73	3.7	4.6	8.3	44.3
10,000	73	6.3	4.6	10.9	57.8
10,000	73	7.8	5.5	13.3	58.5

Source: CRWMS M&O 2000c [DIRS 151659], Table 7

NOTES: <sup>a</sup> Initial fill and fission gas pressure was 4 MPa at 27°C.

<sup>b</sup> Helium pressure based on Piron and Pelletier 2001 [DIRS 165318]

<sup>c</sup> Helium pressure based on Piron and Pelletier 2001 [DIRS 165318], average burnup of 44.1 MWd/kgU.

<sup>d</sup> Mean value of fill and fission gas pressure from CRWMS M&O 2000c [DIRS 151659], Table 12

Additional corroborating information is available. *Initial Cladding Condition* (CRWMS M&O 2000c [DIRS 151659], Section 6.3.4) provides the initial screening for the effect of helium production. This analysis could be considered an alternative conceptual model to Piron and Pelletier. The internal gas in a fuel rod consists of initial fill gas, fission product gases, and helium gas from alpha decay. The helium gas pressure will slowly increase over time by the production of helium as a result of alpha decay. Manaktala (1993 [DIRS 101719], Figure 3-4, p. 3-12) presents the helium pressure buildup for 100°C as a function of time for a PWR fuel rod with 36 MWd/kgU burnup and a conservative analysis that 100 percent helium is released from the fuel into the fuel rod gap. This figure was used to develop an equation for helium buildup in a fuel rod. Table 6.10-1 provides the pressure change as a function of time for a typical rod (36 MWd/kgU). The pressures have been adjusted to reflect the current maximum temperatures of 268°C (peak) and 73°C (10,000 years) using the ideal gas law. Ambient (27°C) pressure was increased by 1.80 (541 K/300 K) for the peak temperature and 1.15 (346 K/300 K) for 73°C temperature. The table shows that there are two competing effects. Over time, the rod cools, decreasing the pressure and the helium production increases the pressure. After 10,000 years, the pressure is doubled from that at the time of peak temperature. This increase is not enough to change any failure mechanisms that were evaluated at the peak temperature. Cladding failure from pressure, stress, or stress intensity factors is not expected. Creep rupture (FEP 2.1.02.19.0A) is also driven by stress and is not in expected to contribute to cladding failure. This is discussed further in FEPs 2.1.02.19.0A, 2.1.02.21.0A, and 2.1.02.22.0A where the individual failure modes are discussed.

Other corroborating information is available. Rothman (1984 [DIRS 100417], Table 6) predicted that helium pressure buildup would be offset by the cooling of the rods and the pressure at 10,000 years would be slightly less than that at the peak temperature of 322°C. He also considered that 100 percent of the gas was released. Both Rothman and Piron and Pelletier concluded that the pressurization from helium after 10,000 years is not significant to cause rod failure.

Although these results are based on complete release of the helium, this is actually unlikely to occur. Piron and Pelletier (2001 [DIRS 165318], p. 232) point out that  $\text{UO}_2$  can hold  $0.66 \text{ cm}^3$  (STP) of helium per gram of fuel. A rod weighs approximately 2,200 gm ( $201 \text{ cm}^3$  (CRWMS M&O 2000c [DIRS 151659], Table 2)  $\times 10.97 \text{ gm/cm}^3$  (BSC 2003a [DIRS 162153], Table 8)). The fuel in a rod can contain  $1,500 \text{ cm}^3$  (STP) of helium, larger than the  $1,171 \text{ cm}^3$  (STP) expected to be formed. Therefore, even if microscopic bubbles of gas are formed, total gas release is not expected. M. Peehs (1998 [DIRS 109219], p. 5) shows that fission gas release during dry storage is not expected because the diffusion coefficients decrease by approximately 8 orders of magnitude for dry storage temperatures (hotter than repository temperatures) compared to reactor operation. While helium diffusion is greater than fission gas diffusion, complete release is both conservative and unlikely.

In conclusion, cladding degradation from internal pressurization of the cladding is excluded from TSPA-LA. The NRC requirements in 10 CFR 63.114 (e and f) allow the omission because internal pressurization of the fuel rods is too low to cause damage to the cladding and therefore will not significantly change the magnitude and time of the resulting radiological exposures to the reasonably maximally exposed individual (RMEI), or radionuclide releases to the accessible environment.

## 6.11 STRESS CORROSION CRACKING (SCC) OF CLADDING

### **FEP Number:**

2.1.02.21.0A

### **YMP FEP Description:**

Stress corrosion cracking mechanisms can contribute to cladding failure. These mechanisms can operate both from the inside out from the action of fission products, or from the outside in from the actions of salts or other chemicals within the waste package.

### **Descriptor Phrases:**

Cladding high stress locations (external stress corrosion crackings)  
Cladding radiolysis (internal stress corrosion cracking)  
Cladding threshold stress (stress corrosion cracking)

### **Screening Decision:**

Excluded – Low Consequence

### **TSPA-LA Disposition:**

NA

### **Related FEPs:**

2.1.02.16.0A, Localized (pitting) corrosion of cladding  
2.1.02.20.0A, Internal Pressurization of Cladding  
2.1.09.09.0A, Electrochemical effects in EBS

**Screening Argument:** Stress corrosion cracking (SCC) of cladding is excluded from the TSPA-LA on the basis of low consequence.

SCC is the formation of brittle cracks on a metal surface through the simultaneous action of a tensile stress and a corrosive environment. SCC requires a certain chemical environment and sufficiently high stresses (stress intensity factors at the crack tip). Chloride-induced SCC could occur on the outside of the cladding. Chloride induced stress corrosion cracking requires that the passive layer of oxides on the zirconium surface be unstable (Cragolino et al. 1999 [DIRS 152354], p. 4-15; Cox 1973 [DIRS 152920], Abstract; Farina et al. 2002 [DIRS 163639], p. 5; Yau and Webster 1987 [DIRS 100494], p. 718). These are the same conditions under which pitting occurs. As demonstrated in FEP 2.1.02.16.0A, the chemical conditions for pitting and SCC do not exist in the waste package. Therefore, chloride-induced SCC is not expected.

Even if the chemical environment existed, stresses and stress intensities are too low for SCC to occur. Table 6.11-1 provides the pressure, stresses and stress intensity factors for cladding at three different conditions. The first column contains ambient temperature conditions at closure, from *Initial Cladding Condition* (CRWMS M&O 2000c [DIRS 151659], Sections 6.3.6, 6.3.7, and 6.10.2). They represent a statistical distribution for PWR fuel with burnups ranging to 75 MWd/ kgU. Only upper values of the distributions are provided because these are of interest in this type of failure. Column 2 contains the values at the time of the peak temperature (10 years after closure, 268°C for rods located in the center of the waste package), and is calculated from column 1 using the ideal gas law. Column 3 represents the pressure, stress and stress intensity factor at the end of the 10,000-year regulatory period. At this time, the maximum center rod temperature has decreased to 73°C (Table A-3). This has been offset by the buildup of helium pressure from alpha decay (FEP 2.1.02.20.0A). Table 6.10-1 (last row) concludes that if all of the helium were released from the fuel matrix, the helium would contribute 7.7 MPa of pressure to the initial pressure distribution for the initial fill gas and released fission gas. Stresses and stress intensity factors are then estimated.

During the times of interest (peak temperature or peak helium pressure) the maximum stress intensity factors vary from 0.47 mean value to 2.73 MPa-m<sup>0.5</sup>. This is less than the threshold stress intensity factor for SCC, the value at which crack propagation will start. Table 10b of *Clad Degradation – Summary and Abstraction* (CRWMS M&O 2001a [DIRS 151662]) provides the threshold values for various chemical solutions. Table values are greater than or equal to 4 MPa-m<sup>0.5</sup>. The threshold stress intensity factor ( $K_{ISCC}$ ) of 28 MPa-m<sup>0.5</sup> for moist chlorine is included in this table and pertinent to the case of external cracking (Cox 1990 [DIRS 152778], Figure 20, p. 15). This value is for 70°C. The threshold stress intensity decreases with increasing temperature (Cox 1990 [DIRS 152778], Figure 14). At a boiling point of 100°C, when water, possibly carrying chlorides, could enter the WP, the threshold stress intensity could be about 24 MPa-m<sup>0.5</sup>. This value is still well above values predicted in Table 6.11-1. Since the estimated stress intensities are less than the threshold values, chloride-induced cracking is not expected.

Table 6.11-1. Pressures, Stresses and Stress Intensity Factors for Fuel Rods During Repository Emplacement

	Ambient Temperature Properties	Properties at Peak Temperature	Properties at Peak Temperature, Regulatory Limit
Time, years	0	10	10,000
Temperature, °C	27	268	73
<b>Pressure</b>			
Mean, MPa	4.8	8.7	13
95% MPa	7.3	13	16
98%, MPa	8.9	16	18
Max, MPa	18	32	28
<b>Stress</b>			
Mean, MPa	38	69	107
95%, MPa	62	111	137
98%, MPa	76	136	154
Max, MPa	146	263	233
<b>Stress Intensity<sup>a</sup></b>			
Mean, MPa-m <sup>0.5</sup>	0.26	0.47	0.73
95%, MPa-m <sup>0.5</sup>	0.61	1.09	1.34
98%, MPa-m <sup>0.5</sup>	0.77	1.38	1.56
Max, MPa-m <sup>0.5</sup>	1.52	2.73	2.42

Source: CRWMS M&O 2000c [DIRS 151659]

NOTE: <sup>A</sup> For a sharp crack, (Reed-Hill 1973 [DIRS 121838], p. 800)

Stress corrosion cracking on the interior surface of the cladding from iodine is not expected. In “NRC Issue Resolution Status Report Key Technical Issue: Container Life and Source Term” (Beckman 2001 [DIRS 156122], p. 103), the NRC concluded:

The possibility of SCC induced by iodine as discussed in the WF PMR [Process Model Report] does not appear so important because it is limited essentially by the availability of iodine. The phenomenon as such has been postulated as the cause of pellet cladding interaction failure under reactor operating conditions following steep power ramps, but it does not seem plausible under repository conditions.

Iodine concentrations are too low for SCC (Beckman 2001 [DIRS 156122], p. 103). Failure has not been observed in dry storage tests with similar conditions to early repository closure. Stress intensities for a sharp crack, (a limiting case, Reed-Hill 1973 [DIRS 121838], p. 800)(up to 2.73 MPa-m<sup>0.5</sup>) are lower than the range of threshold stress intensity factors (4.0 – 15 MPa-m<sup>0.5</sup>) identified for iodine induced SCC (Tasooji et al. 1984 [DIRS 102093], Figure 12, p. 612). Cragolino et al. (1999 [DIRS 152354], p. 4-27) suggested that lower threshold stress intensity factors could cause failure when considering small cracks. The Dry Storage Characterization Project (EPRI 2002 [DIRS 161421]) studied the condition of fuel assemblies that were exposed to various thermal transients (peak temperatures to 415°C) followed by 15 years of dry storage (peak temperature at 342°C and slowly decreasing). These temperatures are higher than

expected at the repository (Appendix A of this report). Rod failure during dry storage was not observed, suggesting that iodine induced SCC from small cracks did not fail rods.

In conclusion, the magnitude and time of the resulting radiological exposures to the reasonably maximally exposed individual (RMEI), or radionuclide releases to the accessible environment, would not be significantly changed by the omission of this FEP (stress corrosion cracking (SCC) of cladding) from the performance assessment (TSPA-LA) model.

## **6.12 HYDRIDE CRACKING OF CLADDING**

### **FEP Number:**

2.1.02.22.0A

### **YMP FEP Description:**

Cladding contains hydrogen after reactor operation. The cladding might also pick up more hydrogen from cladding general corrosion (wet oxidation) after the waste package is breached. The hydrogen can exist both as zirconium hydride precipitates and as hydrogen in solid solution with zirconium. Hydrides might also form from UO<sub>2</sub> oxidation (after waste package and cladding perforation). In addition, hydrides may dissolve in warmer areas of the cladding and migrate to cooler areas. Hydrogen can also move from places of low stress to places of high stresses, causing hydride reorientation or delayed hydride cracking (DHC). The buildup of hydrides can cause existing cracks to propagate by DHC or hydride embrittlement.

### **Descriptor Phrases:**

Delayed hydride cracking (DHC) (cladding)  
Galvanic coupling (cladding – carbon steel)  
Hydride cracking (cladding)  
Hydride embrittlement (cladding)  
Hydride reorientation in cladding  
Hydrogen induced cracking (HIC) cladding  
Zirconium oxidation of cladding

### **Screening Decision:**

Excluded – Low Consequence

### **TSPA-LA Disposition:**

NA

### **Related FEPs:**

2.1.02.13.0A, General Corrosion of Cladding  
2.1.02.20.0A, Internal Pressurization of Cladding

**Screening Argument:** Hydride cracking and embrittlement of the cladding is excluded from the TSPA-LA on the basis of low consequence.

The stresses in the cladding are not sufficient to fail the cladding at the repository temperatures and experimental data indicate that the in-package environment and cladding stresses are not

conductive to hydride cracking and embrittlement. A more detailed discussion is provided elsewhere (Sections 6.12.1 through 6.12.6 of this report)

As the waste package internals corrode, hydrogen is generated, although little is expected to be absorbed directly by the fuel cladding, because H<sub>2</sub> molecules do not migrate through the high-density ZrO<sub>2</sub> fuel cladding layer (FEP 2.1.12.03.0A). Available data on zirconium hydriding indicate that corrosion of waste package internals will not result in hydriding of fuel cladding, as long as an oxidizing environment exists in the waste package (IAEA 1998 [DIRS 150560], p. 92).

Cladding surface oxidation is minor at repository temperatures and hydrogen absorption will be negligible. Hydride embrittlement from galvanic corrosion of waste package contacting cladding has been excluded based on low consequence. Cladding has a thick, electrically insulating, oxide layer that is produced during reactor operation. This film prevents both direct absorption of hydrogen gas in the environment and galvanic coupling to dissimilar metals. If the passive film has been mechanically removed, the unprotected cladding oxidizes within seconds and forms a passive layer if exposed to water or humid air. Therefore, cladding would undergo little hydrogen charging because the oxide layer prevents hydrogen absorption in the metal (FEP 2.1.12.03.0A).

Cladding failure by DHC is unlikely and has not been included in the abstraction for the TSPA-LA. Stresses (and stress intensity factors) are too low for crack propagation (see Section 6.12.3 of this report).

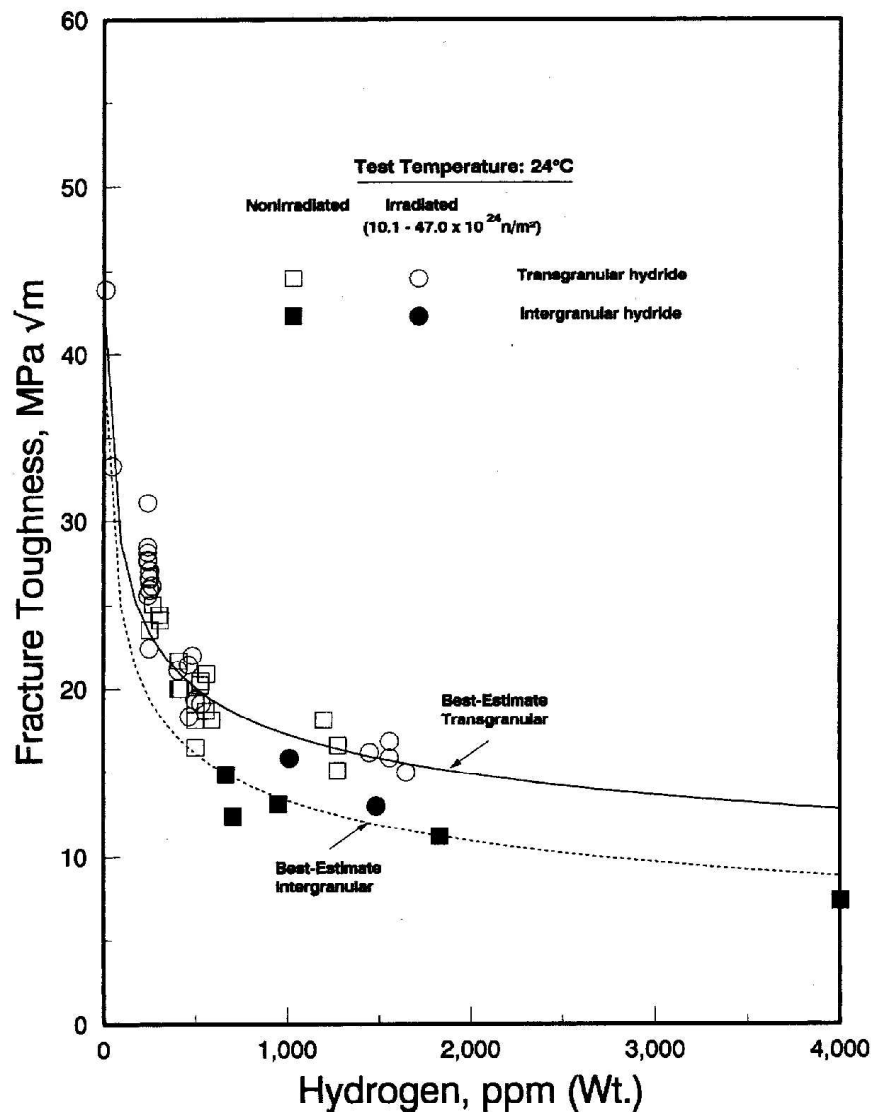
Cladding failure by hydride reorientation is unlikely (see Section 6.12.4 of this report), because the maximum temperatures are too low to dissolve much hydrogen and most rods have stresses too low for reorientation. The cladding material will maintain sufficient strength, even if hydride reorientation occurs, such that failure would not be expected.

Hydrogen axial migration will be limited at the temperatures expected during emplacement (268°C maximum). Failure of the cladding by hydrogen embrittlement is unlikely. Hydrogen absorption in the cladding from UO<sub>2</sub> fuel corrosion only occurs in fuel with already failed cladding. Such reaction, if it should occur, has little consequence (see Section 6.12.5 of this report).

Hydrogen embrittlement results in a generally reduced resistance to fracture. In Zircaloy, hydrogen embrittlement is normally caused by precipitation of zirconium hydride. Since the hydride precipitates are quite brittle, a crack can propagate more readily by preferentially following the hydrides. Resistance to fracture (fracture toughness  $K_{IC}$ ) is a measure of resistance to crack propagation through the material. Fracture toughness is typically measured in terms of the critical stress intensity factor, that is, the stress intensity factor value that will cause growth of a crack. The stress intensity factor is proportional to the far-field stress times the square root of the crack length. Kreyns et al. (1996 [DIRS 100462], Figure 5, reproduced here as Figure 6.12-1) show that for both irradiated and unirradiated material, such hydrides could decrease the fracture toughness ( $K_{IC}$ ) from 42 MPa·m<sup>0.5</sup> to 8 MPa·m<sup>0.5</sup> as the hydrogen content increases from zero to 4,000 ppm. As shown in Table 6.11-1 the maximum stress intensity ( $K_I$ ) for the statistical distribution of rods and crack sizes varies from 0.47 to 2.73 MPa m<sup>0.5</sup> and therefore,

failure is not expected, even with hydride concentrations of 4,000 ppm. In the limit (100 percent hydride and no metal), the fracture toughness is about  $1 \text{ MPa}\cdot\text{m}^{0.5}$ . The outer surface of the cladding could be fairly brittle (hydrogen content greater than 800 ppm) but much of the cladding thickness has a reasonable toughness.

In conclusion, hydride cracking and embrittlement of the cladding is excluded from the TSPA-LA on the basis of low consequence. The NRC requirements in 10 CFR 63.114 (e and f) allow this omission because the small amount of hydride cracking and embrittlement that will occur during the regulatory period will not significantly change the magnitude and time of the radiological exposures to the reasonably maximally exposed individual (RMEI), or radionuclide releases to the accessible environment. The stresses in the cladding are not sufficient to fail the cladding at the repository temperatures and experimental data indicate that the in-package environment and cladding stresses are not conducive to hydride cracking and embrittlement.



Source: Keyns et al. 1996 [DIRS 100462]

Figure 6.12-1. Fracture Toughness vs. Hydrogen Content of Zircaloy-4

### **6.12.1 Hydride Embrittlement from Zirconium Corrosion (of Cladding)**

The hottest rods will pick up only small quantities of hydrogen from cladding surface general corrosion after the waste package fails. Waste packages are failed at various times, permitting water or moist air to enter. Wet oxidation (or steam oxidation if the local temperature is above boiling) occurs, and approximately 17 percent of the hydrogen released from the water is absorbed by the fuel cladding in the failed waste package (Lanning et al. 1997 [DIRS 101704], Volume 1, p. 8.4, Figure 8.2). However, the fuel cladding picks up little hydrogen because the corrosion rate is so slow (see FEP 2.1.02.13.0A). Even the hottest rods will pick up only small quantities of hydrogen from cladding surface general corrosion.

### **6.12.2 Hydride Embrittlement from Galvanic Corrosion of Waste Package Contacting Cladding**

Hydride embrittlement from galvanic corrosion of waste package contacting cladding has been excluded based on low consequence. Cladding has a thick oxide layer that is produced during reactor operation. The oxide coating is electrically insulating and will prevent electric contact of dissimilar metals. It is kinetically noble (Yau and Webster 1987 [DIRS 100494], Table 15, p. 718) and, for zirconium, the most noted effect is accelerated corrosion of the other material. If passive film has been mechanically removed the unprotected cladding oxidizes and forms a passive layer within seconds if exposed to water or humid air (Hansson 1984 [DIRS 101676], p. 6). Inside the failed waste package, the cladding would behave as a cathode and the steel box would be an anode if they were electronically coupled (Yau and Webster 1987 [DIRS 100494], Table 15, p. 718). The cladding would undergo little hydrogen charging because the oxide layer prevents hydrogen absorption in the metal (IAEA 1998 [DIRS 150560], p. 92, see FEP 2.1.12.03.0A). The consequence of hydrogen charging would be to hydride the zirconium. Direct absorption of hydrogen gas in the environment into zirconium has occurred with clean zirconium metals that have nickel coatings to prevent oxidation of the surface. It is unlikely to occur with irradiated cladding, which has heavy oxide coatings.

Other corroborating information is available. The importance of galvanic hydrogen conditions can be inferred from results in “Corrosion Properties of Zirconium in Chloride Solutions” (Yau 1983 [DIRS 149233], p. 26/10). Yau discusses a series of experiments in which zirconium alloy U-bend samples were exposed to boiling seawater for 365 days. Each sample was loaded by an uninsulated steel coupling. Three compositions (Zr 702, Zr 704 with up to 1.3 percent nickel, and Zr 704 without nickel) were considered and tested in both unwelded and welded conditions. Of the six samples, only the welded sample of Zr 704 with nickel showed hydrogen pickup. Clayton (1984 [DIRS 131741]) also observed the role of nickel in hydrogen absorption. The composition limit for these materials is the maximum hydrogen content of 50 ppm. Except for the welded sample of Zr 704 with nickel, the U-bend samples had hydrogen contents of 5 to 9 ppm at the end of the test. It is apparent that contact with a steel surface alone does not lead to galvanic hydrogen charging. Other factors, such as relative surface areas of the coupled anode and cathode, also affect the degree of radiolysis.

It is also important to compare the amount of nickel in various zirconium alloys. Zr 704 contains up to 1.3 percent nickel, Zr 702 contains up to 0.8 percent nickel, Zircaloy-2 contains up to 0.08 percent nickel, and Zircaloy-4 contains no more than 0.007 percent nickel. It is clear that

the Zircalloys contain small amounts of nickel, so hydriding as a result of contact with the steel basket tubes is not expected. It might be argued that, because of its nickel content, Zircaloy-2 cladding could be hydrided. However, Zircaloy-2 fuel cladding is used only for boiling water reactors, and most of the fuel cladding will be separated from the basket tubes by the fuel channels. Electrical coupling does not require physical contact, but the physical separation reduces the risk of galvanic corrosion. However, physical contact is required when insulating surface films (e.g., oxide coating) exist. Since the assemblies are loosely placed in the waste package and coated with thick oxides, they will not undergo hydrogen absorption. Therefore, this FEP is screened out as low consequence.

Hydriding of zirconium alloys as a result of contact with dissimilar materials has been observed, so it is important to consider the conditions that promote hydriding. In this case, the dissimilar metal forms a hydrogen window, not galvanic coupling. Clayton (1984 [DIRS 131741], p. 578) lists a series of experiments in which Zircaloy-4 fasteners clamped onto a sample of nickel-base alloy were hydrided by exposure to hot water with dissolved hydrogen. Clayton (1984 [DIRS 131741], p. 573) discusses the mechanism:

. . . in mechanically attaching a Zircaloy fuel rod fastener to an Inconel support plate, relative motion occurred during assembly. The relative motion was sometimes sufficiently severe and the bearing stress sufficiently high to overcome the protective effects of the corrosion oxide film and graphite lubricant. Smearing and bonding of Inconel onto local regions of the mating Zircaloy contact surface occurred and provided the potential for accelerated hydriding. Inconel has a relatively high permeability for hydrogen and acts as a “window” for hydrogen entry into the Zircaloy.

A similar but localized effect was noted for Zircaloy-4 smeared with Inconel alloy (75.2 percent nickel, 16.7 percent chromium, 3.5 percent copper, and 4.6 percent iron).

Although hydriding was observed in the experiments discussed above, it does not follow that hydriding will occur under repository conditions. As is noted in Clayton (1984 [DIRS 131741], p. 587), “Nickel alloy smearing and bonding to filmed Zircaloy, rather than just tight surface contact, is necessary for accelerated hydriding.” Since fuel assemblies will be lowered carefully into waste package baskets, high contact pressures typical of fastener tightening are not expected. After emplacement, the fuel assembly will simply rest on the basket. Therefore, smearing and bonding should not occur. Few, if any, rods might undergo hydride embrittlement from galvanic coupling and, therefore, this FEP is being screened out as low consequence.

However, if it is supposed that there is some bonding between the fuel assembly and the basket, the significance of the effect must be examined. It should be noted that accelerated hydriding is a transient, not a persistent, effect. Clayton (1984 [DIRS 131741], p. 572) notes that the initial high accelerated hydrogen ingress rate was effectively shut off during exposure at 271°C in about 25 days. Because of the extremely small size of contact spots, corrosion of the carbon steel rack would quickly break the electrical contact between the two materials. Since the time of contact will be short, the amount of hydrogen absorbed as a result of contact will also be small (low consequence). This conclusion is supported by the discussion of U-bend hydriding above.

Ralph et al. (2002 [DIRS 161992]) report an example of intimate contact between cladding and steel (due to corrosion of the fuel racks) in a spent fuel pool at a U.S. commercial nuclear plant. After an extended lay-up period, the spent fuel pool water was found to contain a significant amount of algae and bacteria. During the period when the water chemistry in the spent fuel pool was not maintained, this water still could be a poorer electrolyte than water seeping into the failed repository waste package. Biological agents were purged using controlled additions of chlorine and hydrogen peroxide before the pool was returned to normal operating chemistries. The assessment revealed that the steel rack corrosion products were up to 2.5 cm thick, and the corrosion products had started to engulf the individual fuel rods or flow channels of the stored assemblies in the region where the rack and plates contacted the fuel assemblies. The corrosion product had adhered to the fuel. The iron oxide was composed of FeO, Fe<sub>2</sub>O<sub>3</sub>, and Fe<sub>3</sub>O<sub>4</sub>. Ralph et al. (2002 [DIRS 161992], p. 6) states:

One fuel assembly was removed from its storage location and its channel was removed. The oxide from contact with the carbon steel rack was removed with a water lance utilizing 350 to 700 kg/cm<sup>2</sup> of water pressure. A camera with resolution of 0.025 mm was used to inspect the channel. The channel surface appeared uniform and smooth. No pitting, white discoloration or surface anomalies were observed.

The paper concluded: “The fuel cladding was not affected through any type of corrosion. Therefore, the corrosion did not change the classification of the fuel as intact or damaged.” While it is not likely that galvanic corrosion occurred, if it had, the passivated zirconium alloy would have served as the cathode. Thus, a lack of zirconium corrosion does not demonstrate that galvanic corrosion did not occur. A lack of zirconium hydriding, however, would.

### **6.12.3 Delayed Hydride Cracking (of Cladding)**

Failure of the cladding by DHC has been excluded from the TSPA-LA analysis because few, if any, fuel rods will fail from DHC (low consequence, would not have a significant effect on the resulting radionuclide exposures to the RMEI). The stresses (and stress intensity factors,  $K_I$ ) are lower than the threshold stresses and stress intensity factors ( $K_{IH}$ ) and therefore, few, if any, cracks will propagate and fuel rod failure is not expected.

Peehs (1998 [DIRS 109219], pp. 5, 6) concluded that DHC would not occur in dry storage. The thermal history for dry storage is similar to the earlier period of repository closure, except the repository is cooler (i.e., a maximum temperature of 268°C in [Appendix A of this report] vs. 400°C [NRC 2002 [DIRS 164593]]). Cragolino et al. (1999 [DIRS 152354], p.4-21) reviewed the stress intensity factors and threshold values and also concluded that DHC is not relevant under repository conditions.

Additional corroborating information follows. Rothman (1984 [DIRS 100417], pp. 33 to 39) reviewed DHC in Zircaloy cladding in a repository. He concludes that DHC is unlikely unless the fuel rods have large existing cracks (exceeding approximately 50 percent of wall thickness) and high stresses (exceeding approximately 137 MPa). Reviews of DHC are available in Section 6.3 of *Hydride-Related Degradation of SNF Cladding Under Repository Conditions* (CRWMS M&O 2000f [DIRS 148251]) and *Initial Cladding Condition* (CRWMS M&O 2000c

[DIRS 151659], Section 6.10.2). During delayed hydride cracking, hydrides slowly form at a crack until it propagates through the hydride region at the crack tip and stops. This sequence repeats itself as the crack propagates slowly through the metal. The hydrides preferentially collect at the crack tip. The hydrogen diffuses to a stressed crack tip because the locally high stress reduces the hydrogen chemical potential. The higher tensile stress also reduces the solubility in that region. The critical stress intensity factor ( $K_{IH}$ ) is the minimum stress intensity that will permit any DHC, regardless of velocity (velocity approaches 0). For this analysis (CRWMS M&O 2000d [DIRS 136058]), the stress intensities ( $K_I$ ) were calculated and compared to the threshold stress intensity factor  $K_{IH}$ . If  $K_I > K_{IH}$ , then the crack will start to propagate and, because of long repository times, failure will occur. The threshold stress intensity for DHC is the minimum stress intensity where crack propagation is possible (at a slow velocity). DHC failure occurred in some zirconium coolant tubes in a CANDU reactor where high temperature gradients caused excess hydride buildup in a specific location (Cox 1990 [DIRS 152778], p. 2).

The stress intensity factor,  $K_I$ , is a measure of the increased stress at the tip of a crack. The stress intensity factor is proportional to the far-field stress times the square root of the crack depth. For a sharp crack, a limiting case, the stress intensity factor is (Reed-Hill 1973 [DIRS 121838], p. 800):

$$K_I = St \times \sqrt{\pi w} \quad (\text{Eq. 6.12-1})$$

where

$K_I$  = Stress intensity factor, MPa·m<sup>0.5</sup>

$St$  = Cladding stress, MPa

$w$  = Crack depth, m

Equation 6.12-1 is slightly modified from the form given by Reed-Hill; the crack depth  $w$  is used in place of  $c/2$ , where  $c$  is the crack length (Dieter 1961 [DIRS 147973], p. 194).

DHC is analyzed in Section 6.10.2 of *Initial Cladding Condition* (CRWMS M&O 2000c [DIRS 151659]). The calculated crack size distribution is given in Figure 17 of *Initial Cladding Condition* (CRWMS M&O 2000c [DIRS 151659], Section 6.6). The median ( $P = 50$  percent) value is 13  $\mu\text{m}$  and the average crack is 18.6  $\mu\text{m}$ . The largest size crack of the 2000 samples is 119  $\mu\text{m}$ . The calculated stress distribution (CRWMS M&O 2000c [DIRS 151659], Section 6.7) is given in Figures 18 and 26 of that report. DHC is unlikely at temperatures above 260°C (Mahmood et al. 2000 [DIRS 152241], p. 139), because of the plasticity of the material. Rothman (1984 [DIRS 100417], p. 37) reports that DHC is unlikely above 250°C because of the plasticity of the material. For this calculation, the temperature of 268°C (maximum cladding temperature, see Table A-2) is used and the pressure is adjusted accordingly. The peak stress intensity factor,  $K_I$ , was calculated for both peak temperature and temperature after 10,000 years of alpha decay and ranges in value from 0.47 to 2.73 MPa·m<sup>0.5</sup> (Table 6.11-1).

The work of Shi and Puls (1994 [DIRS 102084], p. 239, Fig. 7), shows experimental  $K_{IH}$  in the range of 5 to 12 MPa·m<sup>0.5</sup> for zirconium alloy containing 2.5 percent Nb. Rothman (1984 [DIRS 100417], p. 37), reports a  $K_{IH}$  of 6 MPa·m<sup>0.5</sup> for Zircaloy-2. Pescatore et al. (1990 [DIRS 101230], Table 6, p. 50) report values of 5 and 14. Huang (1995 [DIRS 101683], p. 195) shows  $K_{IH}$  for irradiated Zircaloy-2 approached 6 MPa·m<sup>0.5</sup>. For this report, Huang's and Rothman's

value for irradiated cladding of  $6 \text{ MPa}\cdot\text{m}^{0.5}$  was used. Because the  $K_I$  values are well below the threshold values, exactly which  $K_{IH}$  value is selected is not important. No  $K_I$  values in this report's sampling (Table 6.11-1) of rods are near the threshold stress intensity value. The maximum  $K_I$  was  $2.73 \text{ MPa}\cdot\text{m}^{0.5}$  and the mean value was  $0.73 \text{ MPa}\cdot\text{m}^{0.5}$ .

Cragolino et al. (1999 [DIRS 152354], p. 4-27) suggested that, when considering small cracks, lower threshold stress intensities ( $K_{IH}$ ) could cause failure. The Dry Storage Characterization Project (EPRI 2002 [DIRS 161421]) studied the condition of fuel assemblies that were exposed to various thermal transients (peak temperatures to  $415^\circ\text{C}$ ) followed by 15 years of dry storage (peak temperature at  $342^\circ\text{C}$  and slowly decreasing). These temperatures are higher than expected at the repository (Appendix A of this report). Rod failure during dry storage was not observed suggesting that delayed hydride cracking from small cracks did not fail rods, even in a 15 year cooldown.

#### **6.12.4 Hydride Reorientation (of Cladding)**

Hydride reorientation has been excluded on the basis of low consequence since few if any rods will undergo reorientation and reoriented rods might not fail. Because of the low peak temperatures (less than  $270^\circ\text{C}$  for center rod), few rods will undergo reorientation. Hydride reorientation does not necessarily indicate cladding failure. Puls (1988 [DIRS 102067]) measurements showed significant strength after reorientation. Dry storage tests (EPRI 2002 [DIRS 161421]), which exposed irradiated fuel rods to numerous thermal cycles, showed little or no reorientation.

Cragolino et al. (1999 [DIRS 152354], p. 4-22) concluded that reorientation is unlikely if stresses are below 100 MPa and the maximum temperatures are below the hydrogen solvus temperature ( $290\text{-}300^\circ\text{C}$ ). Table 6.11-1 provides the stress distribution value for the hottest rods (center location of the hottest waste package). Only about 8.4 percent of the center rods exceed 100 MPa stress at peak temperature. At other locations in the waste package, a lower percent will exceed 100 MPa. No rods are expected to exceed the solvus temperature since the maximum temperature is  $268^\circ\text{C}$  (Appendix A of this report). Using the screening arguments suggested by Cragolino et al. (1999 [DIRS 152354]), few, if any, rods are expected to undergo reorientation.

Additional corroborating information follows. Section 6.4 of *Hydride-Related Degradation of SNF Cladding Under Repository Conditions* (CRWMS M&O 2000f [DIRS 148251]) reviewed hydride reorientation. The total hydrogen content in the fuel cladding is not as important as the amount of hydrogen in hydrides aligned perpendicular to the largest principal tensile stress. In commercial reactor cladding during irradiation, hydrides form in a circumferential orientation (the normal to the platelet is in the radial direction). Such hydrides do not significantly weaken the cladding against hoop stress. Reorientation usually occurs under tensile stresses ranging from 69 to 208 MPa (with temperature dependency). Test rods at the low end of this range, but significantly higher than the stress expected for most rods at the repository temperatures, showed no hydride reorientation. This lack of reorientation indicates that there should be little, if any, cladding degradation due to hydrides under normal repository temperatures (Einzig et al. 1982 [DIRS 101604], p. 65). In one dry storage test, reorientation to the radial direction was observed in one rod (Einzig and Kohli 1984 [DIRS 101605], p. 119) although rod failure did not occur.

This occurred in a fuel rod with high stresses (145 MPa at 323°C). Reorientation was not observed in fuel rods with lower stresses (13 to 26 MPa). The hydride reoriented so that the normals in the circumferential direction could possibly weaken the cladding. Reorientation was also observed in CANDU reactor coolant pipes. Hydride reorientation under repository conditions was investigated as a potential cladding degradation mode.

Using reorientation data collected by Pescatore et al. (1990 [DIRS 101230], pp. 52 to 55), Section 6.2.6 of *Clad Degradation – Summary and Abstraction* (CRWMS M&O 2001a [DIRS 151662]) developed a reorientation equation that defines the temperatures and stresses where reorientation is observed. This line can be defined as:

$$S_r = 335 - 0.6 \times T^{\circ}\text{C} \quad (\text{Eq. 6.12-2})$$

where

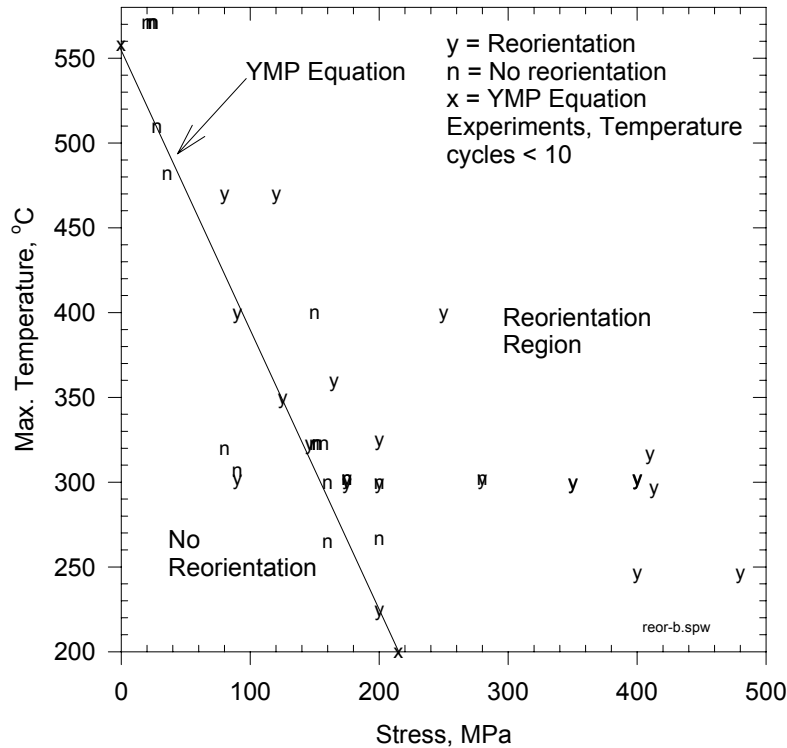
$S_r$  = stress, MPa, required for reorientation

$T$  = Peak Temperature, °C, required for reorientation.

Additional data (Cappelaere et al. 2002 [DIRS 164195], p. 9, Chan 1996 [DIRS 111876], Coleman 1982 [DIRS 111999], Einziger et al. 1982 [DIRS 101604], Einziger and Kohli 1984 [DIRS 101605], Simpson and Chow 1987 [DIRS 164483], Wallace et al. 1989 [DIRS 112344], p. 68) are compared with the equation in Figure 6.12-2. Compared to the repository cooldown period, the time periods for those tests were short, but inspection of rods exposed to dry storage cooldown (15 years cooldown) also showed no hydride reorientation. If Equation 6.12-2 is considered a model, then Figure 6.12-2 could be considered validation of this model since the sources cited above are independent of the source for the equation (Pescatore et al. 1990 [DIRS 101230], pp. 52 to 55).

Figure 6.12-2 and Equation 6.12-2 show that at the cladding maximum temperature of 268°C, the stress would have to be greater than 174 MPa before reorientation would occur. This corresponds to about 94 MPa at ambient temperature. Based on *Initial Cladding Condition* (CRWMS M&O 2000c [DIRS 151659]), an estimated 0.45 percent of the rods could have stresses this high and might undergo some reorientation. This is a small amount of the total inventory and supports the screening argument of low consequence. Rothman (1984 [DIRS 100417]) also studied cladding degradation in a repository and concluded that hydride reorientation would not occur. He did not consider fuel with burnups and stresses as high as considered in *Initial Cladding Condition* (CRWMS M&O 2000c [DIRS 151659]).

Pescatore et al. (1990 [DIRS 101230], pp. 54, 69) state that even with hydride reorientation, stress levels will be insufficient to result in DHC and clad failure. Rothman (1984 [DIRS 100417], pp. 33 to 39) concludes that hydride reorientation is also unlikely because of the lack of large temperature gradients in the repository and the cladding stresses are lower than needed for reorientation. Peehs (1998 [DIRS 109219], pp. 5, 6) concluded that hydride reorientation would not occur in dry storage. The temperature history for dry storage is similar to that of the early times (first 100 years) of repository closure and, therefore, similar hydride motion would be expected to be negligible.



Source: CRWMS M&O 2001a [DIRS 151662]

Figure 6.12-2. Comparison of the YMP Reorientation Equation with Additional Experimental Data

Puls (1988 [DIRS 102067], p. 1507-1522) performed a series of strain tests on Zircaloy-2 with reoriented hydrides. His results are summarized in Table 6.12-1. He took samples of CANDU coolant tubing and performed strain tests in the circumferential direction. The tubing is made in a similar fashion as cladding and develops hydride platelets with their normals in the radial direction. All tests were performed at ambient temperature. He used samples with both 20 ppm and 90 ppm hydrogen content and used two reorientation techniques to form hydrides of various lengths. One technique cooled the samples from 250°C with the stress near the yield point (designated y in Table 6.12-1). Other samples were cooled from 350°C at a stress of 200 MPa. This stress is more than twice that expected for most cladding in the repository (CRWMS M&O 2000c [DIRS 151659], Figure 26). Longer hydrides were produced by cooling samples in a furnace, while shorter ones were produced by bench cooling samples. Table 6.12-1 provides the range of hydride lengths. Two types of samples were used, smooth and notched (designated by “n” in the table). The table provides the stress ( $\sigma_y$ ) for which 0.2 percent strain was measured. Also provided is the ultimate stress at which necking and imminent failure was observed (or, for the arrested tests, was expected). For some experiments, the tests were stopped when the sample started to neck, but before failure (designated a for arrested in the table). In all of these tests, the reoriented hydrides did not significantly change the stress for 0.2 percent strain or the ultimate stress. Both stresses are much higher than those expected in repository cladding. The yield and ultimate strains reported are also higher than the strain failure criteria of 1 percent used in the cladding strain failure analysis developed by Peehs and Fleisch (1986 [DIRS 102065]).

Table 6.12-1. Puls' Zircaloy-2 Strain Tests on Zirconium with Reoriented Hydrides

Hydride Length (μm)	Type*	Yield Stress (0.2%) (MPa)	Tensile Stress (MPa)	Uniform/Total Strain (%)
Initial Material		627	650	-
7-20	-	632	678	4.7/15.8
7-20	y	627	675	4.7/15.8
7-20	-	612	659	4.7/15.8
7-20	n	783	885	-
7-20	n, y	774	882	-
7-20	n	933	1095	-
7-20	n	766	858	-
7-20	a	628	698	6 / 9
30-60	-	627	689	4.7/14.3
30-60	y	605	661	4.7/14.3
30-60	n	861	958	-
30-60	n, y	776	921	-
50-90	-	1079	1160	4.1/13.6
50-90	y	689	741	4.1/13.6
50-90	-	625	647	4.1/13.6
50-90	n	721	803	-
50-90	n, y	923	1032	-
50-90	n	811	936	-
50-90	a	633	701	- / 6
50-90	a	643	730	- / 6

\*Type, y= hydride reoriented near yield stress, n - notched, a = arrested (test terminated before failure)

Source: Puls 1988 [DIRS 102067], Tables 1,3,6

Hydride reorientation might require all the hydride platelets to be dissolved before cool-down and reprecipitation starts. This could be necessary because the hydrides prefer to reprecipitate on existing platelets and these earlier, existing platelets are oriented in the circumferential direction. For all the hydrides to dissolve at a maximum cladding temperature of 268°C, the initial concentration must be less than 44 ppm (see Table 6.12-2). *Initial Cladding Condition* (CRWMS M&O 2000c [DIRS 151659], Figure 15) shows that less than 5 percent of the fuel has an average concentration this low. Knowing that the hydride concentration is directly proportional to the oxide thickness, *Initial Cladding Condition* (CRWMS M&O 2000c [DIRS 151659], Figure 12) shows the fuel that could reorient under this hypothesis is the fuel with the lower burnups and, therefore, lower stresses. Mardon et al. (1997 [DIRS 109213], Figure 3, p. 408) show hydride content as a function of burnup. To have less than 21 ppm, the figure shows that Zircaloy 4 fuel with burnups less than 10 MWd/kgU has low enough hydride concentrations to dissolve all the hydrides at 350°C. Again, these fuels would have the lowest stresses. Rods clad with M5™ or ZIRLO have thinner oxide coatings (see Figure 6.3-1) and therefore, lower hydride content. These rods would be susceptible to reorientation at higher burnups if complete dissolution is needed. The rod that Einziger observed to undergo reorientation was exposed to a 570°C transient which would support a solubility of 729 ppm (Table 6.12-2). It is possible that all the hydrides were dissolved in that experiment.

Table 6.12-2. Saturation Limits ( $T_{ssd}$ ) for Hydrogen in Unirradiated Zirconium as a Function of Temperature

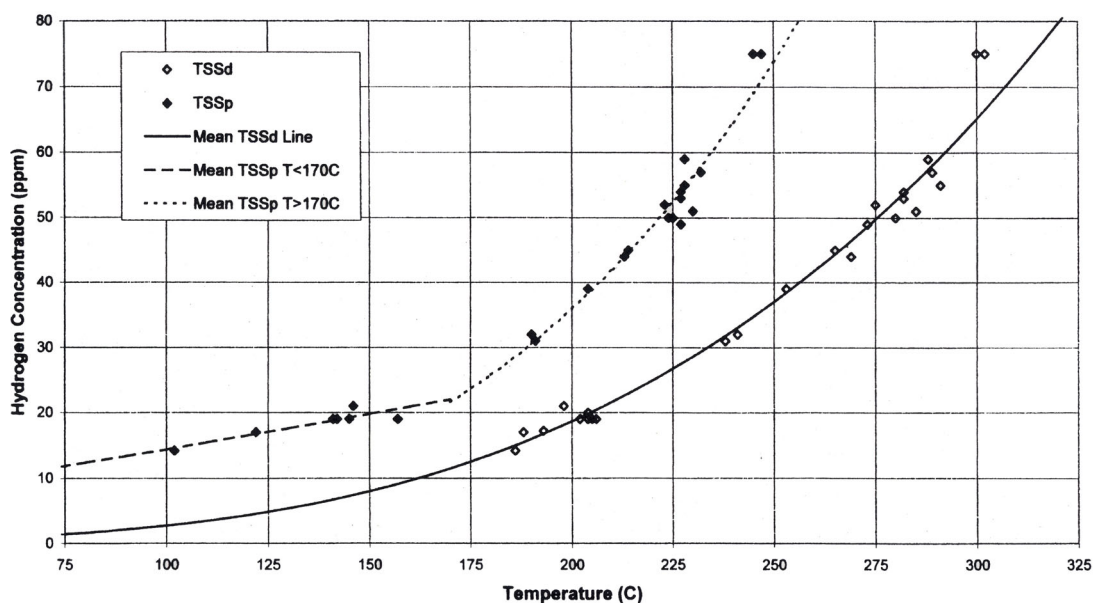
Temperature (°C)	H Concentration (ppm)	Temperature (°C)	H Concentration (ppm)
40	0.1	300	66
50	0.2	310	75
60	0.3	320	85
70	0.4	330	96
80	0.6	340	108
90	0.9	350	120
100	1.2	360	134
110	1.6	370	149
120	2.1	380	165
130	2.8	390	182
140	3.6	400	201
150	4.6	410	221
160	5.8	420	242
170	7.3	430	264
180	9.0	440	288
190	11	450	313
200	13	460	339
210	16	470	367
220	19	480	396
226	22	490	427
230	23	500	459
240	27	510	493
250	32	520	529
260	38	530	565
<b>270</b>	<b>44</b>	540	604
280	50	550	644
290	58	560	686
300	66	570	729

Source: Pescatore et al. 1990 [DIRS 101230], Eq. 6, p. 44

Further support for these conclusions is provided by Figure 8 of “Effects of Irradiation and Hydriding on the Mechanical Properties of Zircaloy-4 at High Fluence” (Garde 1989 [DIRS 113614]), which shows a clear correlation between oxide thickness and hydrogen content. Of greater significance however is the conclusion that low ductility values were obtained on guide tube tensile samples (dog-bone and ring tensile samples) at 300°C because of the high value of the hydride orientation factor and the fact that the hydrogen concentration was barely above the solubility limit for these samples (see comment column in Garde’s Table 5). This observation implies that the hydrogen content of these samples was sufficiently low to go back into solution and then reorient on favorable precipitation sites. By contrast, cladding samples with higher hydrogen concentrations retained a number of hydride platelets and these sites were preferential locations for reprecipitation.

Recently, fuel from a Dry Storage Characterization Project at the Idaho National Engineering and Environmental Laboratory was examined after about 15 years of dry storage. Rods were exposed to stresses up to 62 MPa at temperatures approaching 415°C (EPRI 2002 [DIRS 161421], p. II-4-6) and there were few, if any, radial hydrides in the Surry fuel rods. These rods were exposed to a slower cooldown period (15 years) than those used in the reorientation experiments plotted in Figures 6.12-2 and 6.12-3, yet reorientation was not observed. Comparison of these temperatures and pressures with the equation plotted in Figure 6.12-2 suggests that reorientation would not be expected. Recent NRC Interim Staff Guidance (NRC 2002 [DIRS 164593], Appendix, p. 2) for dry storage and transportation suggests that reorientation is not significant if temperatures are below 400°C, which is well above the maximum temperature of 268°C.

In summary, few, if any, rods will undergo hydride reorientation and their failure is unlikely. If cladding failure from hydride reorientation had been included in the abstraction for TSPA-LA no changes would be seen. Stresses and temperatures are too low for hydride reorientation to occur in most of the fuel, and since the cladding material will maintain sufficient toughness even if hydride reorientation did occur, failure would not be expected.



Source: McMinn et al. 2000 [DIRS 112149], Figure 15, p. 187

Figure 6.12-3. Dissolution and Precipitation Solubilities for Hydrogen in Irradiated Zirconium Metal

### 6.12.5 Hydride Axial Migration (of Cladding)

Hydride axial migration has been excluded from further consideration based on low consequence of occurrence. It is unlikely that sufficient hydrogen can be moved because of a lack of large temperature gradients (limits the driving force) in the waste packages and the low peak temperatures (limiting the amount of hydrogen in solution).

Hydrides can form in cooler parts of the rod (end sections) because the hydrogen can dissolve into the fuel cladding metal matrix at a warmer area, diffuse toward the cooler area, and

condense there. The effect was studied for dry storage (Cunningham et al. 1987 [DIRS 101591], Appendix C) and, for a 90-year period, was determined not to be a problem. Cappelaere et al. (2002 [DIRS 164195], p. 5) studied axial hydrogen redistribution under dry storage conditions and concluded that with a maximum cladding temperature of 470°C, and an axial temperature gradient of 180°C, after 100 years, the amount of hydrogen in the cold end would increase by 110 ppm. They conclude that axial hydrogen migration towards the ends of the rods is small. With the lower peak temperatures (268°C) and temperature differences from rod center to ends (19°C) (CRWMS M&O 2000e [DIRS 147881], Table 6-4) in the repository, even less migration is expected. Replacing the helium fill gas with humid air would increase the temperature difference, but not to the degree reported by Cappelaere et al.

As the repository cools, the driving forces for this redistribution (hydrogen solubility, temperature gradient, and diffusion rate) all decrease. The waste package internals will act to minimize the temperature variation along the length of the fuel assembly. Figure 15 by McMinn et al. (2000 [DIRS 112149]) (reproduced here as Figure 6.12-3) gives the solubility of hydrogen. The solubility varies whether one dissolves or precipitates the hydrogen to form hydrides. Zirconium hydrides have a larger volume than the zirconium metal that they displace and the difference in the dissolution solubility (TSSd) and the solubility for precipitation (TSSp) represents a type of super-saturation. This difference in temperatures is required to have axial migration along the rod. The figure shows that in order to move the hydrogen, a minimum temperature difference of 42°C between the hot location and cold location is needed. At temperatures below 200°C, temperature differences over 75°C are needed to move the hydrogen. At a peak cladding center temperature of 268°C, a difference of at least 50°C is needed to move and precipitate hydrogen. After repository closure, temperature differences of 19°C are predicted (CRWMS M&O 2000e [DIRS 147881], Table 6-4). Therefore, little or no axial migration is expected based on the difference between condensation and dissolution solubility.

#### **6.12.6 Hydride Embrittlement from Fuel Reaction (Causes Failure of Cladding)**

Cladding failure from hydride embrittlement due to fuel reaction has been excluded from further consideration based on low consequence. Clad degradation from fuel reaction is always associated with further degradation of failed fuel, and is mostly observed in failed BWR rods Edsinger 2000 [DIRS 154433]. Both high temperatures and steam environments are required for rod unzipping (propagation of the initial failure from a DHC type cracking). The conditions inside the fuel rod become reducing with the UO<sub>2</sub> consuming any free oxygen. The protective oxide film on the cladding interior becomes disturbed and hydrogen is absorbed into the cladding. In the repository reducing conditions are not expected and therefore hydrogen absorption from fuel/cladding interaction would be minor. In an intact rod, the pellet gap and plenum are inert, so the fuel does not react. Failure of intact rods is not expected. In summary, hydride cracking of the cladding has been excluded from TSPA-LA because of low consequence since the stresses are not sufficient to fail the cladding at repository temperatures.

### **6.13 CLADDING UNZIPPING**

#### **FEP Number:**

2.1.02.23.0A

**YMP FEP Description:**

In either dry or wet oxidizing conditions and with perforated fuel cladding, the UO<sub>2</sub> fuel can oxidize. The volume increase of the fuel as it oxidizes can create stresses in the cladding that may cause gross rupture of the fuel cladding (unzipping).

**Descriptor Phrases:**

Cladding unzipping after initial perforation  
Dry oxidation/unzipping of cladding  
Volume increase of corrosion products (cladding unzipping)  
Wet oxidation/unzipping of cladding

**Screening Decision:**

Included

**TSPA-LA Disposition:** Cladding axial splitting or unzipping is included in the TSPA-LA as being instantaneous once the waste package fails and the cladding is perforated. The cladding degradation abstraction models all failed rods (after initial perforation) as bare fuel pellet fragments for the full length of the fuel rod. Failed fuel rod unzipping (cladding axially splits down its length) is caused by the volume increase of corrosion products, FEP 2.1.09.03.0A, (fuel or cladding). It is based on experimental observations at Argonne National Laboratory, where 2 of 2 rods unzipped in less than 2 years. Unzipping leaves fuel pellets exposed to the waste package internal environment. Details of the scientific analysis that describes the disposition in greater detail is presented in *Clad Degradation – Summary and Abstraction for LA* (BSC 2003a [DIRS 162153]).

Unzipping by dry oxidation (oxidation of UO<sub>2</sub> to U<sub>3</sub>O<sub>8</sub>) of the fuel requires low humidity and high temperature conditions. Dry oxidation is expected to occur in the repository if the waste package fails at closure and the fuel is exposed to the temperature transients presented in Appendix A of this report. If it should occur, it also would cause rapid unzipping and is well modeled with the instant unzipping model used in TSPA-LA. Unzipping by wet oxidation was not observed in the ANL tests because unzipping due to the fuel-side cladding corrosion occurred first. Wet oxidation is still fast and can be modeled by the instant unzipping model where necessary.

**Related FEPs:**

2.1.02.12.0A, Degradation of cladding prior to disposal  
2.1.09.03.0A, Volume increase of corrosion products impacts cladding

**6.14 MECHANICAL IMPACT ON CLADDING**

**FEP Number:**

2.1.02.24.0A

**YMP FEP Description:**

Mechanical failure of cladding may result from external stresses such as rockfall or impact from waste package internals. Seismic induced impacts are addressed in a separate FEP.

**Descriptor Phrases:**

Rockfall (cladding damage)  
Waste package internals – cladding contact (cladding damage)

**Screening Decision:**

Excluded – Low Probability

**TSPA-LA Disposition:**

NA

**Related FEPs:**

1.2.03.02.0A, Seismic ground motion damages EBS components  
2.1.07.01.0A, Rockfall  
2.1.09.03.0A, Volume increase of corrosion products impacts cladding

**Screening Argument:** Mechanical failure of the cladding from external stresses originating outside the waste package has been excluded from the TSPA-LA on the basis of low probability. According to *FEPs Screening of Processes and Issues in Drip Shield and Waste Package Degradation* (CRWMS M&O 2001b [DIRS 153937], FEP 2.1.07.01.0A), nominal rockfall could damage the drip shield but will not deflect the drip shield sufficiently to contact the waste package. Waste package damage from rockfall was screened out based on low probability of occurrence. Therefore, during the 10,000-year regulatory period, no damage to the waste package is expected. The CSNF (waste form and cladding) is located inside the waste package and no damage is expected.

Mechanical failure of the cladding from external stresses originating inside the waste package, such as from the degradation of basket components and other WP internals, has also been excluded from the TSPA-LA on the basis of low probability of occurrence. Volume increase from the waste package corrosion products is addressed in BSC 2003c [DIRS 163935], Section 6.5.1.2.1.3.2. Initially the WP void fraction is 64% (4.7 m<sup>3</sup> free volume) but after the WP internals corrode, the void fraction is 26% (1.9 m<sup>3</sup> free volume). Because of the high void fraction, even after corrosion, the waste package corrosion products do not mechanically load and fail the cladding and there is sufficient free volume for any helium that is released from the fuel (see FEP 2.1.12.02.0A).

Another approach is to consider dimensional changes in the fuel channel that could be produced from hematite (Fe<sub>2</sub>O<sub>3</sub>) formation. The inside width of fuel channel is 22.64 cm and the steel component (fuel basket tube) is 0.5 cm thick (BSC 2003c [DIRS 163935], Table 34). The iron (density = 7.85 g/cm<sup>3</sup>) would change to hematite (density = 5.24 g/cm<sup>3</sup>) (BSC 2003c [DIRS 163935], Table 11). Considering the corrosion products can only form in the fuel channel, the inside dimension would decrease by 0.5 cm [(2 × 0.5 × 7.85/5.24) – 2 × 0.5 = 0.5 cm]. The standard Westinghouse 17×17 assembly is 21.4 cm wide (DOE 1996 [DIRS 100320], p. 123). Although the free clearance would decrease from 1.2 cm to 0.7 cm after the formation of the hematite, fuel failure is not expected. In a fuel assembly, the rods do not contact each other and there is coolant spacing between the rods. Since no fuel failure is expected from the iron corrosion, this FEP is excluded in the TSPA-LA.

Effects of longer term loading due to volume increase from waste form and cladding corrosion products (i.e., internal stresses) are addressed in FEP 2.1.09.03.0A, Volume Increase of Corrosion Products Impacts Cladding. Seismic-induced rockfall, drift degradation, and ground motion are also not treated within this FEP. A full discussion of seismic effects is contained in FEPs 1.2.03.02.0A, Seismic Ground Motion Damages EBS Components; 1.2.03.02.0B, Seismic Induced Rockfall Damages EBS Components; and 1.2.03.02.0C, Seismic Induced Drift Collapse Damages EBS Components. The effect of seismic events on fuel and cladding is addressed in *Seismic Consequence Analysis* (BSC 2004e) [DIRS 167780].

## 6.15 NAVAL SNF CLADDING

### **FEP Number:**

2.1.02.25.0B

### **YMP FEP Description:**

DSNF to be disposed of in Yucca Mountain has a variety of fuel types that may not be similar to the CSNF to be disposed. Some of the fuel types may have initial cladding-degradation characteristics that are different from those for the CSNF. Therefore, the effectiveness of DSNF cladding as a barrier to radionuclide mobilization might be different from CSNF. This FEP addresses Naval SNF cladding only.

### **Descriptor Phrases:**

Degradation of Naval SNF cladding

### **Screening Decision:**

Included

**TSPA-LA Disposition:** Naval SNF cladding is modeled in the TSPA cladding degradation abstraction as CSNF cladding. The 300 waste packages containing naval SNF have been added to the CSNF inventory (approximately 7,500 waste packages) and both of these fuels are modeled as CSNF in the TSPA-LA. More information is available in *Initial Radionuclide Inventories* (BSC 2003d [DIRS 161961]). A previous comparison with an equivalent amount of Zircaloy-clad CSNF indicates that the effect on the resulting radionuclide exposures to the RMEI from the TSPA simulation using the commercial-fuel equivalent is significantly higher than the effect on the resulting radionuclide exposures to the RMEI from the source-term simulation for naval SNF (BSC 2001a [DIRS 152059], p. 36 and Figure 6.1-2). This analysis shows that modeling naval spent nuclear fuels as CSNF is conservative because of the robustness of naval SNF. Details of the scientific analysis that describes the disposition in greater detail is presented in *Clad Degradation – Summary and Abstraction for LA* (BSC 2003a [DIRS 162153]).

### **Related FEPs:**

All CSNF FEPs addressed in this report

## 6.16 DIFFUSION-CONTROLLED CAVITY GROWTH (DCCG) IN CLADDING

### **FEP Number:**

2.1.02.26.0A

**YMP FEP Description:**

Diffusion-Controlled Cavity Growth (DCCG) was once thought to be a possible creep rupture mechanism that could occur under the temperature and pressure conditions that prevailed during dry storage of spent fuel and might occur during disposal.

**Descriptor Phrases:**

Diffusion-controlled cavity growth (DCCG) cladding creep (rupture)

**Screening Decision:**

Excluded – Low Consequence

**TSPA-LA Disposition:**

NA

**Related FEPs:**

2.1.02.19.0A, Creep rupture of cladding

**Screening Argument:** Diffusion-Controlled Cavity Growth (DCCG) in cladding is excluded from the TSPA-LA on the basis of low consequence.

Glide and Coble creep rupture processes are included in the analysis and would account for creep failed fuel. Applicants for dry storage licenses for CSNF were once required by the U.S. Nuclear Regulatory Commission (NRC) to model diffusion controlled cavity growth (DCCG) to evaluate dry storage designs. That is, NUREG-1536 (NRC 1997 [DIRS 101903], Section 4.V.1) required the use of the DCCG method to calculate a maximum cladding temperature limit for a dry storage design. However, this design limit is overly restrictive and relatively inflexible. The literature does not support the use of this model for zirconium-based materials (Pescatore and Cowgill 1994 [DIRS 102066], p. 83 to 85) since it has not been validated, and voids and cavities are rarely seen in irradiated Zircaloy. Pescatore and Cowgill (1994 [DIRS 102066], p. 85) recommend a methodology of calculating the amount of creep and comparing it to a creep failure criterion. The earlier NRC Interim Staff Guidance (ISG) Number 11 (NRC 2000 [DIRS 147797]) for transportation and storage recognizes the controversy with the DCCG conceptual model and permits license applicants to use other creep models in their license application. ISG 11, Rev 2 (NRC 2002 [DIRS 164593]) does not address specific creep models but concludes that creep failures are unlikely if peak temperatures are below 400°C. The temperature profiles for dry storage (time at temperature, see Figure 6 of *Clad Degradation – Summary and Abstraction* (CRWMS M&O 2001a [DIRS 151662])) are similar to those in the early periods of repository closure when DCCG might occur. With peak cladding temperatures below 268°C (Appendix A of this report), creep failure (including DCCG failures) is not expected.

Hayes et al (1999 [DIRS 164598], Figures 2, 5, 6, 8, and 11) concluded that failure from DCCG is unlikely if the peak temperature is less than 330 to 400°C depending on the specific DCCG model (LLNL vs. PNNL), initial stress, and heat decay curve. None of their work suggests failure by DCCG at temperatures as low as 268°C. In summary, omission of this FEP is justified on the basis that DCCG has a low consequence of occurrence because DCCG, as a mechanism to fail Zircaloy cladding, is not expected to occur at the temperatures (peak temperatures below 268°C) predicted at the repository.

The creep analysis described in FEP 2.1.02.19.0A is an alternative conceptual model for DCCG model. The creep analysis was selected because of the stronger experimental basis for this type of strain.

In conclusion, DCCG in cladding is excluded from the TSPA-LA on the basis of low consequence. The NRC requirements in 10 CFR 63.114 (e and f) allow this omission because DCCG has not been observed experimentally and therefore will not significantly change the magnitude and time of the radiological exposures to the reasonably maximally exposed individual (RMEI), or radionuclide releases to the accessible environment.

## **6.17 LOCALIZED (FLUORIDE ENHANCED) CORROSION OF CLADDING**

### **FEP Number:**

2.1.02.27.0A

### **YMP FEP Description:**

Fluoride is present in Yucca Mountain groundwater, and zirconium has been observed to corrode in environments containing fluoride. Therefore, fluoride corrosion of cladding may occur in waste packages.

### **Descriptor Phrases:**

Localized corrosion of cladding enhanced by fluoride

### **Screening Decision:**

Excluded – Low Consequence

### **TSPA-LA Disposition:**

NA

### **Related FEPs:**

2.1.02.15.0A, Localized (radiolysis enhanced) corrosion of cladding

2.1.02.16.0A, Localized (pitting) corrosion of cladding

**Screening Argument:** Fluoride enhanced corrosion of cladding is excluded from the TSPA-LA on the basis of low consequence.

Hydrofluoric acid can contribute to an accelerated general corrosion with fluoride concentrations greater than 5 ppm and pH less than 3.18 (Pourbaix 1974 [DIRS 100817], p. 583). The in-package chemistry model (BSC 2003f [DIRS 161962], Attachment III) predicts pHs greater than 3.5 and J13 well water contains only 2.2 ppm of fluoride. Since neither of the conditions is met, accelerated corrosion from fluoride is not expected. Even if pH dropped below 3, fluoride enhanced localized corrosion of the cladding would not occur because the fluoride concentration would still be less than 5 ppm.

As corroborating evidence, corrosion of zirconium by fluorides is addressed in *Clad Degradation—Local Corrosion of Zirconium and Its Alloys Under Repository Conditions* (CWRMS M&O 2000d [DIRS 136058], Sections 4.1, 6.1.5, 6.2.2.3, and III.4). Zirconium resists attack by most halides, including halogen acids. The major exceptions are hydrofluoric

acid and ferric chloride (localized (pitting) corrosion of cladding, FEP 2.1.02.16.0A). As shown in Section 6.1.3 of *Clad Degradation–Local Corrosion of Zirconium and Its Alloys Under Repository Conditions* (CWRMS M&O 2000d [DIRS 136058]), zirconium is corrosion resistant to certain fluorides when the pH is sufficiently high. Low fluoride ion concentrations ( $F^-$  ions), on the order of a few ppm, in city or ground water have little effect on zirconium's excellent corrosion resistance. However, a few ppm of hydrofluoric acid (HF molecule in solution) will noticeably increase zirconium's corrosion rate. Hydrofluoric acid only exists in solution at pHs below 3.18 (Pourbaix 1974 [DIRS 100817], p. 583).

For accelerated corrosion to occur, the fluoride must be present as free ions (i.e., not complexed as compounds), and the pH must be low. A high insoluble fluoride concentration (in essence a low fluoride ion concentration) would not be expected to have much impact on the standard zirconium corrosion rate. Section 4.1.1 of *Clad Degradation–Local Corrosion of Zirconium and Its Alloys Under Repository Conditions* (CWRMS M&O 2000d [DIRS 136058], Test 12) shows that fluoride ion concentrations of less than 5 ppm, even at pH values as low as 1, produce similar corrosion rates to those with zero fluoride ion concentration. Thus, it is reasonable to conclude that low fluoride ion concentrations, as distinct from total fluoride content, will have limited impact on the uniform Zircaloy corrosion rate.

Zirconium and its alloys generally exhibit low corrosion rates in fluoride solutions, including relatively high fluoride ion content solutions, if the temperature is sufficiently low and the pH is sufficiently high. This is illustrated with the results in Section 4.1.1 of *Clad Degradation–Local Corrosion of Zirconium and Its Alloys Under Repository Conditions* (CWRMS M&O 2000d [DIRS 136058], Test 13). However, if the metal is in contact with solutions containing HF, the corrosion rate can increase rapidly. From the Pourbaix (1974 [DIRS 100817], p. 583) diagram, HF can exist when the pH is less than 3.18, although this does not necessarily mean that all fluoride ions are immediately converted to HF below this value. The data in Section 4.1.1 of *Clad Degradation–Local Corrosion of Zirconium and Its Alloys Under Repository Conditions* (CWRMS M&O 2000d [DIRS 136058], Tests 10 through 13) can be divided into fluoride ion-containing solutions and HF-containing solutions using a pH of 3.18 as the demarcation point. The calcium fluoride, due to its low solubility, does not contribute to the fluoride ion concentration (about 2 ppm at 25°C and less than 3 ppm at 90°C).

If the fluoride were to react with the cladding, the amount of corrosion would be limited by the amount of fluoride entering the waste package because the fluoride is consumed in the reaction  $Zr + 4F \rightarrow ZrF_4$ . For example, if 1 liter of J-13 well water enters a waste package each year, the total contained fluorine content is 2.2 mg (2.2 wt. ppm). If all the available fluorine reacts with zirconium to produce  $ZrF_4$ , the maximum quantity of zirconium that could be corroded away is 2.6 mg per year ( $4.0 \times 10^{-4}$  cc/year). This volume represents a general corrosion mechanism and would be distributed over the wet area. If it was concentrated at one spot of cladding surface area, 0.008 square centimeters of fuel would be exposed (using nominal wall thickness of 500 microns). This quantity of fuel exposure is not significant and, therefore, fluoride corrosion would be a low consequence degradation mode. Much larger quantities of water containing fluorides than were used in the example must enter the waste package to fail significant quantities of fuel.

Repository conditions (as represented by J-13 well water) would not be expected to produce any significantly different corrosion rates in zirconium and its alloys than in general corrosion (FEP 2.1.02.13.0A). The well water analysis (Table 6.17-1) shows a neutral solution with impurity concentrations too low to be corrosive to zirconium and its alloys. However, it has been hypothesized that ground water entering the repository may be concentrated in impurities as a result of evaporation. Table 6.17-1 provides the predicted values. Of particular note is the fact that the halide content could become enriched due to the high solubility of most chlorides and fluorides. As a result, the corrosive potential of the water increases as the halide concentrations increase. However, the pH of the solution increases at the same time, and this is favorable because zirconium and its alloys are generally corrosion resistant at the higher pH values. That is, J-13 well water will not become oxidizing when the pH is so high. Conceivably, solution pH within crevices may become acidic. As discussed in Section 6.1.10 of *Clad Degradation–Local Corrosion of Zirconium and Its Alloys Under Repository Conditions* (CWRMS M&O 2000d [DIRS 136058]) the condition in a crevice would be too reducing to support the formation of oxidizing ions.

*Clad Degradation – Summary and Abstraction* (CRWMS M&O 2001a [DIRS 151662]) contained an alternative conceptual model for fluoride corrosion. In that model the fluoride, at any concentration, was modeled to concentrate onto a 1-cm length of one rod and consume that rod until failure and then concentrate onto another rod. This sequential failure occurred well after the regulatory period and was not consistent with experimental observations cited above. This model has been dropped from TSPA-LA.

Table 6.17-1. Compositions of J-13 Well Water and Its Concentrates

Ion	Concentration (mg/liter)			
	J-13	Long Term Test Solution (1000x)	Beaker Evaporation (1000x)	90°C / 85% Relative Humidity
SO <sub>4</sub>	18.4	13,000	15,700	29,500
Cl	7.14	7,200	6,120	14,800
NO <sub>3</sub>	8.78	6,440	6,730	14,200
F	2.18	1,580	1,520	3,400
HCO <sub>3</sub>	128.9	47,326	31,471	11,370
Na	45.8	42,500	37,700	77,400
K	5.04	3,580	3,720	9,700
Ca	13.0	3	7	25
Mg	2.01	1	0	0
SiO <sub>2</sub> (aq)	61.0	109	7,124	22,500
pH	7.4	10.1	9.9	10

NOTE: Beaker Evaporation 1000X solution and Long Term Test 1000X solution agree reasonably well except the concentration of SiO<sub>2</sub> (aq). This disagreement could be attributed to the attack of the glass beaker by fluoride ions.

Source: BSC 2001b [DIRS 155640], Table 18

In conclusion, the magnitude and time of the resulting radiological exposures to the reasonably maximally exposed individual (RMEI), or radionuclide releases to the accessible environment, would not be significantly changed by the omission of this FEP (fluoride enhanced corrosion) from the performance assessment (TSPA-LA) model. Few, if any, rods would experience

accelerated corrosion because the pH is too high (> 3.18) for the formation of hydrofluoric acid and the concentration of fluorine is too low (<5 ppm).

## 6.18 ROCKFALL

**FEP Number:**

2.1.07.01.0A

**YMP FEP Description:**

Rockfalls may occur with blocks that are large enough to mechanically tear or rupture drip shields and/or waste packages. Seismic induced rockfall is addressed in a separate FEP.

**Descriptor Phrases:**

Rockfall (cladding damage)

**Screening Decision:**

Excluded – Low Probability

**TSPA-LA Disposition:**

NA

**Related FEPs:**

- 1.2.03.02.0A, Seismic ground motion damages EBS components
- 1.2.03.02.0B, Seismic induced rockfall damages EBS components
- 2.1.02.24.0A, Mechanical impact on cladding

**Screening Argument:** Rockfall damage of the cladding has been excluded from the TSPA-LA on the basis of low probability of occurrence because the drip shield prevents rocks from striking the waste package and possibly damaging the cladding. According to *FEPs Screening of Processes and Issues in Drip Shield and Waste Package Degradation* (CRWMS M&O 2001b [DIRS 153937]), nominal rockfall could damage the drip shield but will not deflect the drip shield sufficiently to contact the waste package. Therefore, during the 10,000-year regulatory period, no damage to the waste package is expected. The CSNF (waste form and cladding) is located inside the waste package and no damage is expected. While the fuel and cladding might experience some minor vibration from rockfall, no damage is expected. Fuel and cladding are exposed to vibration during transportation and damage is not observed (Debes 1999 [DIRS 161193]).

Seismic induced rockfall and drift degradation are not considered within this FEP. A full discussion of seismic effects is contained in FEPs 1.2.03.02.0A, Seismic Ground Motion Damages EBS Components; 1.2.03.02.0B, Seismic Induced Rockfall Damages EBS Components; and 1.2.03.02.0C, Seismic Induced Drift Collapse Damages EBS Components. The effect of seismic events on fuel and cladding is addressed in *Seismic Consequence Analysis* (BSC 2004e [DIRS 167780]).

## 6.19 VOLUME INCREASE OF CORROSION PRODUCTS IMPACTS CLADDING

### FEP Number:

2.1.09.03.0A

### YMP FEP Description:

Corrosion products have a higher molar volume than the intact, uncorroded material. Increases in volume during waste form and cladding corrosion could change the stress state in the material being corroded and lead to cladding unzipping.

### Descriptor Phrases:

Volume increase of corrosion products (cladding unzipping)

### Screening Decision:

Included

**TSPA-LA Disposition:** The volume increase of corrosion products causes cladding axial splitting, or unzipping, and is included in TSPA cladding degradation abstraction (BSC 2003a [DIRS 162153], Section 6.2.4). This FEP applies to failed cladding where water or moist air can interact with the fuel or cladding interior. The volume increase of corrosion products inside the cladding causes stress on the cladding and the cladding to tear open. This tearing is modeled to be instantaneous. All failed rods contain fuel pellet fragments for the full length of the fuel rod that are available for dissolution. Failed fuel rod unzipping (cladding axially splits down its length) is caused by the volume increase of corrosion products (fuel or cladding). It is based on experimental observations of two rods at ANL where both rods unzipped in less than two years. Unzipping leaves the fuel pellets exposed to the waste package internal environment. The scientific analysis that describes the disposition in greater detail is presented in *Clad Degradation – Summary and Abstraction for LA*, (BSC 2003a [DIRS 162153], Section 6.2.4).

Unzipping by dry oxidation (oxidation of  $\text{UO}_2$  to  $\text{U}_3\text{O}_8$ ) of the fuel requires low humidity and high temperature conditions. It is expected to occur in the repository if the waste package fails at closure and the fuel is exposed to the temperature transients given in Appendix A of this report. If dry oxidation should occur, it also would cause rapid unzipping and is well modeled with the instant unzipping model used in TSPA-LA.

The effects of basket component degradation on external cladding integrity have been evaluated in the FEP Mechanical Impact on the Cladding, FEP 2.1.02.24.0A.

### Related FEPs:

2.1.02.23.0A, Cladding unzipping

2.1.02.12.0A, Mechanical Impact of Cladding

## 6.20 ELECTROCHEMICAL EFFECTS IN EBS

### FEP Number:

2.1.09.09.0A

**YMP FEP Description:**

Electrochemical effects may establish an electric potential within the drift or between materials in the drift and more distant metallic materials. Migration of ions within such an electric field could affect corrosion of metals in the EBS and waste, and could also have a direct effect on the transport of radionuclides as charged ions.

**Descriptor Phrases:**

Electrophoresis/electro-osmosis  
Galvanic coupling (cladding)  
Galvanic coupling (waste form)

**Screening Decision:**

Excluded – Low Consequence

**TSPA-LA Disposition:**

NA

**Related FEPs:**

2.1.02.22.0A, Hydride cracking of cladding  
2.1.02.16.0A, Localized (pitting) corrosion of cladding

**Screening Argument:** Electrochemical effects (electrophoresis and galvanic coupling) are excluded from the TSPA-LA on the basis of low consequence.

Cladding, with its thick oxide layer produced in reactor operation, is kinetically noble (Yau and Webster 1987 [DIRS 100494], Table 15, p. 718). Any unprotected cladding oxidizes and forms a passive layer within seconds if exposed to water or humid air after being removed mechanically (Hansson 1984 [DIRS 101676], p. 6). Inside the waste package, the cladding would behave as a cathode and the steel box would be an anode if they are electronically coupled. The cladding can not undergo hydrogen charging because the oxide layer prevents hydrogen absorption in the metal (See FEP 2.1.12.03.0A). The consequence of such hydrogen charging would be to hydride the zirconium. Direct absorption of hydrogen gas in the environment into zirconium has occurred with clean zirconium metals with nickel coatings to prevent oxidation of the surface. It is unlikely to occur with irradiated cladding, which has heavy oxide coatings.

The Center for Nuclear Waste Regulatory Analysis (Cragolino 1999 [DIRS 152354], p. 4-13) surveyed various corrosion mechanisms for zirconium cladding under repository conditions. They concluded:

Zr is not susceptible to galvanic corrosion because the protective  $ZrO_2$  passive film leads to  $E_{corr}$  values in the galvanic series in flowing seawater close to those of noble metals and graphite but slightly lower than that of Ag (Yau and Webster, 1987). However, local corrosion promoted by galvanic coupling to a more noble metal may occur if the film is mechanically disrupted. Nevertheless, the repassivation rate of Zr and its alloys is sufficiently fast in many aqueous solutions that unless fretting is continuously occurring no substantial corrosion can be expected.

Possible effects of galvanic coupling between cladding and the carbon steel rack are likely to have a low consequence. After reactor operation, fuel assemblies are coated with a thick oxide, which has a high electrical resistance and would minimize the galvanic effect. After the waste package is breached, the carbon steel rack would behave as an anode if coupled with the cladding and could corrode more quickly. An increase in corrosion of the carbon steel rack at assembly contact points would have a low consequence. Stainless steel and aluminum plates would maintain the geometry for some time. Galvanic corrosion of cladding or fuel boxes is excluded from the TSPA because of low consequence.

Electrochemical effect on the waste form will also be minimal. The CSNF waste form is surrounded by the split zirconium cladding and would not be in direct contact with the waste package internals. If the  $\text{UO}_2$  did contact the steel fuel boxes and galvanic coupling did occur, the steel boxes would see the accelerated reaction and not the fuel pellets. As the  $\text{UO}_2$  corrodes, it coats itself with reaction products, which will minimize galvanic effects. Omission of electrochemical effects (electrophoresis and galvanic coupling) in the waste would not have a significant effect on the resulting radionuclide exposures to the RMEI because those effects are much smaller than the effects of modeling with a minimum flow rate through a failed container of 15 liters/yr used in performing the equilibrium-model calculations (CRWMS M&O 2000d [DIRS 136058]). This flow rate has a much greater effect than can be created by electrophoresis or electro-osmosis (Soderman and Jonsson 1996 [DIRS 149441]).

Galvanic coupling could theoretically affect the rate of redox reactions involved in waste form matrix degradation when the waste form matrix is an electronic conductor. For example, galvanic coupling between the CSNF matrix (a semiconductor) and cladding could influence the corrosion potential, and hence, the rate of oxidative dissolution of the CSNF matrix. However, data from tests performed on CSNF rod segments (which include the cladding) and on CSNF fragments in Zircaloy holders indicate that such hypothetical galvanic coupling has a negligible effect on the rate of corrosion of the fuel matrix and the associated radionuclide release rate. The effects of galvanic coupling on the corrosion and associated radionuclide release rate from DSNF are also negligible because the base case model for DSNF corrosion causes it to corrode completely in one TSPA time step. Electrochemical effects on DHLW degradation are negligible because the principal reactions involved are glass network hydrolysis reactions that are not influenced by electrochemical effects.

Electrochemical effects of various solutions that might cause pitting of the cladding are addressed in FEP 2.1.02.16.0A. The pitting model (BSC 2003g [DIRS 164667]) is an electrochemical model and the in-package chemistry model (BSC 2003f [DIRS 161962]) addresses the effect of EBS and waste package corrosion on chemistry. Figure 6.5-1 shows pH variation with time, including the effects of radiolysis. The depression of pH in this figure is caused by waste package steel corrosion. The result (Section 6.5 of this report (FEP 2.1.02.15.0A) and Section 6.6 of this report (FEP 2.1.02.16.0A)) is that no failure is expected.

In conclusion, electrochemical effects (electrophoresis and galvanic coupling) are excluded from the TSPA-LA on the basis of low consequence. The NRC requirements in 10 CFR 63.114 (e and f) allow this omission because electrochemical effects are expected to be small and will not significantly change the magnitude and time of the resulting radiological exposures to the

reasonably maximally exposed individual (RMEI), or radionuclide releases to the accessible environment.

## 6.21 CHEMICAL EFFECTS OF WASTE-ROCK CONTACT

### FEP Number:

2.1.09.11.0A

### YMP FEP Description:

Waste (CSNF, DSNF, and HLW) and rock are placed in contact by mechanical failure of the drip shields and/or waste packages. Chemical effects on the waste (e.g., dissolution) of waste may be enhanced or altered in a system where waste, rock minerals, and water are all in physical contact, relative to a system where only waste and water are in physical contact.

### Descriptor Phrases:

Chemical effects of waste-rock contact

### Screening Decision:

Excluded – Low Consequence

### TSPA-LA Disposition:

NA

### Related FEPs:

- 2.1.02.13.0A, General corrosion of cladding
- 2.1.02.14.0A, Microbially influenced corrosion (MIC) of cladding
- 2.1.02.15.0A, Localized (radiolysis enhanced) corrosion of cladding
- 2.1.02.16.0A, Localized (pitting) corrosion of cladding

**Screening Argument:** The chemical effects of waste–rock contact are excluded from the TSPA-LA on the basis of low consequence.

Waste–rock contact will have no effect on CSNF, DSNF, and HLW dissolution. Water that contacts SNF will have previously been in contact (i.e., equilibrium with the host rock) and therefore, placement of the rock in physical contact with the SNF will not affect the waste/rock/water system chemistry. Furthermore, *In-Package Chemistry Abstraction* (BSC 2003f [DIRS 161962]) demonstrated that variations in the chemistry of the water contacting the waste package internal components, including the SNF, had an insignificant effect on the pH and total carbonate, the two key chemical parameters controlling the solubility of CSNF, DSNF, and HLW, of the in-package fluids. Waste form and cladding interaction with igneous intrusions are addressed in FEP 1.2.04.04.0A, *Igneous intrusion interactions with EBS components*. This FEP is addressed in *Igneous Intrusion Impacts on Waste Package and Waste Forms* (BSC 2003e [DIRS 165002]).

The chemical effect of waste-rock contact has been excluded from TSPA-LA because of low consequence. Even if near-field chemistry contacts the cladding or waste form, accelerated corrosion is not expected. Tests involving the contact of zirconium with soils have not shown

corrosion. Adler Flitton et al. (2002 [DIRS 161991], p. 4) buried various metal samples including zirconium in an arid vadose zone environment for three years. These samples were in intimate contact with the vadose (unsaturated) zone environment. They reported indications of pitting on some of the other metals, but observed no pitting on the zirconium samples when in contact with rock. Other corroborating information is also available. The waste form is protected from the rocks by both the drip shield and waste package during the 10,000-year regulatory period. Zirconium is impervious to most chemical solutions (CRWMS M&O 2000d [DIRS 136058]) and only severe chemicals will pit cladding (BSC 2003g [DIRS 164667]). Yau (1984 [DIRS 102050]) performed corrosion tests with zirconium in geothermal fluids and reports no corrosion. Yau and Webster (1987 [DIRS 100494]) review the limited conditions where corrosion of zirconium is observed. This review suggests that contact with YMP tuff would not corrode the cladding.

The CSNF and DSNF waste forms will have little contact with the rock because the stainless steel inner barrier and Alloy 22 outer barrier waste package will prevent contact. For the CSNF and some forms of DSNF, the zirconium alloy cladding surrounding the UO<sub>2</sub> pellets will prevent contact. Contact of the UO<sub>2</sub> pellets with the rock would have little effect. The uranium in the UO<sub>2</sub> first oxidizes (U<sup>4+</sup> to U<sup>6+</sup>), dissolves, and then precipitates immediately on the pellet surface as a U<sup>6+</sup> mineral. The rock would have little contact with the UO<sub>2</sub> pellets and little effect on the CSNF corrosion. DSNF and DHLW are also unlikely to contact the rock and direct effects of such contact, were it to occur, are also negligible. Indirect effects that could occur through the water chemistry (e.g., effects on dissolved silicon concentration) which would feed back into the rate of glass dissolution are small compared to the effects of the glass dissolution, as indicated by the results of tests conducted in EJ-13 water (i.e., J-13 well water preconditioned by reaction with tuff).

In conclusion, the chemical effects of waste–rock contact are excluded from the TSPA-LA on the basis of low consequence. NRC requirements in 10 CFR 63.114 (e and f) allow this omission because contact is not expected. Even if it did occur, the resulting chemical effects would not significantly change the magnitude and time of the resulting radiological exposures to the reasonably maximally exposed individual (RMEI), or radionuclide releases to the accessible environment. If contact were to occur during the regulatory period, no chemical effect is expected.

## **6.22 THERMAL EXPANSION/STRESS OF IN-PACKAGE EBS COMPONENTS**

### **FEP Number:**

2.1.11.05.0A

### **YMP FEP Description:**

Thermally induced stresses could alter the performance of the waste or EBS. For example, thermal stresses could cause the waste form to develop cracks and create pathways for preferential fluid flow and, thereby, accelerate degradation of the waste.

**Descriptor Phrases:**

- Thermal-mechanical effects on cladding
- Thermal-mechanical effects on CSNF waste form
- Thermal-mechanical effects on DSNF waste form
- Thermal-mechanical effects on HLW waste form

**Screening Decision:**

Excluded – Low Consequence

**TSPA-LA Disposition:**

NA

**Related FEPs:**

2.1.02.19.0A, Creep rupture of cladding

**Screening Argument:** Thermal expansion and stresses of in-package EBS components, including the waste form, are excluded from the TSPA-LA on the basis of low consequence.

The waste package and its internals are designed for the thermal expansion from the thermal cycle shown in Figure A-1. The CSNF and DSNF are designed for the thermal cycles expected in reactors, which are more severe than repository conditions. As discussed in Section 6.2.1 of *CSNF Waste Form Degradation: Summary Abstraction* (BSC 2004c [DIRS 167321]), the in-reactor thermal cycles (principally that associated with the initial power escalation) result in extensive cracking of the fuel matrix. The effects of this cracking are included in the specific surface area parameter. Glass logs crack because of the cooldown during manufacturing. The cracking that results from this cooldown is included in the DHLW model surface area parameter. This cooldown (from molten glass, about 950°C, BSC 2004d [DIRS 167619], Section 7.5.3) is more severe than repository conditions.

Commercial nuclear fuel operates at higher temperatures than expected during the post-closure period at the repository. Under normal conditions, typical cladding operates at about 320°C (Garde et al. 1991 [DIRS 101652], p. 582) with fuel centerline temperatures reaching 1,800°C (Lanning et al. 1997 [DIRS 101704], V3, p. 3.2, Figure 3.1). Fuel is also designed to undergo anticipated operating occurrences (off normal transients that occur during the design life) without damage. These are more severe thermal cycles than normal reactor operation or repository closure. Every time a reactor shuts down and goes to cold shutdown, the fuel is cooled to below 100°C (coolant is less than boiling). These temperature transients are more severe than repository closure (Figure A-1). DSNF is also exposed to reactor transients more severe than the post-closure cooldown. Since the temperature transients for spent fuel from normal in-reactor operations and for DHLW from normal manufacturing cooldown are more severe than the transient associated with repository closure, no further degradation (cracking) is expected from thermal expansion or stress of in-package EBS components.

In conclusion, thermal expansion and stress of in-package EBS components, including the waste form is excluded from the TSPA-LA on the basis of low consequence. The NRC requirements in 10 CFR 63.114 (e and f) allow this omission because thermal expansion will not significantly change the magnitude and time of the resulting radiological exposures to the reasonably maximally exposed individual (RMEI), or radionuclide releases to the accessible environment.

## 6.23 GAS GENERATION (He) FROM WASTE FORM DECAY

### FEP Number:

2.1.12.02.0A

### YMP FEP Description:

Helium (He) gas production may occur by alpha decay in the waste. Helium production might cause local pressure buildup in cracks in the fuel and in the void between fuel and cladding, leading to cladding and waste-package failure.

### Descriptor Phrases:

Chemical effects from He generation  
Internal gas pressure from He (cladding damage)

### Screening Decision:

Excluded – Low Consequence

### TSPA-LA Disposition:

NA

### Related FEPs:

2.1.02.20.0A, Internal pressurization of cladding  
2.1.09.03.0A, Volume increase of corrosion products impacts cladding

**Screening Argument:** Effects of helium gas generation from alpha decay on the cladding in spent fuel are excluded from the TSPA-LA on the basis of low consequence.

Piron and Pelletier (2001 [DIRS 165318], Section 5.3) investigated pressurization of the fuel rods from helium production (alpha decay) and concluded that fuel (47.5 MWd/kgU) would produce 1,171 cm<sup>3</sup> (STP) of helium in a rod after 10,000 years, too low a quantity to damage the fuel. The peak pressure of 13.3 MPa (FEP 2.1.02.20.0A, Table 6.10-1) would have to be significantly higher (about 33 MPa) for the cladding to fail from delayed hydride cracking.

For cladding, delayed hydride cracking, stress corrosion cracking, and strain failures are driven by the cladding stress, which may be caused by the internal gas (including initial fill gas, fission product gases, and helium gas from alpha decay) pressure buildup. The gas pressure will slowly increase over time by the production of helium as a result of alpha decay. For failed rods, the helium would be released into the waste package, possibly increasing the pressure there. Using complete helium release from the fuel is conservative at these temperatures. Helium is an inert gas and will not chemically react with in-package components (internals, cladding or UO<sub>2</sub> pellets). After waste package failure, it will also tend to diffuse out. The helium would have little effect on the corrosion of the UO<sub>2</sub> pellets. UO<sub>2</sub> corrosion is an oxidation/dissolution phenomenon and the presence of traces of an inert gas will not affect this. The effects of microcracking due to pressure buildup in gas bubbles within the fuel matrix on the rate of matrix corrosion are expected to be negligible. As described in Sections 6.2.1 and 6.2.2 of *CSNF Waste Form Degradation: Summary Abstraction* (BSC 2004c [DIRS 167321]), evidence from CSNF testing indicates that the corrosion process is a general corrosion process occurring predominantly at the periphery of the fuel fragments. The effective specific surface area of the corroding fuel is comparable to the geometric surface area and is not sensitive to the internal

grain boundary decohesion or microcracking that may result from helium buildup in the matrix. Likewise, because DHLW dissolution occurs at the periphery of glass fragments the internal microstructural features (including helium gas bubbles) do not affect the dissolution rate.

After the waste package is placed in the repository and closure occurs, the temperature and pressure peak. The waste package then cools down, decreasing the pressure. This is countered by a steady production of helium by alpha decay of transuranic elements. After 10,000 years, total system pressure will increase to about 60 percent higher than at the thermal peak. Because this pressure is not high enough to cause any damage to the cladding (FEP 2.1.02.20.0A), there is a low consequence of this FEP.

For an intact waste package, the free volume is 4.7 m<sup>3</sup> (FEP 2.1.09.03.0A). If the waste package has failed, any helium that is released from the failed fuel can escape the waste package. It is expected that less than 1 percent of the fuel is failed (FEP 2.1.02.12.0A). If all of the rods were considered failed and all of the helium was released from the fuel matrix, then approximately 1,500 cm<sup>3</sup> (STP) of gas (FEP 2.1.02.20.0A) would be released per rod. With 5,544 rods per waste package (BSC 2003a [DIRS 162153], Table 8), there would be 8.3×10<sup>6</sup> cm<sup>3</sup> (STP) of helium available. When distributed into the free volume, 4.7 m<sup>3</sup> (FEP 2.1.09.03.0A), of the waste package at 73°C (peak temperature at 10,000 years, Table A-3), the pressure would increase by 0.22 MPa (2.2 atm). This pressure rise is too small to damage the waste package. With most of the fuel rods intact, and most of the helium tied up in the fuel matrix, the actual pressure rise would be small. An alternative conceptual model for helium generation is discussed in FEP 2.1.02.20.0A.

In conclusion, effects of helium gas generation from alpha decay on the cladding are excluded from the TSPA-LA on the basis of low consequence. The NRC requirements in 10 CFR 63.114 (e and f) allow this omission because the pressures generated by helium generation are insufficient to damage the cladding and, therefore, will not significantly change the magnitude and time of the resulting radiological exposures to the reasonably maximally exposed individual (RMEI), or radionuclide releases to the accessible environment.

## **6.24 GAS GENERATION (H<sub>2</sub>) FROM WASTE PACKAGE CORROSION**

### **FEP Number:**

2.1.12.03.0A

### **YMP FEP Description:**

Gas generation can affect the mechanical behavior of the host rock and engineered barriers, chemical conditions, and fluid flow, and, as a result, the transport of radionuclides. Gas generation due to oxic corrosion of waste containers, cladding, and/or structural materials will occur at early times following closure of the repository. Anoxic corrosion may follow the oxic phase if all oxygen is depleted. The formation of a gas phase around the waste package may exclude oxygen from the iron, thus inhibiting further corrosion.

### **Descriptor Phrases:**

Hydride cracking (cladding)

Internal gas pressure from H<sub>2</sub> (waste package damage)

**Screening Decision:**

Excluded – Low Consequence

**TSPA-LA Disposition:**

NA

**Related FEPs:**

2.1.03.01.0A, Waste package general corrosion

2.1.02.22.0A, Hydride cracking of cladding

**Screening Argument:** Hydrogen gas (H<sub>2</sub>) generation from waste package corrosion, as a degradation mechanism for cladding, is excluded from the TSPA-LA on the basis of low consequence. The cladding absorbs little or no hydrogen from the outside environment such as waste package corrosion and hydride embrittlement will not occur.

Many investigators have considered the hydriding of zirconium alloys (for example, the papers cited in Clayton 1989 [DIRS 149208], Tables 1 through 4). Many of these investigations have been straightforward measurements of the rate of hydriding under various conditions. However, at least one set of experiments directly determined the origin of hydrogen in the metal. *Waterside Corrosion of Zirconium Alloys in Nuclear Power Plants* (IAEA 1998 [DIRS 150560], p. 92) discusses experiments in which zirconium-base alloys were oxidized in normal water (H<sub>2</sub>O) with dissolved tritium gas (T<sub>2</sub>). This experiment is extremely sensitive. If even one ppm of the hydrogen was from dissolved tritium gas, the radioactivity of T<sub>2</sub> would result in thousands of decays per second for one square centimeter of surface. This level of activity would be readily detected. IAEA (1998 [DIRS 150560], p. 92) gives the following discussion of the experiment:

Oxidation studies using T<sub>2</sub>/H<sub>2</sub>O mixtures ... have shown that, during normal oxidation, no T<sub>2</sub> enters the metal ... until the thermally-induced exchange reaction has progressed to the point where a measurable fraction of HTO has been formed. Thus, the hydrogen isotopes which enter the metal do so as an integral part of the reaction of the zirconium with water molecules, and not by reaction with any dissolved hydrogen in the water. Studies have shown that this situation persists ... until hydrogen over-pressures in the system of tens of MPa are present.

Note that, according to this quotation, the hydrogen pressures required to cause hydriding are quite large. By comparison, the highest hydrogen pressure in a breached waste package is pure hydrogen gas at atmospheric pressure, or about 0.1 MPa.

Additional corroborating information follows. The oxide film on the surface of the metal is important in preventing the uptake of hydrogen from the surrounding environment. Under specific experimental conditions, this oxide layer can be removed. At 200°C, the solubility of oxygen in zirconium is greater than 1 percent by weight, and the solubility of oxygen increases with increasing temperature (Baker 1992 [DIRS 149104], p. 2-326). As a result, the oxide film on the surface of a piece of zirconium is normally not thermodynamically stable. In his discussion of experimental procedure, Smith (1966 [DIRS 149107], p. 325) notes, “Zirconium samples were first annealed at 700°C under vacuum (~ 10<sup>-3</sup> mm Hg) to remove any oxide film. The film dissolved into the samples, leaving them a bright metallic color.” It is clear that the oxide film can be damaged or even destroyed by heat treatment in a suitable environment.

However, the film can be maintained if there is a supply of oxygen. Water will serve as a source of oxygen, because the electrochemical domain of stability for zirconium metal lies well below that of water (Pourbaix 1974 [DIRS 100817], p. 226). Spent nuclear fuel has a robust oxide layer from reactor operation. Under the oxidizing and humid environment of a failed waste package, it is expected that the oxide layer will be preserved.

Garzarolli et al. (1979 [DIRS 149256], p. 64) studied the effect of the oxygen supply and stated:

The effect of the composition of the gas atmosphere on the electrical properties of ZrO<sub>2</sub> corrosion films was measured. The results revealed a large decrease in the electric resistance when the atmosphere changed from oxidizing to non-oxidizing, indicating a drastic change of the morphology (passivity of the oxide film) .. the obvious implication of all available results is that massive hydriding can start when the availability of oxygen to continuously repair the protective oxide film falls below a critical value.

Clayton (1989 [DIRS 149208], p. 270) quantified the conditions for hydriding in the equation:

$$(p_{\text{H}_2\text{O}})_{\text{protective}} \leq 0.2(p_{\text{H}_2})^{1/3} \quad (\text{Eq. 6.24-1})$$

where  $p_{\text{H}_2\text{O}}$  and  $p_{\text{H}_2}$  are the pressures of H<sub>2</sub>O and H<sub>2</sub>, respectively. For Equation 6.24-1 to be applicable, both pressures must be given in torr (millimeters of Hg head). This fact is deduced as follows. First, Clayton (1989 [DIRS 149208], Tables 1 through 4) indicates that pressures are measured in “mm.” Second, pressures of “760 mm” (of Hg) (= atmospheric pressure) occur many times in these tables. Third, the “Critical  $p_{\text{H}_2\text{O}}/p_{\text{H}_2}$ ” values given in the tables are consistent since both are expressed in the same units. For  $p_{\text{H}_2} = 101 \text{ kPa} = 760 \text{ torr}$ , it is found that  $p_{\text{H}_2\text{O}} (\text{protective}) = 0.24 \text{ kPa} = 1.8 \text{ torr}$ . Note that, by atmospheric standards, this  $p_{\text{H}_2\text{O}}$  corresponds to a dry gas. For comparison, the vapor pressure of water at 25°C is about 3.2 kPa. For this small amount of humidity, corrosion of the waste package internals is not likely. If no corrosion occurs, no hydrogen is produced, so hydriding is impossible.

It should be noted that hydriding of zirconium by absorption of gas has been observed in the laboratory. For example, Smith (1966 [DIRS 149107], Table 3) provides data on hydrogen absorption. However, the environment for these experiments was hot, extremely pure hydrogen. Smith (1966 [DIRS 149107], Table 3) states that the temperatures for the hydrogen absorption experiments were 210 °C to 700 °C. Smith (1966 [DIRS 149107], p. 325) notes that “hydrogen was purified by passing it through a Deoxo unit, a bed of platinized asbestos (300°C), a tube of P<sub>2</sub>O<sub>5</sub> and a liquid nitrogen trap.” The evident intention is to react any oxygen impurities, and absorb or condense any water vapor that is formed. After this treatment, little oxygen would have been available to maintain the oxide film. Such an environment is not relevant for a repository at Yucca Mountain because air, water vapor, or liquid water will be present and will maintain the protective oxide film.

It is understood that corrosion of waste package internals will occur at temperatures below the range for which the Equation 6.24-1 was developed. Data on hydriding at lower temperatures were not available in the literature.

In some respects, it can be argued that it is conservative to apply Equation 6.24-1 to the repository. Equation 6.24-1 was developed for coupons of Zircaloy-2. This alloy is more susceptible to hydriding than is Zircaloy-4 (Clayton 1989 [DIRS 149208], Table 5), and coupons are more susceptible to hydriding than is tubing (Clayton 1989 [DIRS 149208], Table 5). Therefore, Equation 6.24-1 should give conservative predictions of the susceptibility of spent fuel cladding to hydriding.

In summary, hydrogen will be generated in the waste package as the waste package internals corrode. This hydrogen is not directly absorbed, because the H<sub>2</sub> molecules do not migrate through the high-density ZrO<sub>2</sub> layer on the cladding. Hydrogen is introduced into the coolant in PWRs to reduce oxygen ions and reduce corrosion of components and yet it is not absorbed into the cladding.

Hydrogen would have no effect on in-package chemistry because it would immediately diffuse out of the package before reacting with anything. Also, hydrogen is a reduced gas and is, therefore, unlikely to form in an oxidizing environment. The uranium in the UO<sub>2</sub> first oxidizes (U<sup>4+</sup> to U<sup>6+</sup>), dissolves, and then precipitates immediately on the pellet surface as a schoepite-type mineral. Although the kinetics of hydrogen gas reactions are sluggish under the conditions expected in a breached waste package, the presence of hydrogen would reduce the concentration of oxidizing agents and hence the corrosion rate of the UO<sub>2</sub>; neglecting this effect is therefore, conservative. The presence of some hydrogen gas would not affect the hydrolysis reactions that control the rate of DHLW dissolution. The hydrogen would be generated for the first 500 years while the waste package internals are corroding so this conservatism exists for a limited time.

In conclusion, hydrogen gas (H<sub>2</sub>) generation from waste package corrosion, as a degradation mechanism for cladding, is excluded from the TSPA-LA on the basis of low consequence. The cladding absorbs little or no hydrogen from the outside environment such as waste package corrosion and hydride embrittlement will not occur. The NRC requirements in 10 CFR 63.114 (e and f) allow this omission because H<sub>2</sub> will not damage the cladding and therefore will not significantly change the magnitude and time of the resulting radiological exposures to the reasonably maximally exposed individual (RMEI), or radionuclide releases to the accessible environment.

## 7. CONCLUSIONS

This report summarizes the screening of 24 waste form and cladding degradation FEPs. This screening is for the current LA design without backfill. The earlier screening of the FEPs (CRWMS M&O 2000g [DIRS 153947]) was based on backfill with higher temperatures and generally similar screening was developed. The degradation of cladding is not sensitive to temperature changes when the maximum temperatures are below 400°C. Twenty-four (24) FEPs relevant to cladding degradation processes have been screened (see Sections 6.1 through 6.24) and are summarized in Table 7-1. The last five FEPs in this table also address waste form degradation. This table provides the FEP number, name, screening decision (included/excluded), and basis for the exclusion (i.e., low probability or low consequence). Low consequence means that omitting the FEP will not significantly change the magnitude and time of the resulting radiological exposures to the reasonably maximally exposed individual (RMEI), or radionuclide releases to the accessible environment (10 CFR 63.114 e and f).

For the first nineteen FEPs in Table 7-1, the FEP screening applies to CSNF and naval spent fuel. The last five FEPs in Table 7-1 address both cladding and all waste forms including defense spent nuclear fuel (DSNF) and high-level waste (HLW). Uncertainties are addressed in the included FEPs and are described in *Clad Degradation – Summary and Abstraction for LA* (BSC 2003a [DIRS 162153]). The list of Cladding Degradation FEPs is provided in Section 1.0 and FEP screening analyses are provided in Sections 6.1 through 6.24 of this report.

For the repository, cladding is not an engineered barrier. It is not designed and controlled by the project to reduce release of radionuclides. The behavior can be modeled but the design characteristics are not within the project controls.

Table 7-1. Summary of Cladding Degradation and Waste Form FEPs

Section	FEP Number	FEP Name	Screening Decision	Screening Basis
6.1	2.1.02.11.0A	Degradation of cladding from waterlogged rods	Excluded	Low Consequence
6.2	2.1.02.12.0A	Degradation of cladding prior to disposal	Included	NA
6.3	2.1.02.13.0A	General corrosion of cladding	Excluded	Low Consequence
6.4	2.1.02.14.0A	Microbially influenced corrosion (MIC) of cladding	Excluded	Low Consequence
6.5	2.1.02.15.0A	Localized (radiolysis enhanced) corrosion of cladding	Excluded	Low Consequence
6.6	2.1.02.16.0A	Localized (pitting) corrosion of cladding	Excluded	Low Consequence
6.7	2.1.02.17.0A	Localized (crevice) corrosion of cladding	Excluded	Low Consequence
6.8	2.1.02.18.0A	Enhanced corrosion of cladding from dissolved silica	Excluded	Low Consequence
6.9	2.1.02.19.0A	Creep rupture of cladding	Excluded	Low Consequence
6.10	2.1.02.20.0A	Internal pressurization of cladding	Excluded	Low Consequence
6.11	2.1.02.21.0A	Stress corrosion cracking (SCC) of cladding	Excluded	Low Consequence
6.12	2.1.02.22.0A	Hydride cracking of cladding	Excluded	Low Consequence
6.13	2.1.02.23.0A	Cladding unzipping	Included	NA
6.14	2.1.02.24.0A	Mechanical impact on cladding	Excluded	Low Probability
6.15	2.1.02.25.0B	Naval SNF cladding	Included	NA
6.16	2.1.02.26.0A	Diffusion-controlled cavity growth (DCCG) in cladding	Excluded	Low Consequence
6.17	2.1.02.27.0A	Localized (fluoride enhanced) corrosion of cladding	Excluded	Low Consequence
6.18	2.1.07.01.0A	Rockfall	Excluded	Low Probability
6.19	2.1.09.03.0A	Volume increase of corrosion products impacts cladding	Included	NA
6.20	2.1.09.09.0A	Electrochemical effects in EBS	Excluded	Low Consequence
6.21	2.1.09.11.0A	Chemical effects of waste-rock contact	Excluded	Low Consequence
6.22	2.1.11.05.0A	Thermal expansion/stress of in-package EBS components	Excluded	Low Consequence
6.23	2.1.12.02.0A	Gas generation (He) from waste form decay	Excluded	Low Consequence
6.24	2.1.12.03.0A	Gas generation (H <sub>2</sub> ) from waste package corrosion	Excluded	Low Consequence

## 8. REFERENCES

### 8.1 DOCUMENTS CITED

Adler Flitton, M.K.; Mizia, R.E.; and Bishop, C.W. 2002. "Underground Corrosion of Activated Metals in an Arid Vadose Zone Environment." *Corrosion/2002, [57th Annual Conference & Exposition, April 7-11, 2002, Denver, Colorado]*. Paper No. 02531. Houston, Texas: NACE International. TIC: 253838.

Baker, H. 1992. "Binary Alloy Phase Diagrams." Volume 3 of *ASM Handbook*. Page 2.326. Materials Park, Ohio: ASM International. TIC: 247622.

Beckman, D.A. 2001. "NRC Issue Resolution Status Report on Container Life and Source Term, Revision 3." Memorandum from D.A. Beckman (BSC) to Distribution, February 21, 2001, LV.LAP.AH.02/2001-236, with enclosure. ACC: MOL.20010418.0048.

Bradley, E.R.; Bailey, W.J.; Johnson, A.B., Jr.; and Lowry, L.M. 1981. *Examination of Zircaloy-Clad Spent Fuel After Extended Pool Storage*. PNL-3921. Richland, Washington: Pacific Northwest Laboratory. TIC: 230049.

Brossia, C.S.; Cragolino, G.A.; and Dunn, D.S. 2002. "Effect of Oxide Thickness on the Localized Corrosion of Zircaloy." *Corrosion/2002, 57th Annual Conference & Exposition, April 7-11, 2002, Denver, Colorado*. Paper No. 02549. Houston, Texas: NACE International. TIC: 253839.

BSC 2001a. *Performance Assessment of U.S. Department of Energy Spent Fuels in Support of Site Recommendation*. CAL-WIS-PA-000002 REV 00. Las Vegas, Nevada: Bechtel SAIC Company. ACC: MOL.20010627.0026.

BSC 2001b. *Environment on the Surfaces of the Drip Shield and Waste Package Outer Barrier*. ANL-EBS-MD-000001 REV 00 ICN 02. Las Vegas, Nevada: Bechtel SAIC Company. ACC: MOL.20010724.0082.

BSC 2001c. *The Development of Information Catalogued in REV00 of the YMP FEP Database*. TDR-WIS-MD-000003 REV 00 ICN 01. Las Vegas, Nevada: Bechtel SAIC Company. ACC: MOL.20010301.0237.

BSC 2002. *The Enhanced Plan for Features, Events, and Processes (FEPs) at Yucca Mountain*. TDR-WIS-PA-000005 REV 00. Las Vegas, Nevada: Bechtel SAIC Company. ACC: MOL.20020417.0385.

BSC 2003a. *Clad Degradation – Summary and Abstraction for LA*. ANL-WIS-MD-000021 REV 00. Las Vegas, Nevada: Bechtel SAIC Company. ACC: DOC.20030626.0002.

BSC 2003b. *Multiscale Thermohydrologic Model*. ANL-EBS-MD-000049 REV 01G. Las Vegas, Nevada: Bechtel SAIC Company. ACC: MOL.20031212.0037. TBV-5641

BSC 2003c. *EBS Radionuclide Transport Abstraction*. ANL-WIS-PA-000001 REV 01A. Las Vegas, Nevada: Bechtel SAIC Company. ACC: MOL.20030617.0222. TBV-5179

BSC 2003d. *Initial Radionuclide Inventories*. ANL-WIS-MD-000020 REV 00. Las Vegas, Nevada: Bechtel SAIC Company. ACC: DOC.20031110.0002.

BSC 2003e. *Igneous Intrusion Impacts on Waste Package and Waste Forms*. MDL-EBS-GS-000002 REV 00. Las Vegas, Nevada: Bechtel SAIC Company. ACC: DOC.20030819.0003.

BSC 2003f. *In-Package Chemistry Abstraction*. ANL-EBS-MD-000037 REV 02. Las Vegas, Nevada: Bechtel SAIC Company. ACC: DOC.20030723.0003.

BSC 2003g. *Pitting Model for Zirconium-Alloyed Cladding at YMP*. MDL-WIS-MD-000001 REV 00. Las Vegas, Nevada: Bechtel SAIC Company. ACC: DOC.20031017.0003.

BSC 2004a. *Technical Work Plan for Waste Form Degradation Modeling, Testing, and Analyses in Support of LA*. TWP-WIS-MD-000008 REV 02 ICN 04. Las Vegas, Nevada: Bechtel SAIC Company. ACC: DOC.20040218.0001.

BSC 2004b. *D&E /PA /C IED Typical Waste Package Components Assembly*. 800-IED-WIS0-00206-000-00Ba. Las Vegas, Nevada: Bechtel SAIC Company. ACC: MOL.20040109.0376. TBV-5668.

BSC 2004c. Errata for CSNF Waste Form Degradation: Summary Abstraction. ANL-EBS-MD-000015 REV 01. Las Vegas, Nevada: Bechtel SAIC Company. ACC: DOC.20030708.0004; DOC.20031224.0001; DOC.20040202.0002.

BSC 2004d. *Defense HLW Glass Degradation Model*. ANL-EBS-MD-000016 REV 01 ICN 01. Las Vegas, Nevada: Bechtel SAIC Company. ACC: DOC.20040223.0006.

BSC 2004e. *Errata for Seismic Consequence Abstraction*. MDL-WIS-PA-000003 REV 0 ERRATA 1. Las Vegas, Nevada: Bechtel SAIC Company. ACC: DOC.20030818.0006; DOC.20040218.0002.

Cappelaere, C.; Limon, R.; Bredel, T.; Herter, P.; Gilbon, D.; Bouffieux, P.; and Mardon, J-P. 2002. "Long Term Behavior of the Spent Fuel Cladding in Dry Storage Conditions." *ICEM '01, Proceedings of the 8th International Conference on Radioactive Waste Management and Environmental Remediation, held in Burges, Belgium, September 30-October 4, 2001*. Taboas, A.; Vanbrabant, R.; and Benda, G., eds. 1, New York, New York: American Society of Mechanical Engineers. TIC: 254663.

Chan, K.S. 1996. "A Micromechanical Model for Predicting Hydride Embrittlement in Nuclear Fuel Cladding Material." *Journal of Nuclear Materials*, 227, 220-236. Amsterdam, The Netherlands: Elsevier. TIC: 237164.

Clayton, J.C. 1984. "Out-of-Pile Nickel Alloy-Induced Accelerated Hydriding of Zircaloy Fasteners." *Zirconium in the Nuclear Industry: Sixth International Symposium, Vancouver, British Columbia, June 28- July 1, 1982*. Franklin, D.G. and Adamson, R.B., eds. ASTM STP

824. Pages 572-591. Philadelphia, Pennsylvania: American Society for Testing and Materials. TIC: 241417.

Clayton, J.C. 1989. "Internal Hydriding in Irradiated Defected Zircaloy Fuel Rods." *Zirconium in the Nuclear Industry: Eighth International Symposium, held June 19-23, 1988 San Diego, California*. ASTM STP 1023. Pages 266-288. Philadelphia, Pennsylvania: American Society for Testing and Materials. TIC: 241414.

Coleman, C.E. 1982. "Effect of Texture on Hydride Reorientation and Delayed Hydrogen Cracking in Cold-Worked Zr-2.5Nb." *Zirconium in the Nuclear Industry, Proceedings of the Fifth International Conference, Boston, Massachusetts, 4-7 August 1980*. ASTM STP 754. Pages 393-411. Philadelphia, Pennsylvania: American Society for Testing and Materials. TIC: 247323.

Cox, B. 1973. "Stress Corrosion Cracking of Zircaloy-2 in Neutral Aqueous Chloride Solutions at 25 C." *Corrosion*, 29, (4), 157-166. Houston, Texas: National Association of Corrosion Engineers. TIC: 248988.

Cox, B. 1990. "Environmentally-Induced Cracking of Zirconium Alloys – A Review." *Journal of Nuclear Materials*, 170, 1-23. [Amsterdam, The Netherlands]: North-Holland. TIC: 234774.

Cragolino, G.A.; Dunn, D.S.; Brossia, C.S.; Jain, V.; and Chan, K.S. 1999. *Assessment of Performance Issues Related to Alternate Engineered Barrier System Materials and Design Options*. CNWRA 99-003. San Antonio, Texas: Center for Nuclear Waste Regulatory Analyses. TIC: 248875.

CRWMS M&O 1995. *Analysis of Degradation Due to Water and Gases in MPC*. BB0000000-01717-0200-00005 REV 01. Las Vegas, Nevada: CRWMS M&O. ACC: MOL.19960419.0202.

CRWMS M&O 2000a. *Total System Performance Assessment for the Site Recommendation*. TDR-WIS-PA-000001 REV 00 ICN 01. Las Vegas, Nevada: CRWMS M&O. ACC: MOL.20001220.0045.

CRWMS M&O 2000b. *In-Drift Microbial Communities*. ANL-EBS-MD-000038 REV 00 ICN 01. Las Vegas, Nevada: CRWMS M&O. ACC: MOL.20001213.0066.

CRWMS M&O 2000c. *Initial Cladding Condition*. ANL-EBS-MD-000048 REV 00 ICN 01. Las Vegas, Nevada: CRWMS M&O. ACC: MOL.20001002.0145.

CRWMS M&O 2000d. *Clad Degradation–Local Corrosion of Zirconium and Its Alloys Under Repository Conditions*. ANL-EBS-MD-000012 REV 00. Las Vegas, Nevada: CRWMS M&O. ACC: MOL.20000405.0479.

CRWMS M&O 2000e. *Thermal History of Cladding in a 21 PWR SNF WP Loaded with Average Fuel*. CAL-UDC-ME-000001 REV 00. Las Vegas, Nevada: CRWMS M&O. ACC: MOL.20000216.0105.

CRWMS M&O 2000f. *Hydride-Related Degradation of SNF Cladding Under Repository Conditions*. ANL-EBS-MD-000011 REV 00. Las Vegas, Nevada: CRWMS M&O. ACC: MOL.20000319.0048.

CRWMS M&O 2000g. *Clad Degradation – FEPs Screening Arguments*. ANL-WIS-MD-000008 REV 00 ICN 01. Las Vegas, Nevada: CRWMS M&O. ACC: MOL.20001208.0061.

CRWMS M&O 2001a. *Clad Degradation – Summary and Abstraction*. ANL-WIS-MD-000007 REV 00 ICN 01. Las Vegas, Nevada: CRWMS M&O. ACC: MOL.20010214.0229.

CRWMS M&O 2001b. *FEPs Screening of Processes and Issues in Drip Shield and Waste Package Degradation*. ANL-EBS-PA-000002 REV 01. Las Vegas, Nevada: CRWMS M&O. ACC: MOL.20010216.0004.

CRWMS M&O 2001c. *Miscellaneous Waste-Form FEPs*. ANL-WIS-MD-000009 REV 00 ICN 01. Las Vegas, Nevada: CRWMS M&O. ACC: MOL.20010216.0006.

Cunningham, M.E.; Simonen, E.P.; Allemann, R.T.; Levy, I.S.; Hazelton, R.F.; and Gilbert, E.R. 1987. *Control of Degradation of Spent LWR Fuel During Dry Storage in an Inert Atmosphere*. PNL-6364. Richland, Washington: Pacific Northwest Laboratory. ACC: HQO.19941222.0016.  
Debes, M. 1999. "Transportation in France." Letter from O. Dekens (EDF) to A.J. Machiels (EPRI), November 15, 1999, with attachment. TIC: 249077.

Debes, M. 1999. "Transportation in France." Letter from O. Dekens (EDF) to A.J. Machiels (EPRI), November 15, 1999, with attachment. TIC: 249077.

Dieter, G.E., Jr. 1961. *Mechanical Metallurgy*. 1st Edition. New York, New York: McGraw-Hill Book Company. TIC: 245037.

DOE (U.S. Department of Energy) 1996. *Spent Nuclear Fuel Discharges from U.S. Reactors 1994*. SR/CNEAF/96-01. Washington, D.C.: U.S. Department of Energy. TIC: 232923.

Edsinger, K. 2000. "A Review of Fuel Degradation in BWRs." Proceedings of the 2000 International Topical Meeting on Light Water Reactor Fuel Performance, Park City, Utah, April 10-13, 2000. La Grange Park, Illinois: American Nuclear Society. TIC: 248973.

Einziger, R.E. 1994. "Preliminary Spent LWR Fuel Oxidation Source Term Model." *High Level Radioactive Waste Management, Proceedings of the Fifth Annual International Conference, Las Vegas, Nevada, May 22-26, 1994*. 2, 554-559. La Grange Park, Illinois: American Nuclear Society. TIC: 210984.

Einziger, R.E. and Kohli, R. 1984. "Low-Temperature Rupture Behavior of Zircaloy-Clad Pressurized Water Reactor Spent Fuel Rods Under Dry Storage Conditions." *Nuclear Technology*, 67, (1), 107-123. Hinsdale, Illinois: American Nuclear Society. TIC: 216868.

Einziger, R.E.; Atkin, S.D.; Stellrecht, D.E.; and Pasupathi, V. 1982. "High Temperature Postirradiation Materials Performance of Spent Pressurized Water Reactor Fuel Rods Under Dry

Storage Conditions." *Nuclear Technology*, 57, (1), 65-80. Hinsdale, Illinois: American Nuclear Society. TIC: 237142.

EPRI (Electric Power Research Institute) 2002. *Dry Cask Storage Characterization Project*. EPRI TR-1002882. Palo Alto, California: Electric Power Research Institute. TIC: 253737.

Farina, S.B.; Duffo, G.S.; and Galvele, J.R. 2002. "Stress Corrosion Cracking of Zirconium and Zircaloy-4 in Iodine Containing Solutions." *Corrosion/2002, [57th Annual Conference & Exposition, April 7-11, 2002, Denver, Colorado]*. Paper No. 02436. Houston, Texas: NACE International. TIC: 253841.

Freeze, G. 2003. *KTI Letter Report, Response to Additional Information Needs on TSPAI 2.05 and TSPAI 2.06*. REG-WIS-PA-000003 REV 00 ICN 04. Las Vegas, Nevada: Bechtel SAIC Company. ACC: DOC.20030825.0003

Garde, A.M. 1986. *Hot Cell Examination of Extended Burnup Fuel from Fort Calhoun*. DOE/ET/34030-11. Windsor, Connecticut: Combustion Engineering. TIC: 237128.

Garde, A.M. 1989. "Effects of Irradiation and Hydriding on the Mechanical Properties of Zircaloy-4 at High Fluence." *Zirconium in the Nuclear Industry, 8th International Symposium*. Van Swam, L.F.P. and Eucken, C.M., eds. *ASTM-STP-1023*, 548-569. Philadelphia, Pennsylvania: American Society for Testing and Materials. TIC: 241414.

Garde, A.M. 1991. "Enhancement of Aqueous Corrosion of Zircaloy-4 Due to Hydride Precipitation at the Metal-Oxide Interface." *Zirconium in the Nuclear Industry, Ninth International Symposium, Kobe, Japan, November 5-8, 1990*. Eucken, C.M. and Garde, A.M., eds. *ASTM-STP-1132*, 566-594. Philadelphia, Pennsylvania: American Society for Testing and Materials. TIC: 246113.

Garzarolli, F.; von Jan, R.; and Stehle, H. 1979. "The Main Causes of Fuel Element Failure in Water-Cooled Power Reactors." *Atomic Energy Review*, 17, (1), 31-128. [Vienna, Austria]: International Atomic Energy Agency. TIC: 221365.

Greene, C.A.; Brossia, C.S.; Dunn, D.S.; and Cragolino, G.A. 2000. "Environmental and Electrochemical Factors on the Localized Corrosion of Zircaloy-4." *Corrosion/2000, [55th Annual Conference & Exposition, March 26-31, 2000, Orlando, Florida]*. Paper No. 00210. Houston, Texas: NACE International. TIC: 246988.

Hansson, C.M. 1984. *The Corrosion of Zircaloy 2 in Anaerobic Synthetic Cement Pore Solution*. SKB TR-84-13. Stockholm, Sweden: Svensk Kärnbränsleförsörjning A.B. TIC: 206293.

Hayes, T.A.; Rosen, R.S.; and Kassner, M.E. 1999. *Critical Analysis of Dry Storage Temperature Limits for Zircaloy-Clad Spent Nuclear Fuel Based on Diffusion Controlled Cavity Growth*. UCRL-ID-131098. Livermore, California: Lawrence Livermore National Laboratory. TIC: 254551.

Hillner, E.; Franklin, D.G.; and Smee, J.D. 1998. *The Corrosion of Zircaloy-Clad Fuel Assemblies in a Geologic Repository Environment*. WAPD-T-3173. West Mifflin, Pennsylvania: Bettis Atomic Power Laboratory. TIC: 237127.

Huang, F.H. 1995. *Fracture Properties of Irradiated Alloys*. Richland, Washington: Avante Publishing. TIC: 224548.

IAEA (International Atomic Energy Agency) 1998. *Waterside Corrosion of Zirconium Alloys in Nuclear Power Plants*. IAEA-TECDOC-996. Vienna, Austria: International Atomic Energy Agency. TIC: 248234.

Jangg, V.G.; Webster, R.T.; and Simon, J.M. 1978. "Untersuchung uber das Korrosionsverhalten von Zirkoniumlegierungen." *Werkstoffe und Korrosion*, 29, 16-26. Weinheim, Germany: VCH Gesellschaft GmbH. TIC: 246090.

Knoll, R.W. and Gilbert, E.R. 1987. *Evaluation of Cover Gas Impurities and Their Effects on the Dry Storage of LWR Spent Fuel*. PNL-6365. Richland, Washington: Pacific Northwest Laboratory. TIC: 213789.

Kohli, R. and Pasupathi, V. 1986. *Investigation of Water-logged Spent Fuel Rods Under Dry Storage Conditions*. PNL-5987. Richland, Washington: Pacific Northwest Laboratory. TIC: 246472.

Kreyns, P.H.; Bourgeois, W.F.; White, C.J.; Charpentier, P.L.; Kammenzind, B.F.; and Franklin, D.G. 1996. "Embrittlement of Reactor Core Materials." *Zirconium in the Nuclear Industry, Eleventh International Symposium held in Garmisch-Partenkirchen, Germany, September 11-14, 1995*. Bradley, E.R. and Sabol, G.P., eds. ASTM STP 1295. Pages 758-782. West Conshohocken, Pennsylvania: American Society for Testing and Materials. TIC: 237256.

Lanning, D.D.; Beyer, C.E.; and Painter, C.L. 1997. *FRAPCON-3: Modifications to Fuel Rod Material Properties and Performance Models for High-Burnup Application*. NUREG/CR-6534. Volume 1. Richland, Washington: Pacific Northwest National Laboratory. TIC: 238923.

Little B. and Wagner P. 1996. "An Overview of Microbiologically Influenced Corrosion of Metals and Alloys Used in the Storage of Nuclear Wastes." *Canadian Journal of Microbiology*, 42, (4), 367-374. Ottawa, Canada: National Research Council of Canada. TIC: 246614.

Maguire, M. 1984. "The Pitting Susceptibility of Zirconium in Aqueous Cl-, Br-, and I-Solutions." *Industrial Applications of Titanium and Zirconium: Third Conference, A Symposium Sponsored by ASTM Committee B-10 on Reactive and Refractory Metals and Alloys, New Orleans, Louisiana, September 21-23, 1982*. ASTM STP 830. Pages 177-189. Philadelphia, Pennsylvania: American Society for Testing and Materials. TIC: 237161.

Mahmood, S.T.; Farkas, D.M.; Adamson, R.B.; and Etoh, Y. 2000. "Post-Irradiation Characterization of Ultra-High-Fluence Zircaloy-2 Plate." *Zirconium in the Nuclear Industry: Twelfth International Symposium, Toronto, Canada, 15-18 June 1998*. Sabol, G.P. and Moan, G.D., eds. ASTM STP 1354. Pages 139-169. West Conshohocken, Pennsylvania: American Society for Testing and Materials. TIC: 247102.

Manaktala, H.K. 1993. *Characteristics of Spent Nuclear Fuel and Cladding Relevant to High-Level Waste Source Term*. CNWRA 93-006. San Antonio, Texas: Center for Nuclear Waste Regulatory Analyses. TIC: 208034.

Mardon, J.P.; Garner, G.; Beslu, P.; Charquet, D.; and Senevat, J. 1997. "Update on the Development of Advanced Zirconium Alloys for PWR Fuel Rod Claddings." *Proceedings of the 1997 International Topical Meeting on Light Water Reactor Fuel Performance, Portland, Oregon, March 2-6, 1997*. Pages 405-412. La Grange Park, Illinois: American Nuclear Society. TIC: 232556.

McMinn, A.; Darby, E.C.; and Schofield, J.S. 2000. "The Terminal Solid Solubility of Hydrogen in Zirconium Alloys." *Zirconium in the Nuclear Industry: Twelfth International Symposium, Toronto, Canada, 15-18 June 1998*. Sabol, G.P. and Moan, G.D., eds. Pages 173-195. West Conshohocken, Pennsylvania: American Society for Testing and Materials. TIC: 247102.

McNeil, M. and Odom, A. 1994. "Thermodynamic Prediction of Microbiologically Influenced Corrosion (MIC) by Sulfate-Reducing Bacteria (SRB)." *Microbiologically Influenced Corrosion Testing*. ASTM STP 1232. Pages 173-179. Philadelphia, Pennsylvania: American Society for Testing and Materials. TIC: 246989.

NRC (U.S. Nuclear Regulatory Commission) 1997. *Standard Review Plan for Dry Cask Storage Systems*. NUREG-1536. Washington, D.C.: U.S. Nuclear Regulatory Commission. ACC: MOL.20010724.0307.

NRC (U.S. Nuclear Regulatory Commission) 2000. "Interim Staff Guidance - 11. Storage of High Burnup Spent Fuel." ISG - 11. Washington, D.C.: U.S. Nuclear Regulatory Commission. Accessed March 21, 2000. TIC: 247227. <http://www.nrc.gov/OPA/reports/isg11.htm>

NRC (U.S. Nuclear Regulatory Commission) 2002. *Interim Staff Guidance - 11, Revision 2. Cladding Considerations for the Transportation and Storage of Spent Fuel*. ISG-11, Rev. 2. Washington, D.C.: U.S. Nuclear Regulatory Commission. TIC: 254441.

NRC (U.S. Nuclear Regulatory Commission) 2003. *Yucca Mountain Review Plan, Final Report*. NUREG-1804, Rev. 2. Washington, D.C.: U.S. Nuclear Regulatory Commission, Office of Nuclear Material Safety and Safeguards. TIC: 254568.

Peehs, M. 1998. *Assessment of Dry Storage Performance of Spent LWR Fuel Assemblies with Increasing Burn-Up*. Erlangen, Germany: Bereich Energieerzeugung. TIC: 245171.

Peehs, M. and Fleisch, J. 1986. "LWR Spent Fuel Storage Behaviour." *Journal of Nuclear Materials*, 137, (3), 190-202. Amsterdam, The Netherlands: North-Holland Publishing Company. TIC: 235595.

Pescatore, C. and Cowgill, M. 1994. *Temperature Limit Determination for the Inert Dry Storage of Spent Nuclear Fuel*. EPRI TR-103949. Palo Alto, California: Electric Power Research Institute. TIC: 102933.

Pescatore, C.; Cowgill, M.G.; and Sullivan, T.M. 1990. *Zircaloy Cladding Performance Under Spent Fuel Disposal Conditions, Progress Report May 1 - October 31, 1989*. BNL 52235. Upton, New York: Brookhaven National Laboratory. ACC: NNA.19900710.0055.

Piron, J.P. and Pelletier, M. 2001. "State of the Art on the Helium Issues." Section 5.3 of *Synthesis on the Long Term Behavior of the Spent Nuclear Fuel*. Poinssot, C., ed. CEA-R-5958(E). Volume 1. [Paris], France: Commissariat à l'Énergie Atomique. TIC: 253976.

Pourbaix, M. 1974. *Atlas of Electrochemical Equilibria in Aqueous Solutions*. Houston, Texas: National Association of Corrosion Engineers. TIC: 208955.

Puls, M.P. 1988. "The Influence of Hydride Size and Matrix Strength on Fracture Initiation at Hydrides in Zirconium Alloys." *Metallurgical Transactions A*, 19A, (6), 1507-1522. Metals Park, Ohio: American Society for Metals. TIC: 237143.

Ralph, R.; Purohit, A.; and Dille, E. 2002. "Characterization of Oxide Formation on Dresden Unit 1 Fuel Storage Pool Racks." *Tenth International Conference on Environmental Degradation of Materials in Nuclear Power Systems—Water Reactors, August 5 to 9, 2001, Lake Tahoe, Nevada*. Houston, Texas: NACE International. TIC: 252999.

Reed-Hill, R.E. 1973. *Physical Metallurgy Principles*. Second Edition. 797-801. New York, New York: D. Van Nostrand Company. TIC: 237154.

Riley, W.D. and Covino, B.S., Jr. 1982. Effect of Ferric Ion on Corrosion Resistance of Zirconium in HCl-A1Cl<sub>3</sub> Environment. Report of Investigations 8610. Washington, D.C.: U.S. Department of Interior, Bureau of Mines. TIC: 253837.

Rothman, A.J. 1984. *Potential Corrosion and Degradation Mechanisms of Zircaloy Cladding on Spent Nuclear Fuel in a Tuff Repository*. UCID-20172. Livermore, California: Lawrence Livermore National Laboratory. ACC: NNA.19870903.0039.

Seibold, Angelika; Garzarolli, Friedrich; Manzel, Reiner 2001. *Verification of High Burnup Materials Behavior*. 4A-3. 14. Erlangen, Germany: Framatome ANP GmbH. Copyright Requested. TBV-5665.

Shi, S.Q. and Puls, M.P. 1994. "Criteria for Fracture Initiation at Hydrides in Zirconium Alloys I. Sharp Crack Tip." *Journal of Nuclear Materials*, 208, (3), 232-242. Amsterdam, The Netherlands: North-Holland Publishing Company. TIC: 237135.

Simpson, L.A. and Chow, C.K. 1987. "Effect of Metallurgical Variables and Temperature on the Fracture Toughness of Zirconium Alloy Pressure Tubes." *Zirconium in the Nuclear Industry, Seventh International Symposium, Strasbourg, France, 24-27 June 1985*. Adamson, R.B. and Van Swam, L.F.P. eds. ASTM STP 939. Pages 579-596. [Philadelphia, Pennsylvania: American Society for Testing and Materials]. TIC: 254718.

Smith, T. 1966. "Kinetics and Mechanism of Hydrogen Permeation of Oxide Films on Zirconium." *Journal of Nuclear Materials*, 18, 323-336. Amsterdam, The Netherlands: Elsevier. TIC: 247624.

Soderman, O. and Jonsson, R. 1996. "Electro-Osmosis: Velocity Profiles in Different Geometries with Both Temporal and Spatial Resolution." *Journal of Chemical Physics*, 105, (23), 10300-10311. New York, New York: American Institute of Physics. TIC: 247669.

Štefanić I. and LaVerne, J.A. 2002. "Temperature Dependence of the Hydrogen Peroxide Production in the  $\gamma$ -Radiolysis of Water." *Journal of Physical Chemistry*, 106, (2), 447-452. Washington, D.C.: American Chemical Society. TIC: 255323.

Tasooji, A.; Einziger, R.E.; and Miller, A.K. 1984. "Modeling of Zircaloy Stress-Corrosion Cracking: Texture Effects and Dry Storage Spent Fuel Behavior." *Zirconium in the Nuclear Industry, Sixth International Symposium, Vancouver, British Columbia, June 28- July 1, 1982*. Franklin, D.G. and Adamson, R.B., eds. ASTM STP 824. Pages 595-626. Philadelphia, Pennsylvania: American Society for Testing and Materials. TIC: 241417.

Wallace, A.C.; Shek, G.K.; and Lepik, O.E. 1989. "Effects of Hydride Morphology on Zr-2.5Nb Fracture Toughness." *Zirconium in the Nuclear Industry: Eighth International Symposium, held 19-23 June 1988 at San Diego, California*. ASTM STP 1023. Pages 66-88. Philadelphia, Pennsylvania: American Society for Testing and Materials. TIC: 241414.

Wolery, T.J. and Daveler, S.A. 1992. *EQ6, A Computer Program for Reaction Path Modeling of Aqueous Geochemical Systems: Theoretical Manual, User's Guide, and Related Documentation (Version 7.0)*. UCRL-MA-110662 PT IV. Livermore, California: Lawrence Livermore National Laboratory. ACC: MOL.19980701.0459.

Wolfram, J.H.; Mizia, R.E.; Jex, R.; Nelson, L.; Garcia, K.M. 1996. *The Impact of Microbially Influenced Corrosion on Spent Nuclear Fuel and Storage Life*. INEL-96/0335. Idaho Falls, Idaho: Idaho National Engineering Laboratory. ACC: MOL.20030925.0038.

Yau, T-L. 1983. "Corrosion Properties of Zirconium in Chloride Solutions." *Corrosion 83, International Corrosion Forum, Anaheim, California, April 18-22, 1983*. Paper No. 26. Pages 26/1 - 26/13. Houston, Texas: National Association of Corrosion Engineers. TIC: 243849.

Yau, T. L. 1984. "Zirconium Versus Corrosive Species in Geothermal Fluids." Paper 140 of *Corrosion 84*. Houston, Texas: National Association of Corrosion Engineers. TIC: 238987.

Yau, T.L. and Maguire, M. 1990. "Control of Localized Corrosion of Zirconium in Oxidizing Chloride Media." *Advances in Localized Corrosion, Proceedings of the Second International Conference on Localized Corrosion, June 1-5, 1987, Orlando, Florida*. Isaacs, H.S.; Bertocci, U.; Kruger, J. and Smialowska, S., eds. Pages 311-319. Houston, Texas: National Association of Corrosion Engineers. TIC: 247083.

Yau, T.L. and Webster, R.T. 1987. "Corrosion of Zirconium and Hafnium." In *Corrosion*, Volume 13, Pages 707-721 of *ASM Handbook*. Formerly 9th Edition, Metals Handbook. Materials Park, Ohio: ASM International. TIC: 240704.

## **8.2 CODES, STANDARDS, REGULATIONS, AND PROCEDURES**

10 CFR 63. Disposal of High-Level Radioactive Wastes in a Geologic Repository at Yucca Mountain, NV. Readily available.

10 CFR 60. Energy: Disposal of High-Level Radioactive Wastes in Geologic Repositories. Readily available

AP-2.22Q, Rev. 1. *Classification Analyses and Maintenance of the Q-List*. Washington, D.C.: U.S. Department of Energy, Office of Civilian Radioactive Waste Management. ACC: DOC.20030807.0002.

AP-SI.1Q Rev. 5. ICN 2 *Software Management*. Washington, DC: U.S. Department of Energy, Office of Civilian Radioactive Waste Management. ACC: DOC.20030902.0003.

AP-SIII.2Q Rev. 1. ICN 2 *Qualification of Unqualified Data*. Washington, DC: U.S. Department of Energy, Office of Civilian Radioactive Waste Management. ACC: DOC.20040127.0008.

AP-SIII.9Q, Rev. 1. ICN 3. *Scientific Analyses*. Washington, D.C.: U.S. Department of Energy, Office of Civilian Radioactive Waste Management. ACC: DOC.20040301.0002.

ASTM C 1174-97. 1998. *Standard Practice for Prediction of the Long-Term Behavior of Materials, Including Waste Forms, Used in Engineered Barrier Systems (EBS) for Geological Disposal of High-Level Radioactive Waste*. West Conshohocken, Pennsylvania: American Society for Testing and Materials. TIC: 246015.

## **8.3 SOURCE DATA, LISTED BY DATA TRACKING NUMBER**

MO0307SEPFEPS4.000. LA FEP List. Submittal date: 07/31/2003.

**APPENDIX A**  
**CLADDING TEMPERATURE ESTIMATES FOR POSTCLOSURE**

INTENTIONALLY LEFT BLANK

## APPENDIX A - CLADDING TEMPERATURE ESTIMATES FOR POSTCLOSURE

Many of the features, events, and processes (FEPs) depend on temperature. Peak temperatures are important for some FEPs such as delayed hydride cracking. Other FEPs such as general corrosion or creep depend on both the temperature levels and how long the temperatures stay elevated. This appendix will develop both best estimate and peak temperatures for the cladding.

The cladding temperatures are predicted by adding the interior temperature rise across the waste package to the waste package surface temperature. The waste package surface temperatures (BSC 2003b [DIRS 166463], Section 6.2) vary with waste package location in the repository, water infiltration flux, and time (from radioactive decay). The temperature rise across the waste package (BSC 2004b) [DIRS 166727] depends on the thermal loading (decay heat power) of the waste package and the loading pattern. The peak cladding temperature for a specific rod will also depend on what location the rod is loaded in the waste package. The maximum cladding temperatures tend to occur in the center location and the coolest locations are along the outer row of locations.

This appendix will first address the expected waste package surface temperatures. It will then discuss the radial temperature distribution across the waste package for the fuel. Finally, these two pieces of information will be combined to give cladding temperatures. A comparison of the current temperature estimates with those used in the cladding degradation evaluation for SR (CRWMS M&O 2000a [DIRS 153246]) will also be made.

### Waste Package Surface Temperature

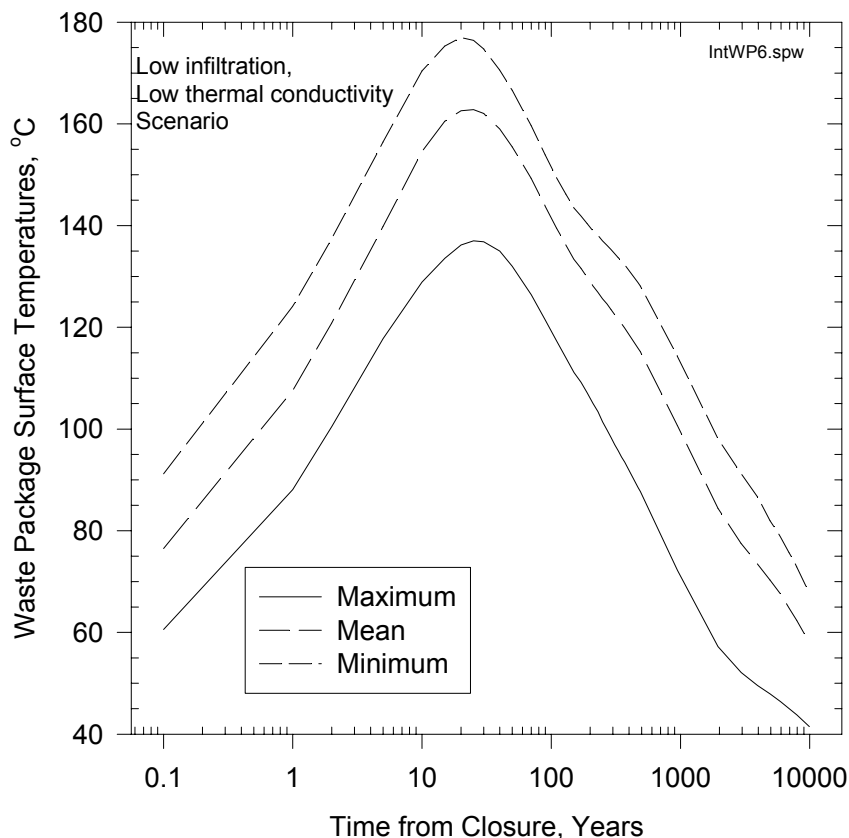
The waste package surface temperatures (BSC 2003b [DIRS 166463], Section 6.2) depend on the location within the repository, the water infiltration flux, and the thermal loading. Table A-1 (BSC 2003b [DIRS 166463], Section 6.2) provides the minimum, maximum and mean waste package surface temperatures for different infiltration fluxes and thermal conductivity of the rock. The overall temperatures (last row of Table A-1) have a minimum temperature of 74°C, mean temperature of 138°C, and the maximum temperature of 177°C. The waste package temperature profiles for Bin 4, low infiltration, low thermal conductivity (bold row in Table A-1) will be used for estimating cladding temperatures. The selection of this group is conservative for estimating mean temperatures because it represents the hottest group. These temperatures are used in the first row of Table A-2 to estimate cladding temperatures. Figure A-1 provides the values of waste package surface temperature of the hottest waste package group (lowest flux, low thermal conductivity). This plot shows that after repository closure (after the 50 year ventilation period) the temperatures increase and reach a peak after about 20 years. They then decrease as the decay heat decreases exponentially (close to a straight line on the semi-log scale of Figure A-1). By 1000 years, the maximum waste package surface temperature is about 114°C. At 10,000 years, the maximum waste package has cooled to about 68°C.

Table A-1. The Minimum, Mean, and Maximum of the Peak CSNF Temperatures (°C) for All Bins for the Three Infiltration Flux Cases for the TSPA-LA Base Case

Bin Number	Infiltration Flux	Thermal Conductivity	CSNF Minimum (°C)	CSNF Mean (°C)	CSNF Maximum (°C)
1	Lower	Mean	129	138	150
1	Mean	Mean	123	133	142
1	Upper	Mean	74	87	96
1	Lower	Low	144	155	170
1	Upper	High	112	121	128
2	Lower	Mean	122	138	152
2	Mean	Mean	121	136	145
2	Upper	Mean	121	134	143
2	Lower	Low	136	156	172
2	Upper	High	112	123	130
3	Lower	Mean	124	142	156
3	Mean	Mean	121	139	145
3	Upper	Mean	118	137	144
3	Lower	Low	138	160	176
3	Upper	High	110	125	130
4	Lower	Mean	123	144	156
4	Mean	Mean	122	140	146
4	Upper	Mean	114	137	144
<b>4</b>	<b>Lower</b>	<b>Low</b>	<b>137</b>	<b>163</b>	<b>177</b>
4	Upper	High	108	125	130
5	Lower	Mean	135	148	156
5	Mean	Mean	133	142	145
5	Upper	Mean	129	139	142
5	Lower	Low	151	166	176
5	Upper	High	119	127	129
Overall			74	138	177

Source: BSC 2003b [DIRS 166463], Section 6.2

The predictions of the waste package surface temperatures have evolved over time as both the analytical tools and the design have evolved. The surface temperatures used for the cladding degradation evaluation for TSPA-SR were from an earlier evaluation (CRWMS M&O 2001a [DIRS 151662], Section 6.2.1) and represented waste packages with backfill. In that analysis, the mean value for waste package peak temperature reached 277°C. An uncertainty of 13.5 percent produced a maximum peak temperature of 315°C. These temperatures are used in the first row of Table A-2 to estimate cladding temperatures.

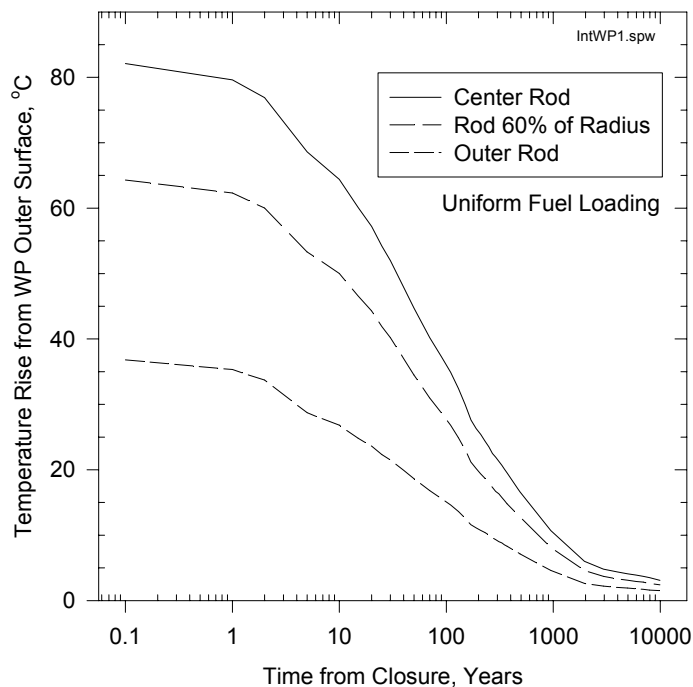


Source: BSC 2003b [DIRS 166463], Section 6.2

Figure A-1. WP Surface Temperature History for Hottest Group

## Interior Temperatures

Sensitivity studies have been performed on the possible loading patterns for assemblies with high decay heat (hot assemblies) (BSC 2004b) [DIRS 166727]. The cladding temperature has a distribution that varies across the radius of the waste package, peaking in the center. The maximum thermal loading of the waste package is 11.8 kW. If the heat load is uniformly distributed to the 21 assemblies (562 W/assembly) then the temperature distribution across the waste package is given in Figure A-2. The center rod is the hottest, starting out 82°C hotter than the waste package surface at closure and the temperature rise decreases with time (due to fission product decay). The outer rod (bottom curve) is the coolest (starting at 37°C above waste package surface and cooling). The intermediate profile represents a rod located about 60 percent of the radial distance toward the outer edge. While only one assembly is placed in the center location, the remaining 20 assemblies are in cooler locations. Twelve assemblies are located in the coolest, outer rows of the waste package. Uniform loading represents the nominal or mean temperature rise. Hotter cladding temperatures are possible if high power assemblies are located in the center region and cooler temperatures are possible with hotter assemblies located in the outer region. This interior temperature rise will be added to the waste package surface temperatures to estimate cladding temperatures.



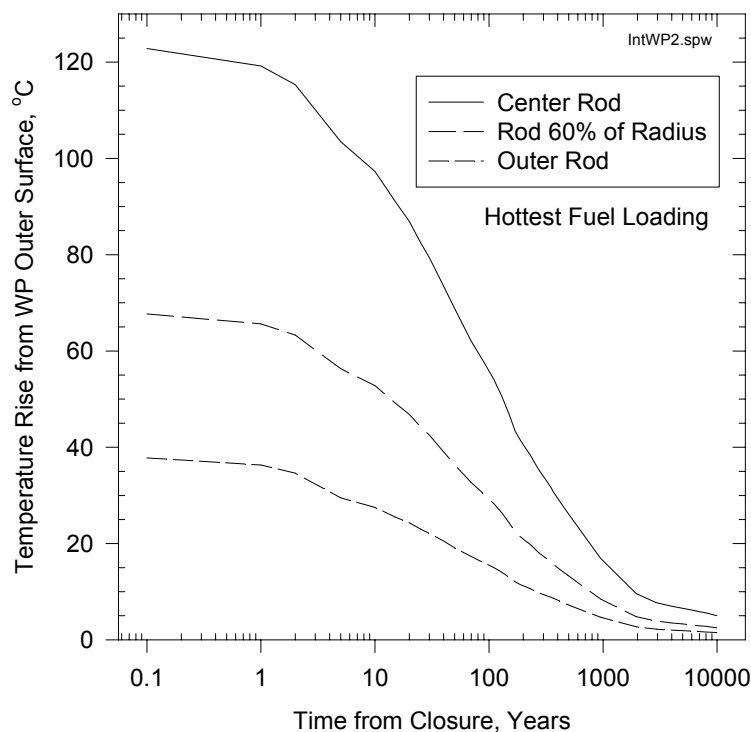
Source: BSC 2004b [DIRS 166727]

Figure A-2. Average Temperature Rise Across the Waste Package

Sensitivity studies of loading patterns were performed to estimate maximum cladding temperatures. Figure A-3 shows the temperature rise when a 2,100 Watt assembly is loaded in the center location and the remaining 20 assembly locations are loaded with 485 Watt assemblies. This is the hottest permitted loading pattern because the center rod is predicted to reach 350°C with a simulated repository closure occurring after 25 years and using conservative design heat transfer codes (used for design conservatism). The current repository design and TSPA are based on 50 years of ventilation before closure. The center rod is the hottest, starting out 123°C hotter than the waste package surface at closure and the temperature rise decreases with time (due to fission product decay). The outer rod (bottom curve) is the coolest (starting at 38°C above waste package surface and again decreasing with time). It is important to note that the temperature rise decreases significantly in the first 100 years. This interior temperature rise will be added to the waste package surface temperatures to estimate cladding temperatures.

In the earlier TSPA-SR analysis, *Thermal History of Cladding in a 21 PWR SNF WP Loaded with Average Fuel* (CRWMS M&O 2000e [DIRS 147881], Table 6-2) was used to give the time dependent temperature distribution across the waste package for the initial average thermal loading of 9.1 kW. The earlier analysis of cladding degradation (CRWMS M&O 2001a [DIRS 151662]) used a 31°C temperature rise for the nominal SR case (thermal loading of 9.1 kW). This design also had a shrink fit between the inner and outer waste package so there was a much smaller temperature rise across the two barriers. The model only addressed uniform fuel loading. The peak temperature occurred three years after closure. The analysis used an uncertainty of 13.5 percent to predict the maximum temperature rise of 35°C. The 13.5 percent uncertainty was based on waste package loading errors and not on variation in waste package power.

Minimum temperature rise across the waste package would occur if the hotter assemblies were loaded on the outside row of the waste package or the waste package has a lower thermal loading than 11.8 kW per waste package (maximum design value). Such loading patterns were not studied and the mean thermal loading will be used to estimate the lower range of cladding temperatures.

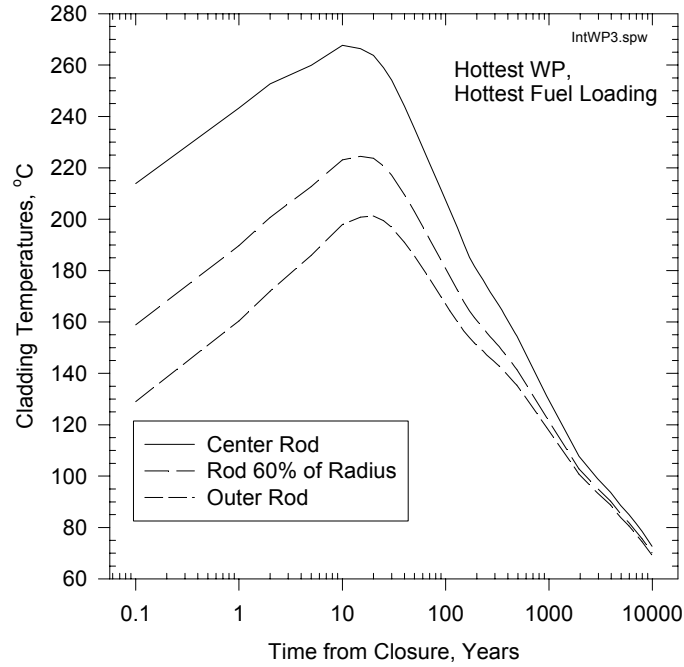


Source: BSC 2004b [DIRS 166727]

Figure A-3. Maximum Temperature Rise Across the Waste Package

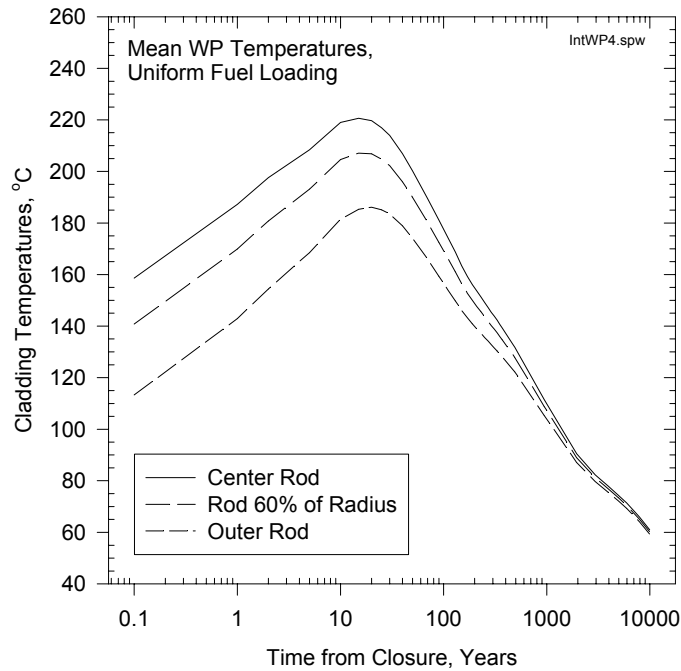
### Cladding Temperatures

The calculated center rod temperature is the sum of waste package surface temperature (see Figure A-1) and the temperature rise across the waste package (either Figure A-2 or A-3). The maximum cladding temperature is generated by placing the hottest possible fuel loading into the hottest waste package. Figure A-4 provides the temperature history of the hottest center rod, rod at 60 percent of radius and outer rod. The current repository design has the maximum cladding temperatures peak at 268°C. The outer rod temperature peaks at 201°C. Figure A-5 provides the temperature history of the average rod loaded into the average waste package. Here the center rod temperature peaks at 221°C and the outer rod peaks at 186°C.



Source: This report

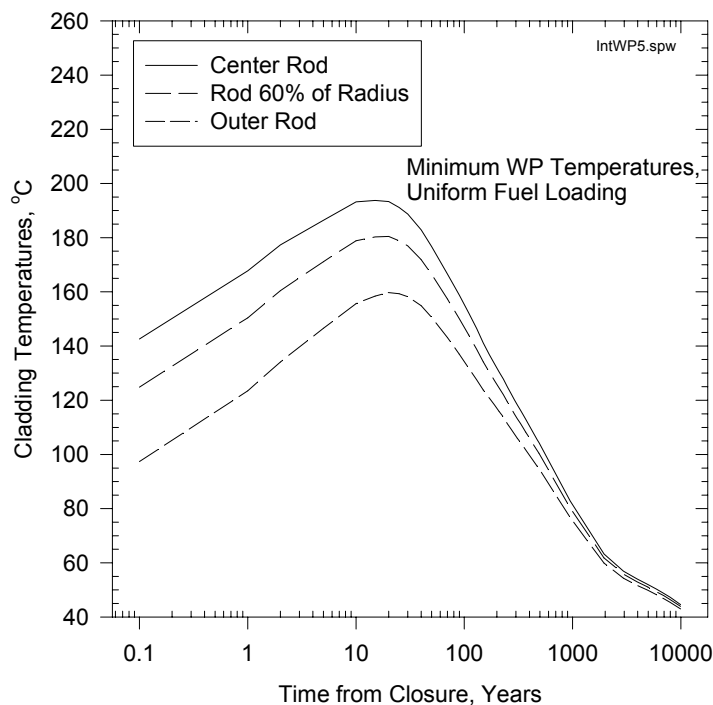
Figure A-4. Temperature Profiles for Maximum Fuel Loading into Hottest Waste Package



Source: This report

Figure A-5. Temperature Profiles for Mean Fuel Loading into Mean Waste Package

Figure A-6 provides the cladding temperature histories for an average loading of rods into the coolest waste package in the group being evaluated (Bin 4, lower infiltration flux, low thermal conductivity, see Table A-1). Here the center rod temperature peaks at 194°C and the outer rod peaks at 160°C. This group contains the hottest waste package. Colder waste packages are contained in other groups so Figure A-6 can not be considered minimum cladding temperatures for the repository.



Source: This report

Figure A-6. Temperature Profiles for Mean Fuel Loading into Coolest Waste Package

Table A-2 provides the cladding temperatures for the rods in the center of the waste package. Two cases are given. The case labeled “Earlier Analysis” shows the temperatures calculated in the cladding degradation for SR (CRWMS M&O 2001a [DIRS 151662]). In this case, maximum cladding temperatures peaked at 350°C. These temperatures were higher than currently expected because they represented a backfill design evaluated in TSPA-VA. Even at these high temperatures, degradation from thermal effects was not expected. The case labeled “Current Analysis” shows the temperatures used for TSPA-LA.

Table A-3 shows the center rod temperature histories for the average fuel loading into the average waste package and the maximum loading into the hottest WP. The temperatures are above 200°C for less than 130 years. The peak temperature of 268°C will be used to evaluate the FEPs in this report. Table A-3 also estimates the temperature of the cladding at the end of the regulatory period. The maximum cladding temperature is 73°C at 10,000 years. This temperature will be used to evaluate FEPs addressing helium production from alpha decay of actinides.

Table A-2. Peak Waste Package Surface Temperatures and Center Rod Cladding Temperatures

	Earlier Analysis			Current Analysis		
	Minimum (°C)	Mean (°C)	Maximum (°C)	Minimum (°C)	Mean (°C)	Maximum (°C)
Waste package surface	245	277	315	134	161	171
Temperature rise across waste package	27	31	35	60	60	97
Center rod cladding peak temperature	272	308	350	194	221	268

Source: CRWMS M&O 2000e [DIRS 147881], BSC 2003b [DIRS 166463], Section 6.2, BSC 2004b [DIRS 166727]

Table A-3. Time Dependency of Temperatures for Center Rod, Average and Maximum

Time (Years)	Temperature, Average Loading, Average Waste Package Temperature (°C)	Temperature, Maximum Fuel Loading, Maximum Waste Package Temperature (°C)
0	159	214
5	208	260
10	219	<b>268</b>
15	<b>221</b>	266
20	220	264
30	214	254
90	181	212
130	169	197
290	145	170
950	111	131
3000	82	99
6000	71	85
10,000	61	73

Source: BSC 2003b [DIRS 166463], Section 6.2, BSC 2004b [DIRS 166727]

Radionuclide transport depends on the water condensing or dripping. For local transportation of radionuclides to occur, the rods must cool to below the boiling point of the water (about 96°C at the repository altitude). Table A-4 provides the approximate time to cool to boiling for rods in three radial locations of three different waste packages.

Table A-4. Time from Closure to Cool Cladding to Boiling Point (96°C)

	Center Rod (Years)	Rod 60% Radius (Years)	Outer Rod (Years)
Cold waste package, Average Loading	670	590	470
Average waste package, Average Loading	1680	1600	1460
Hottest waste package, Hottest Loading	3520	2840	2600

Source: BSC 2003b [DIRS 166463], Section 6.2 BSC 2004b [DIRS 166727]

**APPENDIX B**  
**DATA QUALIFICATION PLAN**

INTENTIONALLY LEFT BLANK

**APPENDIX B - DATA QUALIFICATION PLAN**

<b>Section I. Organizational Information</b>			QA/QA
Qualification Title			ERS 3/15/04
Qualification of Technical Information - Attachment II to Clad Degradation - FEPs Screening Arguments (ANL-WIS-MD-000008)			
Requesting Organization			
Waste Form			
<b>Section II. Process Planning Requirements</b>			
1. List of Unqualified Data to be Evaluated			
156122 ERS 3/15/04			
All sources of technical information that provide direct input to ANL-WIS-MD-000008 will be evaluated. The Document Input Reference System [DIRS] assigns to these sources the following numbers: 156605, 161421, 150560, 101704, 101903, 147797, 164593, 100494, 161991, 161988, 164195, 149208, 152354, <del>153937</del> , 101591, 145073, 101676, 164598, 100455, 100462, 109219, 165318, 100817, 154433, 165268. Authoritative sources will not be qualified.			
2. Type of Data Qualification Method(s) [Including rationale for selection of method(s) (Attachment 3) and qualification attributes (Attachment 4)]			
The information will be qualified by the Technical Assessment method that confirms that the data have been used in similar applications (AP-SIII.2Q, Attachment 3, Section 5 (b)(3)). This method was chosen because documentation or proof of proper data acquisition is unavailable for review.			
One or more of the following qualification attributes (taken from AP-SIII.2Q, Attachment 4) will be considered:			
<ul style="list-style-type: none"> <li>• Qualifications of personnel or organizations generating the information,</li> <li>• Prior peer or other professional reviews of the information and their results, and</li> <li>• Extent and quality of corroborating information.</li> </ul>			
3. Data Qualification Team and Additional Support Staff Required			
Eric Siegmann - Chairman Chris Pflum			
4. Data Evaluation Criteria			
The following data evaluation criteria are based on and in this case are identical to the attributes in block 2:			
<ul style="list-style-type: none"> <li>• Qualifications of personnel or organizations generating the information,</li> <li>• Prior peer or other professional reviews of the information and their results, and</li> <li>• Extent and quality of corroborating information.</li> </ul>			
5. Identification of Procedures Used			
AP-SIII.2Q, AP-SIII.9Q, AP-3.15Q REV4 ICN2 ERS 3/15/04 <del>REV1, ICN3</del> <del>REV1, ICN2</del>			
<b>Section III. Approval</b>			
Qualification Chairperson Printed Name	Qualification Chairperson Signature	Date	
Eric Siegmann	Eric R. Siegmann	2/27/04	
Responsible Manager Printed Name	Responsible Manager Signature	Date	
Howard Adkins	Howard E. Adkins	02-27-04	

INTENTIONALLY LEFT BLANK

**APPENDIX C**

**QUALIFICATION OF TECHNICAL INFORMATION THAT SUPPORTS CLAD  
DEGRADATION - FEPS SCREENING ARGUMENTS (ANL-WIS-MD-000008)**

INTENTIONALLY LEFT BLANK

**APPENDIX C - QUALIFICATION OF TECHNICAL INFORMATION THAT  
SUPPORTS *CLAD DEGRADATION - FEPS SCREENING ARGUMENTS*  
(ANL-WIS-MD-000008)**

**C.1 PURPOSE**

The “Clad Degradation - FEPs (Features, Events and Processes) Screening Arguments” (analysis) relies on technical information that may not have been collected under an approved quality assurance program that meets the requirements of 10 CFR Part 63, Subpart G [DIRS 156605] or its predecessor, 10 CFR Part 60 [DIRS 103540]. This appendix qualifies the technical information that the cladding degradation analysis uses as direct input that is important to waste isolation. With the following exception, the appendix was prepared according to the Project's Procedure "Qualification of Unqualified Data" (AP-SIII.2Q, Revision 1, ICN 2). This appendix assumes "technical information" and "data" are synonymous; the procedure does not<sup>1</sup>. This qualification is being performed under the plan presented in Section C-5.

**C.2 METHODS AND CRITERIA**

The procedure offers five methods by which unqualified data may be qualified. The method of technical assessment was chosen because documentation or proof of proper data, or in this case information acquisition is unavailable for review. The assessment confirms that the information has been used in similar applications. According to AP-SIII.2Q (Attachment 3, Section 5.), this confirmation comprises: "A discussion and documentation that the data have been used in applications that are similar to those for which the data will be used."

In addition to technical assessment, the qualification process considers at least one of the "Qualification Process Attributes" of AP-SIII.2Q Attachment 4.

- Qualifications of personnel or organizations generating the information,
- Prior peer or other professional reviews of the information and their results, and
- Extent and quality of corroborating information.

These criteria also served as the "data evaluation criteria" on which the Data Qualification Team provided judgements (AP-SIII.2Q, Section 5.1.2 (b)(4)).

The team was comprised of two members: Eric Siegmann, a cladding expert and the analysis originator, chaired the team and Chris Pflum, who is technically competent in radioactive waste management, assisted. As the analysis originator, Eric Siegmann is not independent of the information to be qualified (AP-SIII.2Q, Section 5.1.2 (b)(3)). However, the procedure requires that the originator chair the team "... when the qualification is performed within the Analysis or

---

<sup>1</sup> This analysis and attachment were under review when the governing procedures: "Scientific Analyses" (AP-SIII.9Q Rev. 1, ICN 3, 3/1/04) and "Managing Technical Product Inputs" (AP-3.15Q, Rev. 4, ICN 2, 2/25/04) were revised. The new procedures do not recognize "technical information". This attachment considers the factors that AP SIII.9Q (Section 5.2.1 (m)) lists for data that are suitable for intended use. AP- 3.15Q Rev. 4, ICN 3 does not apply to this analysis because the analysis was finished within 30 days of the procedure's effective date.

Model Report" (AP-SIII.2Q Section 5.1.1). Chris Pflum did not participate in the acquisition or development of the information, and was an independent reviewer of the analysis.

### C.3 QUALIFICATION OF TECHNICAL INFORMATION

The procedure does not apply to "Established Fact data or numerical data obtained from an established/authoritative data source". Because some of the technical information comes from authoritative sources (other than the U.S. Department of Energy, Office of Civilian Radioactive Waste Management), it does not need to be qualified. The remaining information is qualified only for its intended use i.e., to justify excluding from performance assessment twenty-one modes of cladding degradation. Some of the exclusionary arguments depend on qualitative arguments from the open literature that the analysis cites as technical information.

Table C-1 lists sources of technical information and the criteria used to qualify the information. When the source is an authoritative source, the table provides only the sources' names. For the remaining sources, the Table designates the attributes or criteria that are used, in conjunction with the technical assessment, to qualify the information.

Table C-1. Sources of Technical Information and Criteria Used to Qualify the Information

Sources	Criteria
Beckman, D.A. 2001. Memorandum from D.A. Beckman (BSC), February 21, 2001, distributing: "NRC Issue Resolution Status Report on Container Life and Source Term, Revision 3," Division of Waste Management, Office of Nuclear Material Safety and Safeguards, U.S. Nuclear Regulatory Commission. ACC: MOL.20010418.0048. DIRS 156122	Authoritative Source / Excluded from Qualification  U.S. Nuclear Regulatory Commission
Cragnolino, G.A.; Dunn, D.S.; Brossia, C.S.; Jain, V.; and Chan, K.S. 1999. Assessment of Performance Issues Related to Alternate Engineered Barrier System Materials and Design Options. CNWRA 99-003. San Antonio, Texas: Center for Nuclear Waste Regulatory Analyses. TIC: 248875. DIRS 152354	Authoritative Source / Excluded from Qualification  Center for Nuclear Waste Regulatory Analyses
10 CFR 63. Energy: Disposal of High-Level Radioactive Wastes in a Geologic Repository at Yucca Mountain, Nevada. Readily available. DIRS 156605	Authoritative Source / Excluded from Qualification  U.S. Nuclear Regulatory Commission
EPRI (Electric Power Research Institute) 2002. Dry Cask Storage Characterization Project. EPRI TR-1002882. Palo Alto, California: Electric Power Research Institute. TIC: 253737. DIRS 161421	Authoritative Source / Excluded from Qualification  Electric Power Research Institute
IAEA (International Atomic Energy Agency) 1998. Waterside Corrosion of Zirconium Alloys in Nuclear Power Plants. IAEA-TECDOC-996. Vienna, Austria: International Atomic Energy Agency. TIC: 248234. DIRS 150560	Authoritative Source / Excluded from Qualification  International Atomic Energy Agency
Lanning, D.D.; Beyer, C.E.; and Painter, C.L. 1997. FRAPCON-3: Modifications to Fuel Rod Material Properties and Performance Models for High-Burnup Application. NUREG/CR-6534. Volume 1. Richland, Washington: Pacific Northwest National Laboratory. TIC: 238923. DIRS 101704	Authoritative Source / Excluded from Qualification  Contractor for the U.S. Nuclear Regulatory Commission

Table C-1. Sources of Technical Information and Criteria Used to Qualify the Information (Continued)

Sources	Criteria
NRC (U.S. Nuclear Regulatory Commission) 1997. Standard Review Plan for Dry Cask Storage Systems. NUREG-1536. Washington, D.C.: U.S. Nuclear Regulatory Commission. ACC: MOL.20010724.0307. DIRS 101903	Authoritative Source / Excluded from Qualification  U.S. Nuclear Regulatory Commission
NRC (U.S. Nuclear Regulatory Commission) 2000. "Interim Staff Guidance - 11. Storage of High Burnup Spent Fuel." ISG - 11. Washington, D.C.: U.S. Nuclear Regulatory Commission. Accessed March 21, 2000. TIC: 247227. <a href="http://www.nrc.gov/OPA/reports/isg11.htm">http://www.nrc.gov/OPA/reports/isg11.htm</a> DIRS 147797	Authoritative Source / Excluded from Qualification  U.S. Nuclear Regulatory Commission
NRC (U.S. Nuclear Regulatory Commission) 2002. Interim Staff Guidance - 11, Revision 2. Cladding Considerations for the Transportation and Storage of Spent Fuel. ISG-11, Rev. 2. Washington, D.C.: U.S. Nuclear Regulatory Commission. TIC: 254441. DIRS 164593	Authoritative Source / Excluded from Qualification  U.S. Nuclear Regulatory Commission
Pourbaix, M. 1974. Atlas of Electrochemical Equilibria in Aqueous Solutions. Houston, Texas: National Association of Corrosion Engineers. TIC: 208955. DIRS 100817	Authoritative Source / Excluded from Qualification  National Association Of Corrosion Engineers
Yau, T.L. and Webster, R.T. 1987. "Corrosion of Zirconium and Hafnium." In Corrosion, Volume 13, Pages 707-721 of ASM Handbook. Formerly 9th Edition, Metals Handbook. [Materials Park, Ohio]: ASM International. TIC: 240704. DIRS 100494	Authoritative Source / Excluded from Qualification  American Society for Metals - Handbook
Adler Flitton, M.K.; Mizia, R.E.; and Bishop, C.W. 2002 "Underground Corrosion of Activated Metals in an Arid Vadose Zone Environment." Corrosion/2002, [57th Annual Conference & Exposition, April 7-11, 2002, Denver, Colorado]. Paper No. 02531. Houston, Texas: NACE International. TIC: 253838. DIRS 161991	Personnel / organization qualifications Peer / professional review Extent and quality of corroborating information.
Brossia, C.S.; Cragnolino, G.A.; and Dunn, D.S. 2002. "Effect of Oxide Thickness on the Localized Corrosion of Zircaloy." Corrosion/2002, [57th Annual Conference & Exposition, April 7-11, 2002, Denver, Colorado]. Paper No. 02549. Houston, Texas: NACE International. TIC: 253839. DIRS 161988	Personnel / organization qualifications Peer / professional review Extent and quality of corroborating information.
Cappelaere, C.; Limon, R.; Bredel, T.; Herter, P.; Gilbon, D.; Bouffieux, P.; and Mardon, J-P. 2002. "Long Term Behavior of the Spent Fuel Cladding in Dry Storage Conditions." [ICEM '01, Proceedings of the 8th International Conference on Radioactive Waste Management and Environmental Remediation, held in Burges, Belgium, September 30-October 4, 2001]. [Taboas, A.; Vanbrabant, R.; and Benda, G., eds]. [1], [New York, New York]: American Society of Mechanical Engineers. TIC: 254663. DIRS 164195	Personnel / organization qualifications Peer / professional review Extent and quality of corroborating information.
Clayton, J.C. 1989. "Internal Hydriding in Irradiated Defected Zircaloy Fuel Rods." Zirconium in the Nuclear Industry: Eighth International Symposium, held June 19-23, 1988 San Diego, California. ASTM STP 1023. Pages 266-288. Philadelphia, Pennsylvania: American Society for Testing and Materials. TIC: 241414. DIRS 149208	Personnel / organization qualifications Peer / professional review
Cunningham, M.E.; Simonen, E.P.; Allemann, R.T.; Levy, I.S.;	Personnel / organization qualifications

Table C-1. Sources of Technical Information and Criteria Used to Qualify the Information (Continued)

Sources	Criteria
Hazelton, R.F.; and Gilbert, E.R. 1987. Control of Degradation of Spent LWR Fuel During Dry Storage in an Inert Atmosphere. PNL-6364. Richland, Washington: Pacific Northwest Laboratory. ACC: HQO.19941222.0016. DIRS 101591	Extent and quality of corroborating information.
Edsinger, K. 2000. "A Review of Fuel Degradation in BWRs." Proceedings of the 2000 International Topical Meeting on Light Water Reactor Fuel Performance, Park City, Utah, April 10-13, 2000. La Grange Park, Illinois: American Nuclear Society. TIC: 248973. DIRS 154433	Personnel / organization qualifications Peer / professional review
Greene, C.A.; Brossia, C.S.; Dunn, D.S.; and Cragolino, G.A. 2000. "Environmental and Electrochemical Factors on the Localized Corrosion of Zircaloy-4." Corrosion/2000, [55th Annual Conference & Exposition, March 26-31, 2000, Orlando, Florida]. Paper No. 00210. Houston, Texas: NACE International. TIC: 246988. DIRS 145073	Personnel / organization qualifications Peer / professional review Extent and quality of corroborating information.
Hansson, C.M. 1984. The Corrosion of Zircaloy 2 in Anaerobic Synthetic Cement Pore Solution. SKB TR-84-13. Stockholm, Sweden: Svensk Kärnbränsleförsörjning A.B. TIC: 206293. DIRS 101676 Verified	Personnel / organization qualifications Peer / professional review Extent and quality of corroborating information.
Hayes, T.A.; Rosen, R.S.; and Kassner, M.E. 1999. Critical Analysis of Dry Storage Temperature Limits for Zircaloy-Clad Spent Nuclear Fuel Based on Diffusion Controlled Cavity Growth. UCRL-ID-131098. Livermore, California: Lawrence Livermore National Laboratory. TIC: 254551. DIRS 164598	Personnel / organization qualifications Extent and quality of corroborating information.
Hillner, E.; Franklin, D.G.; and Smee, J.D. 1998. The Corrosion of Zircaloy-Clad Fuel Assemblies in a Geologic Repository Environment. WAPD-T-3173. West Mifflin, Pennsylvania: Bettis Atomic Power Laboratory. TIC: 237127. DIRS 100455	Personnel / organization qualifications Peer / professional review Extent and quality of corroborating information.
Kreyns, P.H.; Bourgeois, W.F.; White, C.J.; Charpentier, P.L.; Kammenzind, B.F.; and Franklin, D.G. 1996. "Embrittlement of Reactor Core Materials." Zirconium in the Nuclear Industry, Eleventh International Symposium held in Garmisch-Partenkirchen, Germany, September 11-14, 1995. Bradley, E.R. and Sabol, G.P., eds. ASTM STP 1295. Pages 758-782. West Conshohocken, Pennsylvania: American Society for Testing and Materials. TIC: 237256. DIRS 100462	Personnel / organization qualifications Peer / professional review Extent and quality of corroborating information.
Peehs, M. 1998. Assessment of Dry Storage Performance of Spent LWR Fuel Assemblies with Increasing Burn-Up. Erlangen, Germany: Bereich Energieerzeugung. TIC: 245171. DIRS 109219	Personnel / organization qualifications Extent and quality of corroborating information.
Piron, J.P. and Pelletier, M. 2001. "State of the Art on the Helium Issues." Section 5.3 of Synthesis on the Long Term Behavior of the Spent Nuclear Fuel. Poinssot, C., ed. CEA-R-5958(E). Volume 1. [Paris], France: Commissariat à l'Énergie Atomique. TIC: 253976. DIRS 165318	Personnel / organization qualifications Peer / professional review Extent and quality of corroborating information.
Wolfram, J.H.; Mizia, R.E.; Jex, R.; Nelson, L.; and Garcia, K.M. 1996. The Impact of Microbially Influenced Corrosion on Spent Nuclear Fuel and Storage Life. INEL-96/0335. Idaho Falls, Idaho: Idaho National Engineering Laboratory, Lockheed Martin Idaho Technologies Company. ACC: MOL.20030925.0039. DIRS 165268	Personnel / organization qualifications Extent and quality of corroborating information

Both the discussions above and in the following sections fulfill requirements of AP-SIII.2Q to discuss the data (in this case, technical information) for qualification, the method of qualification, and the evaluation criteria (See AP-SIII.2Q, Section 5.3.1, paragraphs (a) (1) through (3)).

A discussion of the remaining requirements follows:

- In regard to AP-SIII.2Q, Section 5.3.1 (a)(4), the team considers the information technically correct because it has undergone a technical assessment and it fulfills at least one of the “Qualification Process Attributes”. However, AP-SIII.2Q (Attachment 3, paragraph 1) does not require "an evaluation of the data quality and correctness" for data that would be qualified by the technical assessment method (referred to as Method 5).
- In regard to AP-SIII.2Q, Section 5.3.1 (a)(5), no data are generated by this evaluation.
- In regard to AP-SIII.2Q, Section 5.3.1 (a)(6), the team finds that the information is qualified for its use only within this document.
- In regard to AP-SIII.2Q, Section 5.3.1 (a)(7), the team recommends that the information be given the status of “qualified data” should the applicable procedures no longer recognize technical information. Until then, the status should remain as “technical information.”
- In regard to AP-SIII.2Q, Section 5.3.1 (a)(8), the team did not “abandon” any qualification method.
- In regard to AP-SIII.2Q, Section 5.3.1 (a)(9), the technical information is qualified only to justify excluding from performance assessment twenty-one modes of cladding degradation. It is not qualified for other potential uses.
- In regard to AP-SIII.2Q, Section 5.3.1 (a)(10), supporting or corroborating information is identified in Section C.3 when used in the qualification effort.
- In regard to AP-SIII.2Q, Section 5.3.1 (a)(11), the qualification was performed under the data qualification plan presented in Section C.4 of this appendix.

### **C.3.1 Qualification of Adler Flitton, M.K.; Mizia, R.E.; and Bishop, C.W. 2002 [DIRS 161991]**

*Technical Assessment*—The Cladding Degradation Analysis (i.e., this analysis, Section 6.21) applies the cladding/rock contact test in a manner that is consistent with the test results. Both the analysis and the test conclude that corrosion of zirconium was not observed after burial in soil.

*Personnel / Organization Qualifications*—The tests were performed at a national laboratory (Idaho National Engineering and Environmental Laboratory).

*Peer / Professional Review*—The source was peer-reviewed.

*Extent and Quality of Corroborating Information*—An authoritative source, Yau and Webster 1987, corroborates this source's observation that zirconium resists corrosion in soil.

**C.3.2 Qualification of Brossia, C.S.; Cragnolino, G.A.; and Dunn, D.S. 2002. [DIRS 161988]**

*Technical Assessment*—Both this analysis (Section 6.7) and the above source apply consistent conclusions regarding localized (crevice) corrosion of the cladding. Both conclude that any crevice corrosion is not observed.

*Personnel / Organization Qualifications*—The authors work for The Center for Nuclear Waste Regulatory Analyses, Southwest Research Institute. This work was sponsored by the NRC and performed under a QA program that is approved and audited by the NRC.

*Peer / Professional Review*— The source was peer-reviewed.

*Extent and Quality of Corroborating Information*—Two sources corroborate the above source. Yau and Webster (1987 [DIRS 100494], p. 717), an authoritative source, reported that zirconium resists crevice corrosion. In low-pH chloride solutions or chlorine gas, for example, zirconium is not subject to crevice attack. Greene et al. (2000 [DIRS 145073]) performed pitting and crevice corrosion tests on Zircaloy-4. They report that no crevice corrosion is observed under the same environment and electrochemical conditions that promote pitting corrosion on exposed surfaces.

**C.3.3 Qualification of Cappelaere, C.; Limon, R.; Bredel, T.; Herter, P.; Gilbon, D.; Bouffioux, P.; and Mardon, J-P. 2002. [DIRS 164195]**

*Technical Assessment*—Both this analysis (Section 6.12.5) and the above source apply consistent conclusions regarding axial migration of hydrogen in the cladding. Both report minor migration.

*Personnel / Organization Qualifications*—The authors work for CEA, which is a reputable source and an authoritative source for this type of information.

*Peer / Professional Review*— The source was peer-reviewed.

*Extent and Quality of Corroborating Information*—Cunningham et al. 1987 [DIRS 101591] corroborates this source's analysis of hydrogen migration.

**C.3.4 Qualification of Clayton, J.C. 1989 [DIRS 149208]**

*Technical Assessment*—Both this analysis (Section 6.24) and the above source (Clayton, J.C. 1989 [DIRS 149208], Tables 1 through 4, page 270) apply consistent conclusions regarding hydrogen absorption into zirconium. Both report that absorption only occurs under high hydrogen pressure.

*Personnel / Organization Qualifications*—The experiments were performed at the Bettis Atomic Power Laboratory.

*Peer / Professional Review*—The source was peer-reviewed, as stated in the publication.

### **C.3.5 Qualification of Cunningham et al. 1987 [DIRS 101591]**

*Technical Assessment*—Both this analysis and the above source (page 5) apply consistent conclusions regarding axial migration of hydrogen in the cladding. Both report minor migration.

*Personnel / Organization Qualifications*—The analysis was performed at Pacific Northwest Laboratory.

*Extent and Quality of Corroborating Information*—Cappelaere et al. 2002 [DIRS 164195] corroborates this source's analysis of hydrogen migration.

### **C.3.6 Qualification of Edsinger 2000 [DIRS 154433]**

*Technical Assessment*—Both this analysis and the above source apply consistent conclusions regarding hydriding cladding and the requirement for a reducing environment.

*Personnel / Organization Qualifications*—The analysis was performed at Global Nuclear Fuel (previously known as General Electric Nuclear Fuel).

*Peer / Professional Review*—The source was peer-reviewed.

### **C.3.7 Qualification of Greene, C.A.; Brossia, C.S.; Dunn, D.S.; and Cragolino, G.A. 2000. [DIRS 145073]**

*Technical Assessment*—Both this analysis (Section 6.7) and the above source apply consistent conclusions regarding localized (crevice) corrosion of the cladding. Both conclude that any crevice corrosion is not observed.

*Personnel / Organization Qualifications*—The lead author works for the NRC. The other authors work for The Center for Nuclear Waste Regulatory Analyses, Southwest Research Institute. This work was sponsored by the NRC and performed under a QA program that is approved and audited by the NRC.

*Peer / Professional Review*— The source was peer-reviewed.

*Extent and Quality of Corroborating Information*—Two sources corroborate the above source. Yau and Webster (1987 [DIRS 100494], p. 717), an authoritative source, reported that zirconium resists crevice corrosion. In low-pH chloride solutions or chlorine gas, for example, zirconium is not subject to crevice attack. Brossia et al. (2002 [DIRS 161988]) performed pitting and crevice corrosion tests on Zircaloy-4. They report that no crevice corrosion is observed under the same environment and electrochemical conditions that promote pitting corrosion on exposed surfaces.

### **C.3.8 Qualification of Hansson 1984 [DIRS 101676]**

*Technical Assessment*— This analysis and the above source (page 6) assess the extent to which silica could affect cladding corrosion. The analysis considers high dissolved silica content in water, the source considers the silica content in concrete, and an authoritative source (Yau and Webster, 1987 [DIRS 100494]) considers the silica concentration in sea water. All three

anticipate little cladding degradation that can be attributed to silica concentrations that far exceed those that the cladding would encounter in the repository.

*Personnel / Organization Qualifications*—This work was performed at the Danish Corrosion Center.

*Peer / Professional Review*—This report was peer-reviewed within the SKB before publication.

*Extent and Quality of Corroborating Information*— An authoritative source, Yau and Webster, 1987 [DIRS 100494] corroborates this source's assessment of cladding's resistance to silica corrosion.

### **C.3.9 Qualification of Hayes et al. 1999 [DIRS 164598]**

*Technical Assessment*— This analysis and the above source (Figures 2, 5, 6, 8, and 11) assess creep as a mechanism to fail Zircaloy cladding. The analysis does not expect creep at peak repository temperatures (< 268°C), and the source expects little creep damage under 400°C.

*Personnel / Organization Qualifications*—The analysis was performed at Lawrence Livermore National Laboratory.

*Extent and Quality of Corroborating Information*—An authoritative source, NRC 2002 [DIRS 164593], corroborates this source's assessment of creep. Both state that cladding failure attributed to creep is unlikely if peak temperatures are below 400°C.

### **C.3.10 Qualification of Hillner et al. 1998 [DIRS 100455]**

*Technical Assessment*— This analysis and the above source (page 11) do not expect microbes to cause cladding failure. Both consider the corrosion of Zircaloy-clad fuels under repository conditions and both support the concept that organic acids produced by microbes are unlikely to significantly accelerate zirconium corrosion.

*Personnel / Organization Qualifications*—The experiments and analysis were performed at the Bettis Atomic Power Laboratory.

*Peer / Professional Review*—The source was peer-reviewed within the Bettis organization before publication as a WAPD report. It was later accepted, peer-reviewed for publication by the Journal of Nuclear Material.

*Extent and Quality of Corroborating Information*—Three independent sources corroborate Hillner et al. 1998. Wolfram et al. 1996 [DIRS 165268] found no evidence in the literature that zirconium or its alloys are susceptible to microbial-induced corrosion. Yau and Webster, 1987 [DIRS 100494], an authoritative source, states that zirconium resists organic acids that microbes produce. And the Yucca Mountain Project (CRWMS M&O 2000b, [DIRS 151561]) evaluated in-drift microbial communities and concluded that they would have little effect on the in-drift geochemistry.

### **C.3.11 Qualification of Kreyns et al. 1996 [DIRS 100462] Figure 5**

*Technical Assessment*—Hydride embrittlement could cause cladding failure. Test results from Kreyns et al. shows that the fracture toughness of the zirconium-alloyed cladding remains sufficiently high for hydrogen contents up to 4000 ppm that cladding failure is not expected.

*Personnel / Organization Qualifications*—The experiments and analysis were performed at the Bettis Atomic Power Laboratory.

*Peer / Professional Review*—The source was peer-reviewed within the Bettis organization before publication.

*Extent and Quality of Corroborating Information*—This reference is cited by the NRC in "NRC Issue Resolution Status Report on Container Life and Source Term, Revision 3" (Beckman 2001 [DIRS 156122]).

### **C.3.12 Qualification of Peehs 1998 [DIRS 109219]**

*Technical Assessment*—Helium produced in fuel rods could pressurize the cladding and cause it to fail. The Cladding Degradation Analysis and this source (pages 5 and 6) consider that the complete release of helium and the resulting pressurization are highly conservative. Piron and Pelletier 2001 [DIRS 165318], who are discussed in Section C.3.13 of this appendix, show that after 10,000 years at repository temperatures, the peak pressure would not cause the cladding to fail. These results assume complete release of the helium. This source shows that fission gas release during dry storage is not expected because the diffusion coefficients decrease by approximately 8 orders as the fuel cools from reactor temperatures. Because repository temperatures are well below dry storage temperatures, assuming complete release of helium is highly conservative.

*Personnel / Organization Qualifications*—This work was performed at Siemens KWU-NBT, a nuclear vendor.

*Extent and Quality of Corroborating Information*—Manaktala 1993 [DIRS 101719] and Rothman 1984 [DIRS 100417] corroborate this source's assertion that complete release of helium is conservative. Both found that helium pressure buildup would be offset by the cooling of the rods. Consequently, the helium pressure that Cladding Degradation Analysis assumes at 10,000 years is conservative.

### **C.3.13 Qualification of Piron and Pelletier 2001 [DIRS 165318]**

*Technical Assessment*—This analysis and the above source consider whether helium could pressurize the cladding and cause it to fail. This source indicates that after 10,000 years at repository temperatures, the peak pressure would reach 13.3 MPa, but pressure would have to reach about 33 MPa for the cladding to fail from delayed hydride cracking. Both conclude that helium production at peak temperatures would not elevate pressure in the fuel rod to a level that would cause cladding failure.

*Personnel / Organization Qualifications*—The French Atomic Energy Commission (CEA) is a reputable and an authoritative source for this type of information.

*Peer / Professional Review*—The source was peer-reviewed.

*Extent and Quality of Corroborating Information*—Manaktala 1993 [DIRS 101719] and a Rothman 1984 [DIRS 100417] corroborate this source's assertion that helium production would not fail the cladding. Both found that helium pressure buildup would be offset by the cooling of the rods. Consequently, the pressure at 10,000 years would be less than what this source predicted, and the likelihood of cladding failure would be even more remote.

### **C.3.14 Qualification of Wolfram et al. 1996 [DIRS 165268]**

*Technical Assessment*—This analysis and the above source (pages iii and iv) do not expect microbes to cause cladding failure. Both found no evidence in the literature that zirconium or its alloys are susceptible to microbial-induced corrosion.

*Personnel / Organization Qualifications*—This work was performed at the Idaho National Engineering Laboratory.

*Extent and Quality of Corroborating Information*—Three independent sources corroborate Wolfram et al. 1996 [DIRS 165268]. Hillner et al. 1998 [DIRS 100455], supports the concept that organic acids produced by microbes are unlikely to significantly accelerate zirconium corrosion. Yau and Webster, 1987 [DIRS 100494], an authoritative source, states that zirconium resists organic acids that microbes produce. And the Yucca Mountain Project (CRWMS M&O 2000b, [DIRS 151561]) evaluated in-drift microbial communities and concluded that they would have little effect on the in-drift geochemistry.

## **C.4 CONCLUSION**

In conclusion, the data or technical information is qualified for its intended use.